AN ABSTRACT OF THE THESIS OF

Razvan Nes for the degree of Master of Science in Nuclear Engineering presented on May 17, 2002.

Title: An Advanced Nodal Discretization for the Quasi-Diffusion Low-Order Equations.

Abstract approved: _____

Todd S. Palmer

The subject of this thesis is the development of a nodal discretization of the low-order quasi-diffusion (QDLO) equations for global reactor core calculations. The advantage of quasi-diffusion (QD) is that it is able to capture transport effects at the surface between unlike fuel assemblies better than the diffusion approximation. We discretize QDLO equations with the advanced nodal methodology described by Palmtag (Pal 1997) for diffusion. The fast and thermal neutron fluxes are presented as 2-D, non-separable expansions of polynomial and hyperbolic functions.

The fast flux expansion consists of polynomial functions, while the thermal flux is expanded in a combination of polynomial and hyperbolic functions. The advantage of using hyperbolic functions in the thermal flux expansion lies in the accuracy with which hyperbolic functions can represent the large gradients at the interface between unlike fuel assemblies. The hyperbolic expansion functions proposed in (Pal 1997) are the analytic solutions of the zero-source diffusion equation for the thermal flux. The specific form of the QDLO equations requires

the derivation of new hyperbolic basis functions which are different from those proposed for the diffusion equation.

We have developed a discretization of the QDLO equations with node-averaged cross-sections and Eddington tensor components, solving the 2-D equations using the weighted residual method (Ame 1992). These node-averaged data are assumed known from single assembly transport calculations. We wrote a code in "Mathematica" that solves k-eigenvalue problems and calculates neutron fluxes in 2-D Cartesian coordinates.

Numerical test problems show that the model proposed here can reproduce the results of both the simple diffusion problems presented in (Pal 1997) and those with analytic solutions. While the QDLO calculations performed on one-node, zero-current, boundary condition diffusion problems and two-node, zero-current boundary condition problems with UO_2-UO_2 assemblies are in excellent agreement with the benchmark and analytic solutions, UO_2-MOX configurations show more important discrepancies that are due to the single-assembly homogenized cross-sections used in the calculations. The results of the multiple-node problems show similar discrepancies in power distribution with the results reported in (Pal 1997). Multiple-node k-eigenvalue problems exhibit larger discrepancies, but these can be diminished by using adjusted diffusion coefficients (Pal 1997). The results of several "transport" problems demonstrate the influence of Eddington functionals on homogenized flux, power distribution, and multiplication factor k.

An Advanced Nodal Discretization for the Quasi-Diffusion Low-Order Equations

By

Razvan Nes

A THESIS

submitted to

Oregon State University

in partial fulfillment of
the requirements for the
degree of

Master of Science

Presented May 17, 2002

Commencement June 2003

Master of Science thesis of Razvan Nes, presented on May 17, 2002.

APPROVED:

Redacted for Privacy

Major Professor, representing Nuclear Engineering

Redacted for Privacy

Head of Department of Nuclear Engineering

Redacted for Privacy

Dean of Graduate School

I understand that my thesis will become part of the permanent collection of Oregon State University libraries. My signature below authorizes release of my thesis to any reader upon request.

Redacted for Privacy

Razvan Nes, Author

ACKNOWLEDGMENTS

First and foremost, I am deeply thankful to my major professor and advisor, Dr. Todd S. Palmer, who has contributed the most to my education. I would like to thank him for his insight and wisdom during our work, and for teaching me how to do research. He has provided me with patient direction through this project, his confidence in my work being very supportive and encouraging me a lot. Undoubtedly, I could not have found a better major professor, teacher and advisor.

My special thanks go to Dr. Kathryn A. Higley, my minor professor, for being very supportive of me during my time at the Oregon State University. I greatly appreciate her friendly advice and guidance.

I would like to thank Dr. Stephen E. Binney, distinguished professor, for carefully reading my thesis, evaluating my work, and taking time from his busy schedule to serve in my Master's Committee.

I also like to thank Dr. Vinod Narayanan, my Graduate Council Representative. The quality of this thesis has improved through his comments.

This work was supported by DOE Nuclear Energy Research Initiative (NERI) Program. Further acknowledgement goes to the NERI participants, who generously donated their time and expertise. Many interesting and stimulating discussions with Dr. Marvin Adams (Texas A&M University), Dr. Dimitriy Anistratov (North Carolina State University), Dr. Scott Palmtag and Dr. Kord Smith (Studsvik Scandpower, Inc.) have been highly valuable to me and this thesis.

I would like to extend my appreciation to the faculty and staff at the Radiation Center, for creating an excellent environment for learning.

TABLE OF CONTENTS

TABLE OF CONTENTS (CONTINUED)

TABLE OF CONTENTS (CONTINUED)

LIST OF FIGURES

LIST OF FIGURES (CONTINUED)

LIST OF TABLES

LIST OF TABLES (CONTINUED)

LIST OF APPENDICES

NOMENCLATURE

Symbol	Description	Dimension
$\hat{\Omega}$	Unit vector in the direction of the velocity	
Ω_i, Ω_j	Projection after i and j axes (i, j= x, y, z) of $\hat{\Omega}$	
$d\Omega$	Unit of the solid angle	srad
ψ_g	Angular flux of neutrons in group g	$cm^{-2}s^{-1}srad$
Σ_g	Macroscopic total cross-section for neutrons in group g	cm^{-1}
$\Sigma_{gg'}$	Macroscopic scattering cross-section for neutrons between group g' and g	cm^{-1}
$\Sigma_{fg'}$	Macroscopic fission cross-section for neutrons in group g'	cm^{-1}
Φ_g	Scalar flux for neutrons in group g	$cm^{-2}s^{-1}$
χ_g	Fission neutrons with energies within group g	
k	Multiplication factor	
$\hat{J}_g$	Current of neutrons in group g	$cm^{-2}s^{-1}$
$\hat{J}_{gi}$	Projection on i axis (i=x, y, z) of the current of neutrons in group g	$cm^{-2}s^{-1}$
υ	Averaged neutrons number emitted per fission	

Symbol	Description	Dimension
E_g	Eddington tensor for neutrons in group g	
E_{gij}	(i, j) component of Eddington tensor for neutrons in group g	
$\hat{J}_1$	Fast neutron current	$cm^{-2}s^{-1}$
$\hat{J}_2$	Thermal neutron current	$cm^{-2}s^{-1}$
Σ_{f1}	Macroscopic fission cross-section for fast neutrons	cm^{-1}
Σ_{f2}	Macroscopic fission cross-section for thermal neutrons	cm^{-1}
Φ_1	Fast neutron flux	$cm^{-2}s^{-1}$
Φ_2	Thermal neutron flux	$cm^{-2}s^{-1}$
Σ_{r1}	Macroscopic removal cross-section for fast neutrons	cm^{-1}
Σ_{r2}	Macroscopic removal cross-section for thermal neutrons	cm^{-1}
D_g	Diffusion coefficient for neutrons in group g	cm
Σ_1	Macroscopic total cross-section for fast neutrons	cm^{-1}

Symbol	Description	Dimension
Σ_2	Macroscopic total cross-section for thermal neutrons	cm^{-1}
E_{1ij}	(i, j) component of Eddington tensor for fast neutrons (i,j=x, y)	
E_{2ij}	(i, j) component of Eddington tensor for thermal neutrons (i,j=x, y)	
Σ_{12}	Macroscopic scattering cross-section for neutrons from group 1 (fast) to group 2 (thermal)	cm^{-1}
$\bar{\bar{\Phi}}_1$	Node-average fast flux	$cm^{-2}s^{-1}$
$\bar{\bar{\Phi}}_2$	Node-average thermal flux	$cm^{-2}s^{-1}$
$\bar{\Phi}^{ij}_{gx+/-}$, $\bar{\Phi}^{ij}_{gy+/-}$	surface-averaged flux of neutrons in group g in node (i,j)	$cm^{-2}s^{-1}$
$\bar{J}^{ij}_{gx+/-}$, $\bar{J}^{ij}_{gy+/-}$	surface-averaged current of neutrons in group g in node (i,j)	$cm^{-2}s^{-1}$
M	Matrix of the linear system of equations in expansion coefficient from leakage + removal terms of QDLO	
F	Matrix of the linear system of equations in expansion coefficient from fission terms of QDLO	
B^2	Geometric buckling	cm^{-2}

AN ADVANCED NODAL DISCRETIZATION FOR THE QUASI-DIFFUSION LOW-ORDER EQUATIONS

1. INTRODUCTION

In nuclear reactor analysis there are many situations in which the multiplication factor and full, three-dimensional calculations of the neutron flux are required. In these instances, although the diffusion equation can be directly solved numerically on digital computers, practical limitations on computer storage and prohibitively-long execution time are making impossible a "pin-by-pin" modeling of a light water reactor (LWR). Since the diffusion length characterizes the spatial variation of the neutron flux, accuracy requires that the mesh spacing be comparable or less than the diffusion length (Dud 1976). Consequently, in each of the three spatial dimensions of a nuclear reactor core, a large number of mesh points must be chosen and multidimensional core calculations are more expensive.

Neutrons in a reactor have energies between 10^7 eV and 10^{-2} eV, and the interaction cross sections for neutrons are sensitively dependent on the energy of incident neutrons. Therefore, a realistic treatment requires taking into account the neutron energy dependence. For this purpose, in reactor calculations, energy is discretized into "energy groups". Most LWR calculations are performed using a four-group diffusion model, while for fast reactors 20 groups are often used (Dud 1976). Neutrons can undergo scattering interactions resulting in significant changes in their kinetic energy, changing neutron migration between energy groups. This leads to a system of coupled multigroup diffusion equations, one equation for each energy group. As a conclusion multidimensional fine-mesh, fine-energy reactor calculations are leading to large linear systems of equations, which are difficult to handle even by current computers.

A similar situation is encountered in transport calculations. Here, in addition to spatial and energy discretizations, the angular directions are discretized by requiring the transport equation to hold only for a number of distinct angles (Lew 1993).

Problems become even more time-consuming if one is interested in repeatedly performing reactor calculations in order to investigate the effect of particular parameters on multiplication factor or flux distribution, or in the case of a changing core-composition due to fuel burn-up and fission product accumulation.

The difficulties originating from the spatial dependence of the neutron flux, energy spectrum and anisotropic scattering are addressed by the development of coarse-mesh nodal methods: equivalent few-group diffusion parameters, determined for relatively large homogeneous regions called "nodes" are used to compute global solutions like full-core eigenvalues and power distributions. Often the homogenized regions consist of entire fuel assemblies and the computational effort is oriented towards the node-averaged flux over each homogenized region. Traditionally, homogenized node parameters are calculated with the flux determined by transport calculations in an assembly (Law 1986), (Smi 1986). With advanced nodal schemes, the truncation errors in flux solution are smaller than those introduced by the use of flux-weighted homogenization. This drove the development of more accurate homogenization procedures (Law 1986). Accurate node-homogenized fission cross-sections and node-averaged flux yield accurate power distributions.

The work presented here is part of a project that concentrates upon two areas: the creation of a full-core few-group coarse-mesh diffusion-like method that will produce the same results as full-core many-group fine-mesh transport calculations, and the construction of "group constants" (i.e. cross sections and discontinuity factors) to be used in the diffusion-like calculations. The subject of this thesis is the development of a nodal discretization of the quasi-diffusion (QD) equations, derived in Chapter 2, for global core calculations. The advantage of QD

is that it is able to capture transport effects at the surface between unlike fuel assemblies better than the diffusion approximation.

It is significantly more convenient to store one table of group constants derived from single-assembly calculations for each type of fuel assembly, rather than the much larger data set that would result from multi-assembly calculations (also known as "colorsets"). This is why single-assembly calculations are the second main objective in the project. In order to get accurate group constants for an assembly regardless of its neighbors these group constants should be computed using a methodology that captures interface effects.

Spatially-differenced forms of the discrete-ordinate transport equation are usually solved by the method of iteration on the scattering source (Lew 1993), (Ada 2002). In this case the convergence of the iteration is dictated by the properties of the medium and the size of the problem. In large scattering media, where particles undergo many collisions in a single energy group and the leakage probability is small, iterative techniques converge more slowly than in small absorbant, "leaking" systems (Lew 1993), (Ada 2002). As a result, special methods were developed to accelerate the iterations.

Besides early acceleration schemes (Chebychev acceleration and fine- and coarse-mesh rebalance), the research in the field of efficient iteration strategies has followed two paths: synthetic acceleration methods and quasi-diffusion and related methods (Ada 2002).

Synthetic acceleration methods are based on finding a "low-order" operator, close to the original transport operator but more easily invertible. Synthetic acceleration methods provide additive corrections to the transport sweep solutions that are calculated using the low-order operator instead of inverting the whole transport operator (Ada 2002). The converged solution of the synthetic scheme should satisfy the original transport equation regardless of the way the low-order operator was defined as long as the discrete low-order operator is derived

consistently with the transport operator. A low-order operator used in synthetic acceleration schemes is, for example, the diffusion operator (Ada 2002).

Quasi-diffusion methods are characterized by the fact that they obtain a discrete transport solution, but this solution is influenced by both the discretizations of the transport and the low-order diffusion-like operator. The low-order operator contains transport corrections (Ada 2002); thus the QD-accelerated solution does not converge to the unaccelerated transport solution. QD methods are nonlinear, requiring multiplication and division of unknowns. The advantage of the QD methods is that they provide fast convergence regardless of discretization and consistency (Ada 1994).

The QD method was developed in 1964 by Gol'din as a nonlinear method of solving the linear Boltzmann equation (Gol 1967). In the same paper, Gol'din describes a form of the QD equations that accounts for anisotropy.

In 1970 Troshchiev (Gol 1967) reported consistent discretizations allowing the QD method to obtain the same solution as the unaccelerated transport equations. This made QD a true acceleration scheme (Ada 2002).

Later, in 1972, Gol'din and Chetverushkin (Gol 1972) formulated the generalized QD boundary conditions, i.e. a general relationship between flux and current that involves QD coefficients calculated using the angular flux from a previous transport sweep. To be more specific, the paper (Gol 1972) explains a method of solving the 1-D cylindrical geometry gas dynamics equations. The unknown for which the transport equation is solved is the intensity, and the boundary conditions relate the radiative energy flux to the energy density of radiation by the means of QD coefficients.

In 1978, Aksenov and Gol'din (Aks 1979) successfully used 2-D QD calculations of neutron transport, demonstrating the applicability of the method in two-dimensional problems.

In 1982, Gol'din formulated abstractly the QD method, and applied it to multigroup neutron transport problems with anisotropic scattering (Ada 2002). The

effects of various spatial discretizations of the transport equation given a constant low-order equation discretization were analyzed, in 1986, by Anistratov and Gol'din (Ada 2002).

One year later Miften and Larsen (Mif 1993) developed a symmetrized QD method (SQD) that yields an "accurate and efficiently solvable" discretization of multidimensional transport problems. This method combines the advantages of QD methods (i.e. no consistent discretization required) with the convenience of being solvable with the standard conjugate gradient method; in addition to this, the SQD can be more easily generalized to nonorthogonal grids than the discretized synthetic acceleration technique.

In 1986 and later, in 1996, Gol'din used QD to solve coupled material-temperature and radiative transfer equations (Ada 2002). The QD method applied to anisotropic scattering problems described by Gol'din in (Gol 1967) was implemented in the late 1990s for strongly anisotropic scattering (Ada 2002). In 1993 Aristova developed a finite difference scheme for the QD elliptic operator in oblique-angle cells with applications in studying high-temperature radiative gas dynamics (Ari 1993).

Soon after the QD method was created by Gol'din in 1964, nonlinear QD-related methods were derived by Nikolaishvilli ("Yves-Mertens" approximation in 1966), Germogenova ("Method of averaged fluxes" in 1968), and Gol'din himself in 1969. In 1970 Gol'din extended these methods to electron transport problems. Notable contributions in QD-related methods are due to Anistratov and Larsen (Weighted alpha methods in 1996 and 2001) (Ada 2002).

In the present work, the QD method is discretized with the advanced nodal methodology described by Palmtag (Pal 1997). The advanced method proposed by Palmtag presents the fast and thermal neutron fluxes as 2-D, non-separable expansion of polynomial and hyperbolic functions. The fast flux expansion consists of polynomial functions of degree zero through four, and the thermal flux expansion of a combination of polynomial and hyperbolic functions. The same

polynomial functions are used in fast and thermal flux expansions. The hyperbolic expansion functions in thermal flux are the analytic solutions of the zero-source low-order quasi-diffusion (QDLO) equation of the thermal flux. The advantage of use of hyperbolic functions in thermal flux expansion consists in the accuracy with which hyperbolic functions can represent the large gradients at the interface between unlike fuel assemblies (Pal 1997). On the other hand, polynomials are sufficiently accurate in representing the smooth variations of the fast neutron flux. In addition, the use of hyperbolic functions that mathematically solve the zero-source QDLO equations allows expressing the polynomial expansion coefficients of the thermal flux in terms of polynomial expansion coefficients of the fast flux. The 2-group, 2-D nodal discretization is applied here to the more general case of constant Eddington tensor components (QD model). Consequently, different basis functions are used in the hyperbolic terms of the thermal flux expansion. To prove the validity of this model, we developed a code based on the QD equations. The code, written in "Mathematica", is used to solve k-eigenvalue problems and calculates neutron fluxes in 2-D Cartesian coordinates. The results prove that the model proposed here can reproduce the results of the simple diffusion problems presented in literature (Pal 1997) or derived analytically.

Chapter 2 contains the derivation of the 2-group, Cartesian geometry QDLO equations starting from the general-geometry, k-eigenvalue, multigroup transport equation. Chapter 3 describes the nodal discretization and the solution strategies used to solve the 2-group, 2-D QDLO equations and an outline of the power iteration technique used to determine the multiplication factor. Chapter 4 presents the results of a number of diffusion benchmarks and non-diffusion problems obtained by the use of a computer code that incorporates the QDLO equations. Chapter 5 contains the conclusion and the recommendations for future work. The appendices present the analytic form of the weighted equations, continuity and boundary conditions, as they have been derived.

2. THE QUASI-DIFFUSION METHOD FOR NEUTRON TRANSPORT

2.1. TRANSPORT PRELIMINARIES

In Chapter 1, we argued that the quasi-diffusion method is a nonlinear iteration scheme for solving transport problems. Each iteration consists in a "high-order" transport sweep and a "low-order" diffusion calculation. Here we derive the 3-D, multigroup, isotropic scattering and isotropic fission source, transport equation. Then, low-order quasi-diffusion (QDLO) equations are written in 2-D Cartesian coordinates for two energy groups, assuming constant neutron cross sections and Eddington tensor components in the interior of each node. These are the equations that are solved for the homogeneous 2-D scalar neutron flux. We also demonstrate that, if the angular flux is a linear function of angle, the QDLO equations limit to the diffusion equation.

2.2. DERIVATION OF LOW ORDER QUASI-DIFFUSION EQUATIONS

Consider the general-geometry k-eigenvalue transport equation with isotropic scattering in the conventional multigroup form (Lew 1993), (Dud 1976),

$$\hat{\Omega}\bullet\nabla\psi_g(\hat{r},\hat{\Omega})+\Sigma_g(\hat{r})\psi_g(\hat{r},\hat{\Omega})=\frac{1}{4\pi}\sum_{g'=1}^{G}\Sigma_{g'g}(\hat{r})\Phi_{g'}(\hat{r})+$$
$$+\frac{\chi_g}{4\pi k}\sum_{g'=1}^{G}\upsilon\Sigma_{fg'}(\hat{r})\Phi_{g'}(\hat{r}), \tag{2-1}$$

where

- $\hat{\Omega}$ is the direction,

- $\psi_g(\hat{r},\hat{\Omega})$ is the angular flux,
- $\Sigma_g(\hat{r})$ is the total cross section for neutrons in group g,
- $\Sigma_{g'g}(\hat{r})$ is the scattering cross section for neutrons between groups g' and g (g'<g),
- $\Phi_{g'}(\hat{r})$ is the scalar flux,
- χ_g is the fission neutron spectrum,
- k is the multiplication factor,
- υ is the number of neutrons per fission, and
- $\Sigma_{fg'}(\hat{r})$ is the fission cross section for neutrons in group g'.

Integrating each term of (2-1) by over 4π neutron directions, yields (Mif 1993)

$$\int_{4\pi}\hat{\Omega}\bullet\nabla\psi_g(\hat{r},\hat{\Omega})d\hat{\Omega}=\int_{4\pi}(\Omega_x\frac{\partial\psi_g}{\partial x}+\Omega_y\frac{\partial\psi_g}{\partial y}+\Omega_z\frac{\partial\psi_g}{\partial z})d\hat{\Omega}=$$

$$=\frac{\partial}{\partial x}\int_{4\pi}\Omega_x\psi_g(\hat{r},\hat{\Omega})d\hat{\Omega}+\frac{\partial}{\partial y}\int_{4\pi}\Omega_y\psi_g(\hat{r},\hat{\Omega})d\hat{\Omega}+ \qquad (2\text{-}2)$$

$$+\frac{\partial}{\partial z}\int_{4\pi}\Omega_z\psi_g(\hat{r},\hat{\Omega})d\hat{\Omega}=\frac{\partial J_{gx}(\hat{r})}{\partial x}+\frac{\partial J_{gy}(\hat{r})}{\partial y}+\frac{\partial J_{gz}(\hat{r})}{\partial z}=\nabla\bullet\hat{J}_g(\hat{r}),$$

$$\int_{4\pi}d\hat{\Omega}\Sigma_g(\hat{r})\psi_g(\hat{r},\hat{\Omega})=\Sigma_g(\hat{r})\Phi_g(\hat{r}), \qquad (2\text{-}3)$$

$$\int_{4\pi}d\hat{\Omega}\left(\frac{\chi_g}{4\pi k}\sum_{g'=1}^{G}\nu\Sigma_{fg'}(\hat{r})\Phi_{g'}(\hat{r})\right)=\frac{\chi_g}{k}\sum_{g'=1}^{G}\nu\Sigma_{fg'}(\hat{r})\Phi_{g'}(\hat{r}), \qquad (2\text{-}4)$$

and

$$\int_{4\pi}d\hat{\Omega}\left(\frac{1}{4\pi}\sum_{g'=1}^{G}\Sigma_{g'g}(\hat{r})\Phi_{g'}(\hat{r})\right)=\sum_{g'=1}^{G}\Sigma_{g'g}(\hat{r})\Phi_{g'}(\hat{r}). \qquad (2\text{-}5)$$

In (2-2) the quantities

$$\int_{4\pi}d\hat{\Omega}\Omega_i\psi_g(\hat{r},\hat{\Omega})=J_{gi}(\hat{r}) \qquad (2\text{-}6)$$

are the components of the neutron current vector ($i=x,\ y,\ z$). Thus, (2-1) becomes

$$\nabla \bullet \hat{J}_g(\hat{r}) + \Sigma_g(\hat{r})\Phi_g(\hat{r}) = \sum_{g'=1}^{G} \Sigma_{g'g}(\hat{r})\Phi_g(\hat{r}) + \frac{\chi_g}{k} \sum_{g'=1}^{G} \nu\Sigma_{fg'}(\hat{r})\Phi_{g'}(\hat{r}). \quad (2\text{-}7)$$

Equation (2-7) has the physical meaning of a balance equation: in steady state conditions the number of neutrons with energies within group g leaving a volume by diffusion or as a result of collisions occurring in the same volume is equal to the number of neutrons produced by fission within group g plus the number of neutrons that are scattered from group g' into group g. Defining the macroscopic removal cross section Σ_{rg},

$$\Sigma_{rg}(\hat{r}) = \Sigma_g(\hat{r}) - \Sigma_{g'g}(\hat{r}), \quad (2\text{-}8)$$

then (2-7) takes the following form:

$$\nabla \bullet \hat{J}_g(\hat{r}) + \Sigma_{rg}(\hat{r})\Phi_g(\hat{r}) = \sum_{\substack{g'=1 \\ g' \neq g}}^{G} \Sigma_{g'g}(\hat{r})\Phi_{g'}(\hat{r}) + \frac{\chi_g}{k} \sum_{g'=1}^{G} \upsilon\Sigma_{fg'}(\hat{r})\Phi_{g'}(\hat{r}). \quad (2\text{-}9)$$

If we now multiply on equation (2-1) terms by Ω_x and integrate over 4π we obtain (Mif 1993)

$$\int_{4\pi} d\hat{\Omega}\Omega_x \hat{\Omega} \bullet \nabla \psi_g(\hat{r},\hat{\Omega}) = \int_{4\pi} d\hat{\Omega}(\Omega_x^2 \frac{\partial \psi_g(\hat{r},\hat{\Omega})}{\partial x} + \Omega_x\Omega_y \frac{\partial \psi_g(\hat{r},\hat{\Omega})}{\partial y} +$$

$$+\Omega_x\Omega_z \frac{\partial \psi_g(\hat{r},\hat{\Omega})}{\partial z}) = \frac{\partial}{\partial x} \int_{4\pi} d\hat{\Omega}\Omega_x^2 \psi_g(\hat{r},\hat{\Omega}) + \quad (2\text{-}10)$$

$$+\frac{\partial}{\partial y} \int_{4\pi} d\hat{\Omega}\Omega_x\Omega_y \psi_g(\hat{r},\hat{\Omega}) + \frac{\partial}{\partial z} \int_{4\pi} d\hat{\Omega}\Omega_x\Omega_z \psi_g(\hat{r},\hat{\Omega}),$$

$$\int_{4\pi} d\hat{\Omega}\Omega_x \Sigma_g(\hat{r})\psi_g(\hat{r},\hat{\Omega}) = \Sigma_g(\hat{r})J_{gx}(\hat{r}), \quad (2\text{-}11)$$

$$\int_{4\pi} d\hat{\Omega}\Omega_x \left(\frac{1}{4\pi} \sum_{g'=1}^{G} \Sigma_{g'g}(\hat{r})\Phi_{g'}(\hat{r}) \right) = 0, \quad (2\text{-}12)$$

and

$$\int_{4\pi} d\hat{\Omega}\Omega_x \left(\frac{\chi_g}{4\pi k} \sum_{g'=1}^{G} \upsilon\Sigma_{fg'}(\hat{r})\Phi_{g'}(\hat{r}) \right) = 0. \quad (2\text{-}13)$$

Thus, (2-1) becomes

$$\frac{\partial}{\partial x}\int_{4\pi} d\hat{\Omega}\Omega_x^2\psi_g(\hat{r},\hat{\Omega})+\frac{\partial}{\partial y}\int_{4\pi} d\hat{\Omega}\Omega_x\Omega_y\psi_g(\hat{r},\hat{\Omega})+$$
$$+\frac{\partial}{\partial z}\int_{4\pi} d\hat{\Omega}\Omega_x\Omega_z\psi_g(\hat{r},\hat{\Omega})+\Sigma_g(\hat{r})J_{gx}(\hat{r})=0. \qquad (2\text{-}14)$$

Equations similar to (2-14) are obtained by multiplying (2-1) by Ω_y, Ω_z, and integrating over 4π, as follows:

$$\frac{\partial}{\partial x}\int_{4\pi} d\hat{\Omega}\Omega_y\Omega_x\psi_g(\hat{r},\hat{\Omega})+\frac{\partial}{\partial y}\int_{4\pi} d\hat{\Omega}\Omega_y^2\psi_g(\hat{r},\hat{\Omega})+$$
$$+\frac{\partial}{\partial z}\int_{4\pi} d\hat{\Omega}\Omega_y\Omega_z\psi_g(\hat{r},\hat{\Omega})+\Sigma_g(\hat{r})J_{gy}(\hat{r})=0, \qquad (2\text{-}15)$$

$$\frac{\partial}{\partial x}\int_{4\pi} d\Omega\Omega_z\Omega_x\psi_g(\hat{r},\hat{\Omega})+\frac{\partial}{\partial y}\int_{4\pi} d\Omega\Omega_z\Omega_y\psi_g(\hat{r},\hat{\Omega})+$$
$$+\frac{\partial}{\partial z}\int_{4\pi} d\Omega\Omega_z^2\psi_g(\hat{r},\hat{\Omega})+\Sigma_g(\hat{r})J_{gz}(\hat{r})=0. \qquad (2\text{-}16)$$

Equations (2-14), (2-15) and (2-16) can be written concisely

$$\nabla\bullet\left(\int_{4\pi}\Omega_i\Omega_j\psi_g(\hat{r},\hat{\Omega})d\Omega\right)+\Sigma_g(\hat{r})J_{gi}(\hat{r})=0 \quad \text{for i,j=x,y,z}. \qquad (2\text{-}17)$$

Defining a symmetric, positive-definite tensor of components

$$E_{gij}(\hat{r})=\frac{\int_{4\pi}\Omega_i\Omega_j\psi_g(\hat{r},\hat{\Omega})d\Omega}{\int_{4\pi}\psi_g(\hat{r},\hat{\Omega})d\Omega} \quad \text{for i,j=x,y,z} \qquad (2\text{-}18)$$

equation (2-17) can be written as

$$\nabla(E_{gij}(\hat{r})\Phi_g(\hat{r}))+\Sigma_g(\hat{r})J_{gi}(\hat{r})=0. \qquad (2\text{-}19)$$

In deriving (2-19) we use the definition of scalar neutron flux (Lew 1993)

$$\Phi_g(\hat{r})=\int_{4\pi}\psi_g(\hat{r},\hat{\Omega})d\Omega. \qquad (2\text{-}20)$$

The tensor defined by (2-18) is also known as Eddington's tensor. Due to its symmetry the off-diagonal elements of Eddington's tensor are equal ($E_{gij}=E_{gji}$).

Functionals E_{gij} depend weakly on the angular flux. Equations (2-9) and (2-19) are called the Low-Order Quasi-Diffusion equations.

A frequently used form of the Low-Order Quasi-Diffusion equations is the one written for two neutron energy groups g=1 (fast neutrons) and g=2 (thermal neutrons), no upscattering (neutrons cannot gain energy in scattering events), and fissions produce only fast neutrons.

Under these assumptions the Low-Order Quasi-Diffusion equations take the form

$$\nabla\bullet\hat{J}_1(\hat{r})+\Sigma_{r1}(\hat{r})\Phi_1(\hat{r})=\frac{1}{k}(\upsilon\Sigma_{f1}(\hat{r})\Phi_1(\hat{r})+\upsilon\Sigma_{f2}(\hat{r})\Phi_2(\hat{r})) \qquad (2\text{-}21)$$

and

$$\nabla\bullet\hat{J}_2(\hat{r})+\Sigma_{r2}(\hat{r})\Phi_2(\hat{r})=\Sigma_{12}(\hat{r})\Phi_1(\hat{r}). \qquad (2\text{-}22)$$

In Cartesian coordinates (2-19) is equivalent with the following three equations:

$$\begin{aligned}&\frac{\partial}{\partial x}(E_{gxx}(\hat{r})\Phi_g(\hat{r}))+\frac{\partial}{\partial y}(E_{gxy}(\hat{r})\Phi_g(\hat{r}))+\\&+\frac{\partial}{\partial z}(E_{gxz}(\hat{r})\Phi_g(\hat{r}))+\Sigma_g(\hat{r})J_{gx}(\hat{r})=0,\end{aligned} \qquad (2\text{-}23)$$

$$\begin{aligned}&\frac{\partial}{\partial x}(E_{gyx}(\hat{r})\Phi_g(\hat{r}))+\frac{\partial}{\partial y}(E_{gyy}(\hat{r})\Phi_g(\hat{r}))+\\&+\frac{\partial}{\partial z}(E_{gyz}(\hat{r})\Phi_g(\hat{r}))+\Sigma_g(\hat{r})J_{gy}(\hat{r})=0,\end{aligned} \qquad (2\text{-}24)$$

and

$$\begin{aligned}&\frac{\partial}{\partial x}(E_{gzx}(\hat{r})\Phi_g(\hat{r}))+\frac{\partial}{\partial y}(E_{gzy}(\hat{r})\Phi_g(\hat{r}))+\\&+\frac{\partial}{\partial z}(E_{gzz}(\hat{r})\Phi_g(\hat{r}))+\Sigma_g(\hat{r})J_{gz}(\hat{r})=0,\end{aligned} \qquad (2\text{-}25)$$

where g=1,2.

If the angular flux is a linear function of angle, i.e.

$$\psi_g(\hat{r},\hat{\Omega})\approx\psi_{g0}(\hat{r})+\psi_{gx}(\hat{r})\Omega_x+\psi_{gy}(\hat{r})\Omega_y+\psi_{gz}(\hat{r})\Omega_z, \qquad (2\text{-}26)$$

according to (2-18) Eddington tensor elements are given by

$$E_{gij}(\hat{r}) = \frac{\psi_{g0}(\hat{r})\int_{4\pi}\Omega_i\Omega_j d\Omega + \psi_{gx}(\hat{r})\int_{4\pi}\Omega_i\Omega_j\Omega_x d\Omega + + \psi_{gy}(\hat{r})\int_{4\pi}\Omega_i\Omega_j\Omega_y d\Omega + \psi_{gz}(\hat{r})\int_{4\pi}\Omega_i\Omega_j\Omega_z d\Omega}{\psi_{g0}(\hat{r})\int_{4\pi} d\Omega + \psi_{gx}(\hat{r})\int_{4\pi}\Omega_x d\Omega + \psi_{gy}(\hat{r})\int_{4\pi}\Omega_y d\Omega + \psi_{gz}(\hat{r})\int_{4\pi}\Omega_z d\Omega}. \tag{2-27}$$

It can be shown (Dud 1976) that

$$\int_{4\pi}\Omega_i\Omega_j d\Omega = \frac{4\pi}{3}\delta_{ij} \tag{2-28}$$

and

$$\int_{4\pi}\Omega_x^l\Omega_y^m\Omega_z^n d\Omega = 0 \quad \text{if l,m, or n is odd.} \tag{2-29}$$

In these conditions (2-27) becomes

$$E_{gij}(\hat{r}) = \frac{\delta_{ij}}{3} \tag{2-30}$$

and Eddington tensor is diagonal. In (2-30) δ_{ij} stands for the Kronecker's delta: δ_{ij}=1 for i=j, and δ_{ij}=0 for i$\neq$j. Equations (2-23), (2-24) and (2-25) thus become

$$J_{gi}(\hat{r}) = -\frac{1}{3\Sigma_g(\hat{r})}\frac{\partial\Phi_g(\hat{r})}{\partial q_i} \quad \text{i=1,2,3 and } q_i\text{=x, y, z.} \tag{2-31}$$

An equivalent form for (2-31) would be

$$\hat{J}_g(\hat{r}) = -\frac{1}{3\Sigma_g(\hat{r})}\nabla\Phi_g(\hat{r}) \tag{2-32}$$

which is Fick's approximation, with diffusion coefficient $D_g(\hat{r}) = \frac{1}{3\Sigma_g(\hat{r})}$ (Lew 1993).

Equations (2-23) and (2-24) can be rewritten in the following 2-D form that will be used in the next derivations:

$$J_{gx}(x,y) = -\frac{1}{\Sigma_g(x,y)}\left(\frac{\partial}{\partial x}\left(E_{gxx}(x,y)\Phi_g(x,y)\right) + \right.$$
$$\left. + \frac{\partial}{\partial y}\left(E_{gxy}(x,y)\Phi_g(x,y)\right)\right) \tag{2-33}$$

and

$$J_{gy}(x,y) = -\frac{1}{\Sigma_g(x,y)}\left(\frac{\partial}{\partial x}\left(E_{gyx}(x,y)\Phi_g(x,y)\right) + \right.$$
$$\left. + \frac{\partial}{\partial y}\left(E_{gyy}(x,y)\Phi_g(x,y)\right)\right) \tag{2-34}$$

Assuming constant cross-sections and constant Eddington tensor's components, and using (2-33) and (2-34) combined with (2-21) and (2-22) to eliminate the neutron current, one obtains:

$$-\left(\frac{E_{1xx}}{\Sigma_1}\frac{\partial^2\Phi_1(x,y)}{\partial x^2} + \frac{E_{1xy}}{\Sigma_1}\frac{\partial^2\Phi_1(x,y)}{\partial x\partial y} + \right.$$
$$\left. + \frac{E_{1yx}}{\Sigma_1}\frac{\partial^2\Phi_1(x,y)}{\partial y\partial x} + \frac{E_{1yy}}{\Sigma_1}\frac{\partial^2\Phi_1(x,y)}{\partial y^2}\right) + \tag{2-35}$$
$$+\Sigma_{r1}\Phi_1(x,y) = \frac{1}{k}\left(\upsilon\Sigma_{f1}\Phi_1(x,y) + \upsilon\Sigma_{f2}\Phi_2(x,y)\right)$$

and

$$-\left(\frac{E_{2xx}}{\Sigma_2}\frac{\partial^2\Phi_2(x,y)}{\partial x^2} + \frac{E_{2xy}}{\Sigma_2}\frac{\partial^2\Phi_2(x,y)}{\partial x\partial y} + \right.$$
$$\left. + \frac{E_{2yx}}{\Sigma_2}\frac{\partial^2\Phi_2(x,y)}{\partial y\partial x} + \frac{E_{2yy}}{\Sigma_2}\frac{\partial^2\Phi_2(x,y)}{\partial y^2}\right) + \Sigma_{r2}\Phi_2(x,y) = \Sigma_{12}\Phi_1(x,y). \tag{2-36}$$

2.3. SUMMARY

In Chapter 2 the QDLO equations are derived from the general geometry k-eigenvalue, multigroup transport equation. The Eddington tensor depends weakly on angular flux. At the end of the chapter Cartesian-coordinate, 2-group, constant

node Eddington tensor QDLO are written. The methodology for solving these equations is described in the next chapter.

3. NODAL DISCRETIZATION OF THE LOW-ORDER QUASI-DIFFUSION EQUATIONS

3.1. BACKGROUND

In this chapter the two-dimensional quasi-diffusion equations are solved using the method of weighted residuals, with non-separable polynomial and hyperbolic basis function expansions of the fast and thermal neutron fluxes. To form a set of equations which, when solved, will yield the flux expansion coefficients, several conditions are imposed: weighted moment equations, flux and current continuity, node balance and boundary conditions. In this chapter we solve the QDLO equations by using the weighted residuals method (WRM). This method yields approximate solutions as a finite combination of known functions (Ame 1992). In WRM the coefficients of the expansion are chosen so the difference between the true and the approximate solutions are zero in an average sense. Unlike the discrete method that lead to approximate solutions at isolate points, the WRM solutions are defined everywhere and do not rise so many questions regarding accuracy, convergence, and stability (Ame 1992).

3.2. NODAL DISCRETIZATION

The problem domain is the $x-y$ plane divided into non-overlapping square regions (nodes) of dimension h. Non-dimensional coordinates (u,v) are introduced instead of (x,y). To illustrate coordinates (u,v) consider a square node that occupies the position (i, j) in an array as shown in Figure 3.1.

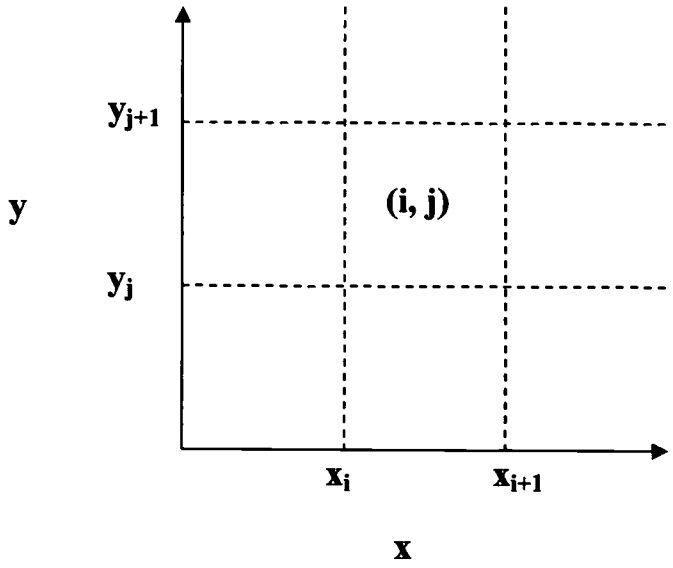

Figure 3.1. 2-D representation of a square node located at position (x_i, y_j)

Based on the geometry of the problem new coordinates (u,v) can be defined.

$$(x_{i+1} - x_i) = (y_{i+1} - y_i) = h, \tag{3-1}$$

$$u = \frac{2x - x_{i+1} - x_i}{2h} \tag{3-2}$$

and

$$v = \frac{2y - y_{i+1} - y_i}{2h}. \tag{3-3}$$

In the new non-dimensional coordinates (u,v) equations (2-35) and (2-36) become

$$\begin{aligned} &-\frac{1}{h^2}\left(\frac{E_{1xx}}{\Sigma_1}\frac{\partial^2\Phi_1(u,v)}{\partial u^2} + \frac{E_{1xy}}{\Sigma_1}\frac{\partial^2\Phi_1(u,v)}{\partial u \partial v} + \right. \\ &\left. + \frac{E_{1yx}}{\Sigma_1}\frac{\partial^2\Phi_1(u,v)}{\partial v \partial u} + \frac{E_{1yy}}{\Sigma_1}\frac{\partial^2\Phi_1(u,v)}{\partial v^2}\right) + \Sigma_{r1}\Phi_1(u,v) = \\ &= \frac{1}{k}(\upsilon\Sigma_{f1}\Phi_1(u,v) + \upsilon\Sigma_{f2}\Phi_2(u,v)) \end{aligned} \tag{3-4}$$

and

$$-\frac{1}{h^2}\left(\frac{E_{2xx}}{\Sigma_2}\frac{\partial^2\Phi_2(u,v)}{\partial u^2}+\frac{E_{2xy}}{\Sigma_2}\frac{\partial^2\Phi_2(u,v)}{\partial u\partial v}+\frac{E_{2yx}}{\Sigma_2}\frac{\partial^2\Phi_2(u,v)}{\partial v\partial u}+\right.$$
$$\left.+\frac{E_{2yy}}{\Sigma_2}\frac{\partial^2\Phi_2(u,v)}{\partial v^2}\right)+\Sigma_{r2}\Phi_2(u,v)=\Sigma_{12}\Phi_1(u,v). \tag{3-5}$$

3.3. SOLUTION STRATEGIES

3.3.1. The method of weighted residuals

The method used to solve equations (2-35) and (2-36) is the method of weighted residuals (MWR). The steps in MWR are (Ame 1992):

1. Approximate the solution $u(x,y)$ of the general form partial differential equation $Lu=f$ with the expansion

$$u(x,y)\sim\sum_{i=1}^{n}a_ib_i(x,y)\equiv U(x,y,a), \tag{3-6}$$

where $b_i(x,y)$ are known basis functions, and a_i are constant to be determined.

2. Build the equation residual

$$R(U)=LU-f \tag{3-7}$$

that is a function of a_i, x and y.

3. Select a set of m functions w_j, called "weight functions".

4. Choose the optimal set of coefficients a_i so that residuals R (U) are zero in an average sense over a domain,

$$<w_j,R(U)>=\int_V w_jR(U)dV=0,\quad \text{for j=1 to m.} \tag{3-8}$$

Integrals (3-8) are also called "weighted residuals". Weighted residuals give m linear equations in coefficients a_i; the rest of the (n-m) equations will be determined by applying boundary conditions, continuity conditions, or other constraints.

3.3.2. Two-dimensional flux expansions

For the neutrons of each energy group a set of basis functions is chosen such that in the interior of each node the flux can be approximated with expansions of basis functions.

3.3.2.1. Fast flux expansion

The fast flux in the interior of each node is approximated by a 2-D, non-separable expansion of polynomial functions (Pal 1997)

$$\Phi_1(u,v) = \sum_{m=0}^{4}\sum_{n=0}^{4} a_{mn} f_m(u) f_n(v), \tag{3-9}$$

where u and v are defined by (3-2) and (3-3). The functions f_m are polynomial basis functions of the form (Law 1986), (Pal 1997),

$$\begin{aligned} f_0(\xi) &= 1, \\ f_1(\xi) &= \xi, \\ f_2(\xi) &= 3\xi^2 - \frac{1}{4}, \\ f_3(\xi) &= 4\xi(\xi + \frac{1}{2})(\xi - \frac{1}{2}), \\ f_4(\xi) &= (\xi^2 - \frac{1}{20})(\xi + \frac{1}{2})(\xi - \frac{1}{2}). \end{aligned} \tag{3-10}$$

The fast flux expansion has only 15 non-zero a_{mn} coefficients (Pal 1997). In matrix form the coefficients are shown below,

$$\begin{bmatrix} a_{00} & a_{10} & a_{20} & a_{30} & a_{40} \\ a_{10} & a_{11} & a_{12} & 0 & 0 \\ a_{20} & a_{21} & a_{22} & 0 & 0 \\ a_{30} & 0 & 0 & a_{33} & 0 \\ a_{40} & 0 & 0 & 0 & a_{44} \end{bmatrix}. \tag{3-11}$$

3.3.2.2. Thermal flux expansion

In the interior of each node, the thermal flux is approximated by a 2-D, non-separable, expansion of polynomial and hyperbolic functions (Pal 1997)

$$\Phi_2(u,v) = \Phi_{2pol}(u,v) + \Phi_{2hyp}(u,v), \tag{3-12}$$

where

$$\Phi_{2pol}(u,v) = \sum_{m=0}^{4}\sum_{n=0}^{4} b_{mn} f_m(u) f_n(v) \tag{3-13}$$

and

$$\Phi_{2hyp}(u,v) = \sum_{l=1}^{8} c_l g_l(u,v). \tag{3-14}$$

The polynomial expansion (3-13) has 19 non-zero b_{mn} coefficients (Pal 1997). The non-zero expansion coefficients are given below in matrix form,

$$\begin{bmatrix} b_{00} & b_{10} & b_{20} & b_{30} & b_{40} \\ b_{10} & b_{11} & b_{12} & b_{13} & 0 \\ b_{20} & b_{21} & b_{22} & 0 & b_{24} \\ b_{30} & b_{31} & 0 & b_{33} & 0 \\ b_{40} & 0 & b_{42} & 0 & b_{44} \end{bmatrix}. \tag{3-15}$$

The symmetry shown by matrix representations (3-11) and (3-15) allows the diagonal symmetry of colorset problems. Non-zero diagonal elements were kept to capture diagonal effects in colorset calculations. To simplify calculations, the high order polynomial functions $f_3(\xi)$ and $f_4(\xi)$ are zero at $u,v=\pm\frac{1}{2}$. The hyperbolic functions $g_p(u,v)$ were determined so that $\Phi_{2hyp}(u,v)$ should satisfy the zero source balance equations for thermal neutron flux

$$-\frac{1}{h^2}\left(\frac{E_{2xx}}{\Sigma_2}\frac{\partial^2\Phi_{2hyp}(u,v)}{\partial u^2}+\frac{E_{2xy}}{\Sigma_2}\frac{\partial^2\Phi_{2hyp}(u,v)}{\partial u\partial v}+\right.$$
$$\left.+\frac{E_{2yx}}{\Sigma_2}\frac{\partial^2\Phi_{2hyp}(u,v)}{\partial v\partial u}+\frac{E_{2yy}}{\Sigma_2}\frac{\partial^2\Phi_{2hyp}(u,v)}{\partial v^2}\right)+\Sigma_{r2}\Phi_{2hyp}(u,v)=0. \tag{3-16}$$

The following set of basis functions (Ani 2001), (Pal 2001) was found to satisfy equations (3-16):

$$\begin{aligned}
&g_1(u,v)=\cosh(\gamma_1 u),\\
&g_2(u,v)=\sinh(\gamma_1 u),\\
&g_3(u,v)=\cosh(\gamma_2 v),\\
&g_4(u,v)=\sinh(\gamma_2 v),\\
&g_5(u,v)=\cosh(\gamma_3(v-\vartheta_1 u)/\sqrt{2}),\\
&g_6(u,v)=\sinh(\gamma_3(v-\vartheta_1 u)/\sqrt{2}),\\
&g_7(u,v)=\cosh(\gamma_3(v-\vartheta_2 u)/\sqrt{2}),\\
&g_8(u,v)=\sinh(\gamma_3(v-\vartheta_2 u)/\sqrt{2}),
\end{aligned} \tag{3-17}$$

where

$$\gamma_1 = \sqrt{\frac{h^2 \Sigma_{r2} \Sigma_{t2}}{E_{2xx}}},$$

$$\gamma_2 = \sqrt{\frac{h^2 \Sigma_{r2} \Sigma_{t2}}{E_{2yy}}},$$

$$\gamma_3 = \sqrt{\frac{h^2 \Sigma_{r2} \Sigma_{t2} E_{2xx}}{E_{2xx} E_{2yy} - E_{2xy}^{\ 2}}}, \qquad (3\text{-}18)$$

$$\theta_1 = \frac{E_{2xy} + \sqrt{-E_{2xy}^{\ 2} + E_{2xx} E_{2yy}}}{E_{2xx}},$$

$$\theta_2 = \frac{E_{2xy} - \sqrt{-E_{2xy}^{\ 2} + E_{2xx} E_{2yy}}}{E_{2xx}}.$$

3.3.2.3. Weight functions

Typical weighted residuals methods for reactor core analysis use one of the following two choices of weight functions (Law 1986):

i. The first choice called "moments weighting" (Pal 1997) uses low-order expansion functions as weight functions.

ii. The second choice, known as "Galerkin weighting", uses higher-order expansion functions as weight functions.

The most accurate results have historically been obtained with moments weighting (Pal 1997). For each energy group seven conditions have been generated using weighting with the following functions:

$$
\begin{aligned}
&w_0(u,v)=1,\\
&w_1(u,v)=f_1(u),\\
&w_2(u,v)=f_1(v),\\
&w_3(u,v)=144f_1(u)f_1(v),\\
&w_4(u,v)=4f_2(u),\\
&w_5(u,v)=4f_2(v),\\
&w_6(u,v)=16f_2(u)f_2(v).
\end{aligned}
\tag{3-19}
$$

3.3.2.4. Equation residuals

Let

$$R_g(u,v)=\Phi_g^e(u,v)-\Phi_g(u,v) \tag{3-20}$$

be the residuals, where $\Phi_g^e(u,v)$ are the exact solutions of (2-35) and (2-36), and $\Phi_g(u,v)$ are the expansions (3-9) and (3-12). Accordingly,

$$R_1(u,v)=\Phi_1^e(u,v)-\sum_{m=0}^{4}\sum_{n=0}^{4}a_{mn}f_m(u)f_n(v) \tag{3-21}$$

and

$$R_2(u,v)=\Phi_2^e(u,v)-\sum_{m=0}^{4}\sum_{n=0}^{4}b_{mn}f_m(u)f_n(v)-\sum_{l=1}^{8}c_l g_l(u,v). \tag{3-22}$$

Substituting residuals (3-21) and (3-22) in equations (3-4) and (3-5), one obtains the equation residuals for the two neutron fluxes,

$$
\begin{aligned}
&-\frac{1}{h^2}\left(\frac{E_{1xx}}{\Sigma_1}\frac{\partial^2 R_1(u,v)}{\partial u^2}+\frac{E_{1xy}}{\Sigma_1}\frac{\partial^2 R_1(u,v)}{\partial u\partial v}+\frac{E_{1yx}}{\Sigma_1}\frac{\partial^2 R_1(u,v)}{\partial v\partial u}+\right.\\
&\left.+\frac{E_{1yy}}{\Sigma_1}\frac{\partial^2 R_1(u,v)}{\partial v^2}\right)+\Sigma_{r1}R_1(u,v)=\frac{1}{k}\left(\upsilon\Sigma_{f1}R_1(u,v)+\upsilon\Sigma_{f2}R_2(u,v)\right)
\end{aligned}
\tag{3-23}
$$

and

$$-\frac{1}{h^2}\left(\frac{E_{2xx}}{\Sigma_2}\frac{\partial^2 R_2(u,v)}{\partial u^2}+\frac{E_{2xy}}{\Sigma_2}\frac{\partial^2 R_2(u,v)}{\partial u\partial v}+\frac{E_{2yx}}{\Sigma_2}\frac{\partial^2 R_2(u,v)}{\partial v\partial u}+\right.$$
$$\left.+\frac{E_{2yy}}{\Sigma_2}\frac{\partial^2 R_2(u,v)}{\partial v^2}\right)+\Sigma_{r2}R_2(u,v)=\Sigma_{12}R_1(u,v). \tag{3-24}$$

Since $\Phi_1^e(u,v)$ and $\Phi_2^e(u,v)$ are exact solutions of (3-4) and (3-5) one can write the equation residuals in the following form:

$$-\frac{1}{h^2}\left(\frac{E_{1xx}}{\Sigma_1}\frac{\partial^2 \Phi_{1pol}(u,v)}{\partial u^2}+\frac{E_{1xy}}{\Sigma_1}\frac{\partial^2 \Phi_{1pol}(u,v)}{\partial u\partial v}+\frac{E_{1yx}}{\Sigma_1}\frac{\partial^2 \Phi_{1pol}(u,v)}{\partial v\partial u}+\right.$$
$$\left.+\frac{E_{1yy}}{\Sigma_1}\frac{\partial^2 \Phi_{1pol}(u,v)}{\partial v^2}\right)+\Sigma_{r1}\Phi_{1pol}(u,v)= \tag{3-25}$$
$$=\frac{1}{k}(\upsilon\Sigma_{f1}\Phi_{1pol}(u,v)+\upsilon\Sigma_{f2}(\Phi_{2pol}(u,v)+\Phi_{2hyp}(u,v)))$$

and

$$-\frac{1}{h^2}\left(\frac{E_{2xx}}{\Sigma_2}\frac{\partial^2 (\Phi_{2pol}(u,v)+\Phi_{2hyp}(u,v))}{\partial u^2}+\right.$$
$$+\frac{E_{2xy}}{\Sigma_2}\frac{\partial^2 (\Phi_{2pol}(u,v)+\Phi_{2hyp}(u,v))}{\partial u\partial v}+ \tag{3-26}$$
$$\left.\frac{E_{2yx}}{\Sigma_2}\frac{\partial^2 (\Phi_{2pol}(u,v)+\Phi_{2hyp}(u,v))}{\partial v\partial u}+\frac{E_{2yy}}{\Sigma_2}\frac{\partial^2 R_2(u,v)}{\partial v^2}\right)+$$
$$+\Sigma_{r2}(\Phi_{2pol}(u,v)+\Phi_{2hyp}(u,v))=\Sigma_{12}\Phi_{1pol}(u,v).$$

3.3.2.5. Weighted residuals of two group equations

Applying the weighted residuals method to equations (3-25) and (3-26) and assuming that all cross sections and Eddington tensor components are spatially constant leads to:

$$
\begin{aligned}
&-\frac{1}{h^2}\left(\frac{E_{1xx}}{\Sigma_1} < w_l(u,v), \frac{\partial^2 \Phi_{1pol}(u,v)}{\partial u^2} > + \right. \\
&+\frac{E_{1xy}}{\Sigma_1} < w_l(u,v), \frac{\partial^2 \Phi_{1pol}(u,v)}{\partial u \partial v} > + \\
&+\frac{E_{1yx}}{\Sigma_1} < w_l(u,v), \frac{\partial^2 \Phi_{1pol}(u,v)}{\partial v \partial u} > + \\
&\left.+\frac{E_{1yy}}{\Sigma_1} < w_l(u,v), \frac{\partial^2 \Phi_{1pol}(u,v)}{\partial v^2} >\right) + \\
&+\Sigma_{r1} < w_l(u,v), \Phi_{1pol}(u,v) >= \frac{1}{k}(\upsilon\Sigma_{f1} < w_l(u,v), \Phi_{1pol}(u,v) > + \\
&+\upsilon\Sigma_{f2} < w_l(u,v), (\Phi_{2pol}(u,v) + \Phi_{2hyp}(u,v)) >
\end{aligned}
\tag{3-27}
$$

and

$$
\begin{aligned}
&-\frac{1}{h^2}\left(\frac{E_{2xx}}{\Sigma_2} < w_l(u,v), \frac{\partial^2 (\Phi_{2pol}(u,v) + \Phi_{2hyp}(u,v))}{\partial u^2} > + \right. \\
&+\frac{E_{2xy}}{\Sigma_2} < w_l(u,v), \frac{\partial^2 (\Phi_{2pol}(u,v) + \Phi_{2hyp}(u,v))}{\partial u \partial v} > \\
&+\frac{E_{2yx}}{\Sigma_2} < w_l(u,v), \frac{\partial^2 (\Phi_{2pol}(u,v) + \Phi_{2hyp}(u,v))}{\partial v \partial u} > + \\
&\left.+\frac{E_{2yy}}{\Sigma_2} < w_l(u,v), \frac{\partial^2 (\Phi_{2pol}(u,v) + \Phi_{2hyp}(u,v))}{\partial v^2} >\right) + \\
&+\Sigma_{r2} < w_l(u,v), (\Phi_{2pol}(u,v) + \Phi_{2hyp}(u,v)) >= \\
&= \Sigma_{12} < w_l(u,v), \Phi_{1pol}(u,v) >,
\end{aligned}
\tag{3-28}
$$

where $w_l(u,v)$, l=0 to 6, are the weight functions (3-19). The "< >" notation is the one introduced by (3-8). After applying the WRM for each weight function to equations (3-27) and (3-28) fourteen equations will result (seven per energy group). These equations together with continuity conditions, boundary conditions, corner balance equations, and balance equations in the thermal group will form the system of linear equations to be solved for the unknown expansion coefficients a_{mn}, b_{mn}, and c_l from expansions (3-9), (3-13), and (3-14).

The zeroth-moment residual of the expansion of the fast flux, i.e. $< w_0(u,v), \Phi_{1pol}(u,v) >$ represents the node averaged fast flux

$$< w_0(u,v), \Phi_{1pol}(u,v) >= \int_{-\frac{1}{2}}^{+\frac{1}{2}} \int_{-\frac{1}{2}}^{+\frac{1}{2}} \Phi_{1pol}(u,v) du dv = \overline{\overline{\Phi_1}} = a_{00}. \qquad (3\text{-}29)$$

The zeroth-moment residual of the expansion of thermal flux, i.e. $< w_0(u,v), \Phi_{2pol}(u,v) + \Phi_{2hyp}(u,v) >$ has the same physical meaning but a more complicated form due to hyperbolic basis functions that appear in $\Phi_{2hyp}(u,v)$:

$$\begin{aligned} &< w_0(u,v), \Phi_{2pol}(u,v) + \Phi_{2hyp}(u,v) >= \\ &= \int_{-\frac{1}{2}}^{+\frac{1}{2}} \int_{-\frac{1}{2}}^{+\frac{1}{2}} \Phi_{2pol}(u,v) du dv + \int_{-\frac{1}{2}}^{+\frac{1}{2}} \int_{-\frac{1}{2}}^{+\frac{1}{2}} \Phi_{2hyp}(u,v) du dv = \\ &= \overline{\overline{\Phi_2}} = b_{00} + \frac{2}{\gamma_1} c_1 \sinh(\frac{\gamma_1}{2}) + \frac{2}{\gamma_2} c_3 \sinh(\frac{\gamma_2}{2}) + \\ &+ \frac{8}{\gamma_3^2 \theta_1} c_5 \sinh(\frac{\gamma_3}{2\sqrt{2}}) \sinh(\frac{\gamma_3 \theta_1}{2\sqrt{2}}) + \frac{8}{\gamma_3^2 \theta_2} c_7 \sinh(\frac{\gamma_3}{2\sqrt{2}}) \sinh(\frac{\gamma_3 \theta_2}{2\sqrt{2}}). \end{aligned} \qquad (3\text{-}30)$$

In the diffusion limit, $E_{gxx} = E_{gyy} = \frac{1}{3}$ and $E_{gxy} = E_{gyx} = 0$, (3-30) becomes:

$$\overline{\overline{\Phi_2}} = b_{00} + \frac{2}{\gamma}(c_1 + c_3) \sinh(\frac{\gamma}{2}) + \frac{8}{\gamma^2}(c_5 + c_7) \sinh^2(\frac{\gamma}{2\sqrt{2}}), \qquad (3\text{-}31)$$

where $\gamma = \sqrt{3h^2 \Sigma_{r2} \Sigma_{t2}}$. An expression similar to (3-31) is derived in (Pal 1997) in the diffusion limit.

3.3.2.6. Surface-averaged flux and current

Node surfaces have been denoted by $x\pm$ or $y\pm$, and they correspond to $u=\pm\frac{1}{2}$ or $v=\pm\frac{1}{2}$ as shown in Figure 3.2.

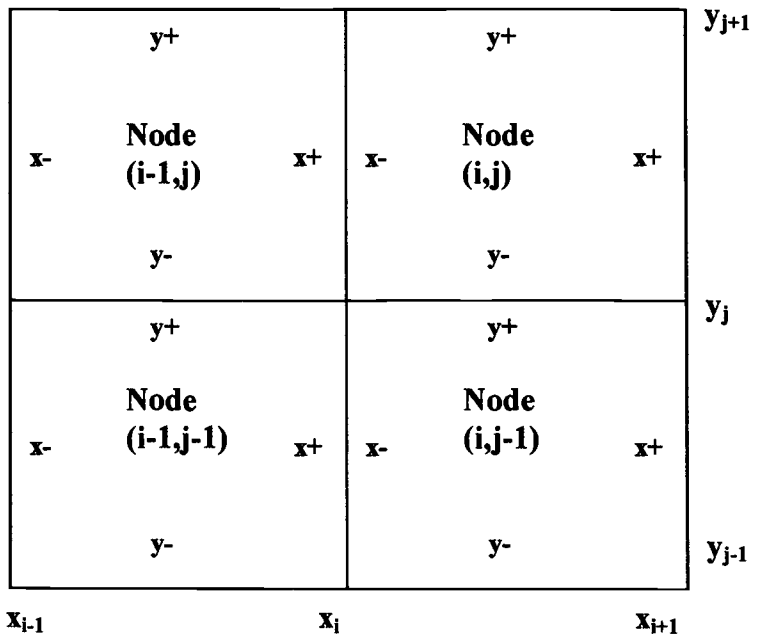

Figure 3.2. Notation of node surfaces

The surface-averaged fluxes on x+ and y+ surfaces of a node (i,j) are defined by:

$$\overline{\Phi^{ij}_{gx+}}=\frac{1}{h}\int_{y_j}^{y_{j+1}}\Phi_g(x_{i+1},y)dy=\int_{-\frac{1}{2}}^{+\frac{1}{2}}\Phi_g(\frac{1}{2},v)dv \qquad (3\text{-}32)$$

$$\overline{\Phi^{ij}_{gy+}}=\frac{1}{h}\int_{x_i}^{x_{i+1}}\Phi_g(x,y_{j+1})dx=\int_{-\frac{1}{2}}^{+\frac{1}{2}}\Phi_g(u,\frac{1}{2})du \qquad (3\text{-}33)$$

In a similar manner we define the surface-averaged flux on x- and y- surfaces of the node (i,j),

$$\overline{\Phi^{ij}_{gx-}} = \frac{1}{h}\int_{y_j}^{y_{j+1}} \Phi_g(x_i, y)dy = \int_{-\frac{1}{2}}^{+\frac{1}{2}} \Phi_g(-\frac{1}{2}, v)dv \tag{3-34}$$

and

$$\overline{\Phi^{ij}_{gy-}} = \frac{1}{h}\int_{x_i}^{x_{i+1}} \Phi_g(x, y_j)dx = \int_{-\frac{1}{2}}^{+\frac{1}{2}} \Phi_g(u, -\frac{1}{2})du. \tag{3-35}$$

Surface-averaged currents across the x+ and y+ surfaces have been defined using similar notations,

$$\begin{aligned}
\overline{J^{ij}_{gx+}} &= \frac{1}{h}\int_{y_i}^{y_{i+1}} J_{gx}(x_{i+1}, y)dy = \\
&= \frac{1}{h}\int_{y_i}^{y_{i+1}} -\frac{1}{\Sigma^{ij}_g}(E^{ij}_{gxx}\frac{\partial\Phi_g(x_{i+1}, y)}{\partial x} + E^{ij}_{gxy}\frac{\partial\Phi_g(x_{i+1}, y)}{\partial y})dy = \\
&= \int_{-\frac{1}{2}}^{+\frac{1}{2}} -\frac{1}{\Sigma^{ij}_g}(E^{ij}_{gxx}\frac{\partial\Phi_g(\frac{1}{2}, v)}{h\partial u} + E^{ij}_{gxy}\frac{\partial\Phi_g(\frac{1}{2}, v)}{h\partial v})dv = \\
&= -\frac{1}{h}\int_{-\frac{1}{2}}^{+\frac{1}{2}} \frac{1}{\Sigma^{ij}_g}(E^{ij}_{gxx}\frac{\partial\Phi_g(\frac{1}{2}, v)}{\partial u} + E^{ij}_{gxy}\frac{\partial\Phi_g(\frac{1}{2}, v)}{\partial v})dv.
\end{aligned} \tag{3-36}$$

Similarly one finds

$$\overline{J^{ij}_{gy+}} = -\frac{1}{h}\int_{-\frac{1}{2}}^{+\frac{1}{2}} \frac{1}{\Sigma^{ij}_g}(E^{ij}_{gyx}\frac{\partial\Phi_g(u, \frac{1}{2})}{\partial u} + E^{ij}_{gyy}\frac{\partial\Phi_g(u, \frac{1}{2})}{\partial v})du, \tag{3-37}$$

$$\overline{J^{ij}_{gx-}} = -\frac{1}{h}\int_{-\frac{1}{2}}^{+\frac{1}{2}} \frac{1}{\Sigma^{ij}_g}(E^{ij}_{gxx}\frac{\partial\Phi_g(-\frac{1}{2}, v)}{\partial u} + E^{ij}_{gxy}\frac{\partial\Phi_g(-\frac{1}{2}, v)}{\partial v})dv, \tag{3-38}$$

and

$$\overline{J^{ij}_{gy-}} = -\frac{1}{h}\int_{-\frac{1}{2}}^{+\frac{1}{2}} \frac{1}{\Sigma^{ij}_g}\left(E^{ij}_{gyx}\frac{\partial\Phi_g(u,-\frac{1}{2})}{\partial u} + E^{ij}_{gyy}\frac{\partial\Phi_g(u,-\frac{1}{2})}{\partial v}\right)du\,. \qquad (3\text{-}39)$$

In deriving equations (3-36) to (3-39) expressions (2-33) and (2-34) are used for x and y neutron current components calculated with constant cross-sections and Eddington tensor components.

3.3.2.7. Continuity equations for flux and current

Using these definitions, the continuity equations for the flux and current on the four surfaces of node (i, j) Figure 3.2 are (Pal 1997):

$$\overline{\Phi^{i-1,j}_{gx+}} = \overline{\Phi^{i,j}_{gx-}}\,, \qquad \text{g=1,2} \qquad (3\text{-}40)$$

$$\overline{\Phi^{i-1,j-1}_{gx+}} = \overline{\Phi^{i,j-1}_{gx-}}\,, \qquad \text{g=1,2} \qquad (3\text{-}41)$$

$$\overline{\Phi^{i-1,j-1}_{gy+}} = \overline{\Phi^{i-1,j}_{gy-}}\,, \qquad \text{g=1,2} \qquad (3\text{-}42)$$

$$\overline{\Phi^{i,j-1}_{gy+}} = \overline{\Phi^{i,j}_{gy-}}\,, \qquad \text{g=1,2} \qquad (3\text{-}43)$$

$$\overline{J^{i-1,j}_{gx+}} = \overline{J^{i,j}_{gx-}}\,, \qquad \text{g=1,2} \qquad (3\text{-}44)$$

$$\overline{J^{i-1,j-1}_{gx+}} = \overline{J^{i,j-1}_{gx-}}\,, \qquad \text{g=1,2} \qquad (3\text{-}45)$$

$$\overline{J^{i-1,j-1}_{gy+}} = \overline{J^{i-1,j}_{gy-}}\,, \qquad \text{g=1,2} \qquad (3\text{-}46)$$

and

$$\overline{J^{i,j-1}_{gy+}} = \overline{J^{i,j}_{gy-}}\,, \qquad \text{g=1,2.} \qquad (3\text{-}47)$$

Equations (3-40) to (3-47) provide another 16 equations for a_{mn}, b_{mn}, and c_l (the unknown expansion coefficients) after replacing in (3-32) to (3-39) the neutron fluxes with their series expansions (3-9) and (3-12) and performing the integrals.

3.3.2.8. Corner flux continuity conditions

Three independent equations can be obtained for each neutron energy group by applying corner flux continuity conditions. If we consider corner (x_i, y_j) in Figure 3.2, these are:

$$\Phi_g^{i,j}(x_i, y_j) = \Phi_g^{i-1,j}(x_i, y_j), \quad \text{g=1,2} \tag{3-48}$$

$$\Phi_g^{i-1,j}(x_i, y_j) = \Phi_g^{i-1,j-1}(x_i, y_j), \quad \text{g=1,2} \tag{3-49}$$

and

$$\Phi_g^{i-1,j-1}(x_i, y_j) = \Phi_g^{i,j-1}(x_i, y_j), \quad \text{g=1,2.} \tag{3-50}$$

The fourth flux corner continuity condition added to (3-48) through (3-50) leads to a system of linear equations non-independent. A fourth independent condition at the corner point will consist of a "corner balance condition" (Pal 1997) that will be described in the next section. Conditions (3-48) to (3-50) bring for each node of the problem, six new equations (three per energy group) to the linear system of equations.

3.3.2.9. Corner balance condition

The corner balance condition is derived by drawing a square box of width 2δ centered on a corner point (x_i, y_j) (Pal 1997), as shown in Figure 3.3.

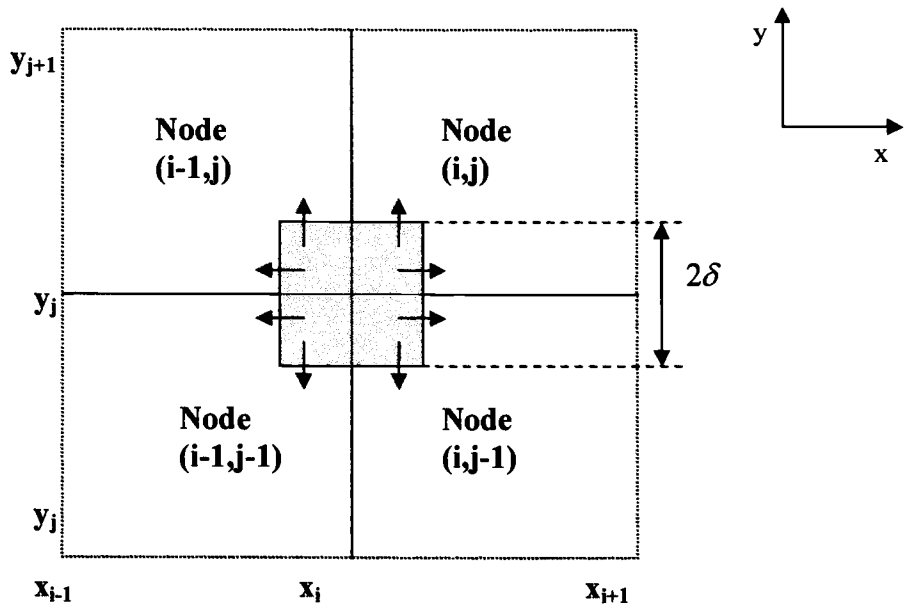

Figure 3.3. 2δ - square box centered around (x_i, y_j) corner, to illustrate the corner balance condition

By reducing the size δ of the imaginary box to zero (box volume approaching zero), no absorptions will occur inside the box (Pal 1997), i.e. there will be no net neutron leakage from the box. The leakage of neutrons of group g from corner (x_i, y_j) is given by (Pal 1997).

$$L_g^{ij} = \frac{1}{\delta}\left(\int_{x_i}^{x_i+\delta} J_{gy}^{ij}(x_i, y_i+\delta)dx + \int_{y_i}^{y_i+\delta} J_{gx}^{ij}(x_i+\delta, y_i)dy\right) \qquad (3\text{-}51)$$

Using the Taylor series expansion for J_{gx}^{ij} and J_{gy}^{ij}, about (x_i, y_j), equation (3-51) takes the form:

$$L_g^{ij} \simeq J_{gy}^{ij}(x_i, y_i) + \delta \left.\frac{\partial J_{gy}^{ij}}{\partial y}\right|_{(x_i, y_j)} + J_{gx}^{ij}(x_i, y_i) + \delta \left.\frac{\partial J_{gx}^{ij}}{\partial x}\right|_{(x_i, y_j)} \qquad (3\text{-}52)$$

At the limit $\delta \to 0$, L_g^{ij} becomes

$$L_g^{ij} = J_{gy}^{ij}(x_i, y_i) + J_{gx}^{ij}(x_i, y_i) \qquad (3\text{-}53)$$

Analogous to (2-88) leakages from corner (i, j) into nodes (i-1, j-1), (i-1, j) are given by:

$$L_g^{i-1,j} = -J_{gx}^{i-1,j}(x_i, y_j) + J_{gy}^{i-1,j}(x_i, y_j) \tag{3-54}$$

$$L_g^{i-1,j-1} = -J_{gx}^{i-1,j-1}(x_i, y_j) - J_{gy}^{i-1,j-1}(x_i, y_j) \tag{3-55}$$

$$L_g^{i,j-1} = J_{gx}^{i,j-1}(x_i, y_j) - J_{gy}^{i,j-1}(x_i, y_j) \tag{3-56}$$

So, as $\delta \to 0$, the corner balance equation becomes (Pal 1997):

$$L_g^{i,j} + L_g^{i-1,j-1} + L_g^{i-1,j} + L_g^{i,j-1} = 0 \tag{3-57}$$

or, in terms of neutron current components,

$$\begin{aligned} &J_{gy}^{i,j}(x_i, y_j) + J_{gx}^{i,j}(x_i, y_j) - J_{gy}^{i-1,j-1}(x_i, y_j) - J_{gx}^{i-1,j-1}(x_i, y_j) + \\ &J_{gy}^{i-1,j}(x_i, y_j) - J_{gx}^{i-1,j}(x_i, y_j) - J_{gy}^{i,j-1}(x_i, y_j) + \\ &+ J_{gx}^{i,j-1}(x_i, y_j) = 0, \quad \text{g=1,2.} \end{aligned} \tag{3-58}$$

For each node of the problem, one can write two equations analogous to (3-58) (one per neutron energy group).

3.3.2.10. Zero-flux boundary surface conditions

For each node and each neutron group, four surface conditions for flux and current and four corner conditions are needed. For interior nodes, these requirements are satisfied by applying equations (3-40) to (3-47). For interior corners, equations (3-48) to (3-58) served this purpose. For exterior nodes, conditions applied to the node depend on the boundary conditions applied to the problem. Zero surface-averaged fluxes are simply imposed. For the simple four-node problem shown in Figure 3.2, zero-flux boundary conditions are described by the following equations:

$$\Phi_{gx-}^{i-1,j-1} = 0\,, \quad \text{g=1,2,} \tag{3-59}$$

$$\Phi_{gx-}^{i-1,j} = 0 , \quad g=1,2, \tag{3-60}$$

$$\Phi_{gy+}^{i-1,j} = 0 , \quad g=1,2, \tag{3-61}$$

$$\Phi_{gx+}^{i,j} = 0 , \quad g=1,2, \tag{3-62}$$

$$\Phi_{gy+}^{i,j} = 0 , \quad g=1,2, \tag{3-63}$$

$$\Phi_{gx+}^{i,j-1} = 0 , \quad g=1,2, \tag{3-64}$$

$$\Phi_{gy-}^{i,j-1} = 0 , \quad g=1,2 \tag{3-65}$$

and

$$\Phi_{gy-}^{i-1,j-1} = 0 , \quad g=1,2. \tag{3-66}$$

3.3.2.11. Zero-flux boundary corner conditions

Zero-flux corner boundary conditions simply require that the neutron flux in the nodes located on the boundaries of the problem is zero. Referring once again to Figure 3.2,

$$\Phi_g(x_{i-1}, y_{j-1}) = 0 , \quad g=1,2, \tag{3-67}$$

$$\Phi_g(x_{i-1}, y_j) = 0 , \quad g=1,2, \tag{3-68}$$

$$\Phi_g(x_{i-1}, y_{j+1}) = 0 , \quad g=1,2, \tag{3-69}$$

$$\Phi_g(x_i, y_{j+1}) = 0 , \quad g=1,2, \tag{3-70}$$

$$\Phi_g(x_{i+1}, y_{j+1}) = 0 , \quad g=1,2, \tag{3-71}$$

$$\Phi_g(x_{i+1}, y_j) = 0 , \quad g=1,2, \tag{3-72}$$

$$\Phi_g(x_{i+1}, y_{j-1}) = 0 , \quad g=1,2 \tag{3-73}$$

and

$$\Phi_g(x_i, y_{j-1}) = 0 , \quad g=1,2. \tag{3-74}$$

3.3.2.12. Zero-current boundary surface conditions

Zero-current boundary surface conditions are mathematically described by zero surface-averaged currents at the exterior surfaces as shown in Figure 3.2,

$$J_{gx-}^{i-1,j-1} = 0\,, \quad \text{g=1,2,} \tag{3-75}$$

$$J_{gx-}^{i-1,j} = 0\,, \quad \text{g=1,2,} \tag{3-76}$$

$$J_{gy+}^{i-1,j} = 0\,, \quad \text{g=1,2,} \tag{3-77}$$

$$J_{gy+}^{i,j} = 0\,, \quad \text{g=1,2,} \tag{3-78}$$

$$J_{gx+}^{i,j} = 0\,, \quad \text{g=1,2,} \tag{3-79}$$

$$J_{gx+}^{i,j-1} = 0\,, \quad \text{g=1,2,} \tag{3-80}$$

$$J_{gy-}^{i,j-1} = 0\,, \quad \text{g=1,2} \tag{3-81}$$

and

$$J_{gy-}^{i-1,j-1} = 0\,, \quad \text{g=1,2.} \tag{3-82}$$

3.3.2.13. Zero-current boundary corner conditions

Zero-current boundary conditions derive from the corner balance equation in each group, equation (3-58). For boundary corners shared by two exterior nodes, such as the (x_{i+1}, y_j) corner from Figure 3.2, we have:

$$\begin{aligned} &-J_{gx}^{i,j}(x_{i+1}, y_j) + J_{gy}^{i,j}(x_{i+1}, y_j) - J_{gy}^{i,j-1}(x_{i+1}, y_j) - \\ &-J_{gx}^{i,j-1}(x_{i+1}, y_j) = 0, \quad \text{g=1,2} \end{aligned} \tag{3-83}$$

and

$$\Phi_g^{i,j-1}(x_{i+1}, y_j) = \Phi_g^{i,j}(x_{i+1}, y_i)\,, \quad \text{g=1,2.} \tag{3-84}$$

Each of the two nodes sharing the (x_{i+1}, y_j) corner accounts for one of equations (3-82) and (3-84). For external boundary corners that belong to only one node (i.e. corner (x_{i+1}, y_{j+1}) from Figure 3.2, equation (3-58) gives:

$$-J_{gy}^{i,j}(x_{i+1}, y_{i+1}) - J_{gx}^{i,j}(x_{i+1}, y_{j+1}) = 0\,, \qquad \text{g=1,2.} \tag{3-85}$$

3.3.2.14. Thermal flux balance equation

As shown in previous sections, for each node and each energy group one can write seven weighted residual moment equations, four surface-averaged continuity equations, and four corner balance equations. This yields 15 equations per neutron energy group and per node (thirty equations per node). In fact, according to (3-9), (3-13) and (3-14), 42 unknown expansion coefficients must be determined for each node. Expressing for each node the thermal flux polynomial expansion coefficients b_{mn} in terms of fast flux polynomial expansion coefficients a_{mn} (Pal 1997) yields a system of equations for 23 unknowns (15 fast polynomial coefficients and eight thermal hyperbolic coefficients).

By substituting expansions (3-9) and (3-12) into the thermal group balance equation (2-36) and taking into account that basis expansion functions (3-18) are exact (analytic) solutions of (3-16), equation (2-36) is reduced to:

$$-\left(\frac{E_{2xx}^{i,j}}{\Sigma_2^{i,j}}\frac{\partial^2\Phi_{2pol}^{i,j}}{\partial x^2} + 2\frac{E_{2xy}^{i,j}}{\Sigma_2}\frac{\partial^2\Phi_{2pol}^{i,j}(x,y)}{\partial x\partial y} + \frac{\Sigma_{2yy}^{i,j}}{\Sigma_2^{i,j}}\frac{\partial^2\Phi_{2pol}^{i,j}(x,y)}{\partial y^2}\right) + \\ +\Sigma_{r2}^{i,j}\Phi_2^{i,j}(x,y) = \Sigma_{12}^{i,j}\Phi_{1pol}^{i,j} \tag{3-86}$$

This is an equation that involves only polynomial terms. Since (3-86) is composed entirely of polynomials, the 19 thermal polynomial expansion coefficients can be found in terms of 15 fast flux expansion coefficients such that (3-86) is true in every point of the node (i, j). By finding the thermal polynomial expansion

coefficients in terms of the fast polynomial expansion coefficients 23 equations per node for the 15 coefficients a_{mn} and 8 coefficients c_l are solved. The rest of the 19 coefficients b_{mn} are determined by simply calculating them using the relations provided by (3-86).

To summarize, in order to solve the Quasi-Diffusion Low Order Equations by the WRM, for each node of the problem 23 equations for 23 coefficients are needed:

- 7 weighted residual moments in the fast group
- 4 surface-averaged continuity conditions in the fast group
- 4 surface-averaged continuity conditions in the thermal group
- 4 corner conditions in the fast group
- 4 corner conditions in the thermal group

However, the expressions of coefficients b_{mn} in terms of a_{mn} coefficients are more complicated in the case of quasi-diffusion than the expressions derived in (Pal 1997) because of the more complicated form of the quasi-diffusion low order equations in which all of the Eddington tensor's components can be non-zero.

3.4. POWER ITERATION TECHNIQUE

The equivalent matrix formulation of a 2-D, (m x n) node problem is

$$\mathbf{M}v = \frac{1}{k}\mathbf{F}v, \tag{3-87}$$

where

- $\mathbf{M}$ is the $(23 \times m \times n)^2$ element square matrix of the source free system of linear equations in expansion coefficients;
- $\mathbf{F}$ is the $(23 \times m \times n)^2$ element square matrix of fission sources;
- v is the $(23 \times m \times n)$ column vector of the expansion coefficients.

Multiplying (3-87) with the inverse of matrix $\mathbf{M}$ and rearranging yields

$$\mathbf{A}v = kv, \tag{3-88}$$

where $\mathbf{A} = \mathbf{M}^{-1}\mathbf{F}$.

Equation (3-88) is the standard form of an eigenvector-eigenvalue problem. It is demonstrated that if one is interested in finding the eigenvalue of the square matrix $\mathbf{A}$ with the greatest absolute value, the numeric procedure recommended is "power iteration".

Starting with a column vector $v^{(1)}$ almost arbitrarily chosen (Rad 1992), after a number of iterations n the vector

$$u^{(n+1)} = \frac{\mathbf{A}v^{(n)}}{\left|\mathbf{A}v^{(n)}\right|}, \quad n \geq 1 \tag{3-89}$$

can be used in (3-89) to approximate the eigenvalue k with the greatest absolute value:

$$k^{(n)} = u_T^{(n)}\mathbf{A}u^{(n)}, \tag{3-90}$$

where $u_T^{(n)}$ is a row vector, the transpose of vector $u^{(n)}$.

3.5 SUMMARY

Chapter 3 presents the discretization of the QDLO, the non-separable function expansion of fast and thermal neutron fluxes, the steps of solving the QDLO by the use of WRM, and briefly the power iteration scheme used to calculate k-eigenvalue.

4. RESULTS AND DISCUSSIONS

4.1. INTRODUCTION

In this chapter the nodal quasi-diffusion low-order (QDLO) equations are solved for several diffusion test problems (diagonal Eddington tensor with diagonal entries equal to 1/3), and "transport" problems (Eddington tensor with diagonal entries different from one-third and zero or positive off-diagonal components). In the transport problems, the Eddington functionals are chosen to be within the range of values representative of two-node UO_2-MOX fuel assembly transport calculations.

The QD method was originally developed as a rapidly-convergent iterative technique for solving transport equations. In this method, the scattering source used in a given transport sweep is obtained from the solution of the QDLO equations, using Eddington functionals (2-18) calculated with the angular fluxes from the previous transport sweep. In applying the QD transport methodology to reactor physics problems, we are assuming that the detailed space, energy, and angle dependence of the angular flux is calculated from single assembly transport calculations (i.e. CASMO). This data, including Eddington tensors, is then homogenized and functionalized for use with the nodal QDLO equations solved for the homogenized scalar flux in the core. For our purposes, the data used in the QLDO equations is assumed known; however, its preparation is also an area of ongoing research.

Our goal in solving the diffusion problems is to illustrate that, for fuel assemblies characterized by "diffusive" data ($E_{xx} = E_{yy} = 1/3,\ E_{xy} = E_{yx} = 0$), the QDLO nodal discretization limits to the nodal diffusion discretization derived by Palmtag (Pal 1997). Palmtag's discretization has been shown to be extremely

accurate for mixed UO_2-MOX cores. We consider a sequence of one-node problems (from the EPRI-9 benchmark specification) with a variety of boundary conditions, a sequence of two-node UO_2-MOX problems from (Pal 1997) and several multi-node problems that demonstrate our ability to model general reactor systems. The transport problems are included to show the effect of representative "non-diffusive" Eddington tensors on homogeneous flux distribution and multiplication factor.

4.2. ONE-NODE, 2-D DIFFUSION PROBLEMS

4.2.1. EPRI-9 assembly calculations results

In this section, three single-assembly benchmark problems are solved with the nodal discretization of the QDLO equations. The data for these assemblies come from the EPRI-9 benchmark problem. The configuration for EPRI-9 problem consists of eight fueled standard 15 x 15 fuel pin PWR assemblies of different enrichments (F1 and F2), and F2-R (a rodded version of F2) (Pal 1997). We use one node per assembly with zero-current boundary conditions to calculate the multiplication factor k_{inf} and the ratio between the node-averaged thermal and fast fluxes, $\bar{\Phi}_2 / \bar{\Phi}_1$.

The multiplication factor k_{inf} obtained from diffusion Eddington functionals is compared with k'_{inf} provided by (Pal 1997). Homogenized cross sections are obtained from single assembly calculations as given in Table 4.1 (Pal 1997). The convergence tolerance for flux and k was set $\leq 10^{-6}$.

Table 4.1. EPRI-9 assembly cross sections

Property	Assembly type		
	F1	F2	F2-R
k_{inf}	1.006603	0.959145	0.656523
Σ_{t1}	0.220260	0.220261	0.227900
Σ_{t2}	0.843809	0.843549	0.874090
Σ_{a1}	0.012099	0.009325	0.015144
Σ_{a2}	0.168560	0.141419	0.183746
Σ_{21}	0.021126	0.021125	0.018810
$\upsilon\Sigma_{f1}$	0.006012	0.004625	0.004633
$\upsilon\Sigma_{f2}$	0.218881	0.164554	0.172501

The results and the relative errors are shown in Table 4.2. The ratio $\bar{\Phi}_2/\bar{\Phi}_1$ is compared with $\left(\bar{\Phi}_2/\bar{\Phi}_1\right)^a = \frac{\Sigma_{12}}{\Sigma_{r1}}$, i.e. the expected ratio according to analytic solution of the diffusion equation in an infinite medium. The other quantities are defined as follows:

$$- \quad k_{\text{inf}}^a = \frac{\upsilon\Sigma_{f1}}{\Sigma_{r1}} + \frac{\upsilon\Sigma_{f2}}{\Sigma_{r2}}\frac{\Sigma_{12}}{\Sigma_{r1}}, \tag{4-1}$$

$$- \quad \varepsilon_1 = \left|\frac{k_{\text{inf}} - k'_{\text{inf}}}{k'_{\text{inf}}}\right|, \tag{4-2}$$

$$- \quad \varepsilon_1 = \left|\frac{k_{\text{inf}} - k_{\text{inf}}^a}{k_{\text{inf}}^a}\right|, \tag{4-3}$$

$$- \quad \varepsilon_3 = \left|\frac{(\bar{\Phi}_2/\bar{\Phi}_1) - (\bar{\Phi}_2/\bar{\Phi}_1)^a}{(\bar{\Phi}_2/\bar{\Phi}_1)^a}\right| \tag{4-4}$$

and

- N= the number of iterations required to reach a convergence tolerance $\leq 10^{-6}$.

Table 4.2. EPRI-9 assembly calculation results

Property	F1	F2	F2-R
k_{inf}	1.00662	0.959142	0.656531
N	12	11	13
k'_{inf} (Pal 1997)	1.00660	0.959145	0.656523
k^{a}_{inf}	1.00662	0.959142	0.656531
ε_1 (%)	$2.5\text{x}10^{-2}$	$5.2\text{x}10^{-4}$	$1.2\text{x}10^{-3}$
ε_2 (%)	0.0	0.0	0.0
$\bar{\Phi}_2 / \bar{\Phi}_1$	0.125332	0.149379	0.102370
$\left(\bar{\Phi}_2 / \bar{\Phi}_1\right)^a$	0.125332	0.149379	0.102370
ε_3 (%)	0.0	0.0	0.0

From Table 4.2 one can see very good agreement between QD code calculations, the results presented in (Pal 1997) and the analytic solutions.

4.2.2. Geometric buckling comparisons

In this sequence of problems, QDLO calculations of geometric buckling for a node with zero-flux or zero-current boundary conditions are compared to analytic predictions. The buckling, B^2, is given by

$$B^2 = \frac{1}{2}(-\alpha + \sqrt{\alpha^2 - 4\beta}), \tag{4-5}$$

where

$$\alpha = 3\left(\Sigma_{r1}\Sigma_{t1} + \Sigma_{r2}\Sigma_{t2} - \frac{1}{k}\upsilon\Sigma_{f1}\Sigma_{t1} \right) \tag{4-6}$$

and

$$\beta = -9\Sigma_{t1}\Sigma_{t2}\left[-\Sigma_{r1}\Sigma_{r2} + \frac{1}{k}(\upsilon\Sigma_{f1}\Sigma_{r2} + \upsilon\Sigma_{f2}\Sigma_{12}) \right]. \tag{4-7}$$

The eigenvalue associated with the fundamental eigenfunction of the Helmholtz equation (Dud 1976) is, for this geometry,

$$B^2 = 2\left(\frac{\pi}{a}\right)^2, \tag{4-8}$$

where a is the dimension of the square node.

Table 4.3 shows in columns 1 through 6 the number of nodes in which an initial (42 x 42) cm^2 assembly is divided, the width h of each of these nodes, the number of iterations (N) required to reach a convergence tolerance $\leq 10^{-6}$, multiplication factor k for zero-flux boundary conditions, and k_{inf}, respectively. Errors shown in columns 7 and 8 take as reference values the 64-node k and 16-node k_{inf}.

Table 4.3. Zero-flux k, zero-current k_{inf} multiplication factors for various node width h

Number of nodes	**h(cm)**	**N**	**k**	**N**	**k_{inf}**	**ε (%)**	**ε_{inf} (%)**
1	2	3	4	5	6	7	8
1	42.0	15	0.771166	35	1.164924	0.38	0.052
4	21.0	19	0.765551	52	1.164925	0.35	0.0
16	10.5	16	0.768218	50	1.164925	0.007	*
64	5.25	17	0.768273	45	1.164925	*	*

The analytic $k_{\inf}$ for zero-current boundary conditions is obtained according to (Dud 1976)

$$k_{\inf} = k_{1\inf} + k_{2\inf} p \tag{4-9}$$

where

$$k_{g\inf} = \frac{\upsilon\Sigma_{fg}}{\Sigma_{rg}}, \quad g=1,2 \tag{4-10}$$

$$p = \frac{\Sigma_{12}}{\Sigma_{r1}} \tag{4-11}$$

According to equations (4-13) – (4-15) the multiplication factor of zero-current boundary conditions problem is $k_{\inf}$=1.16493.

The cross sections used in these calculations correspond to a 5% enriched UO_2 fuel assembly, and are presented in Table 4.4 (Pal 1997). Substituting these cross sections into (4-9) yields $B^2 = 1.11902x10^{-2}$ cm^{-2}. Equation (4-12) gives for a=42.0 cm $B^2 = 1.11900x10^{-2}$ cm^{-2}, very close to the result obtained with (4-9).

Table 4.4. Two-group single assembly cross sections

Property	Assembly type					
	UO_2 3%	**UO_2 4%**	**UO_2 5%**	**MOX 4%**	**MOX 8%**	**MOX 12%**
Σ_{t1}	0.286867	0.286714	0.204091	0.286466	0.285875	0.285233
Σ_{t2}	0.97970	0.980551	0.987944	1.07985	1.16774	1.23263
Σ_{12}	0.016756	0.016229	0.015738	0.013630	0.011853	0.010644
Σ_{a1}	0.009530	0.010234	0.010895	0.012956	0.015327	0.017049
Σ_{a2}	0.082606	0.098603	0.113317	0.197823	0.290164	0.350338
$\upsilon\Sigma_{f1}$	0.006758	0.008092	0.009357	0.008436	0.012259	0.015427
$\upsilon\Sigma_{f2}$	0.129545	0.163555	0.194709	0.321278	0.483443	0.587795
$k_{\inf}$	1.256776	1.323053	1.366686	1.149925	1.177585	1.201939

4.2.3. Power iteration convergence rates

The rate of convergence of the power iteration method is illustrated by a one-node, zero-current test problem in which the width a of the node is increased repeatedly by a factor of two from h to $32h$ (h=42.0 cm). The number of iterations (N) required to reach a convergence tolerance $\leq 10^{-6}$ for k and flux strongly increases with a, while k and $\bar{\Phi}_2 / \bar{\Phi}_1$ remain the same, as shown in Table 4.5.

Table 4.5. Convergence rate results for one node, zero-current problem

Node width (a)	k	$\bar{\Phi}_2 / \bar{\Phi}_1$	**N**
h	1.00635	0.125332	12
$2h$	1.00635	0.125332	33
$4h$	1.00635	0.125332	112
$8h$	1.00635	0.125332	394
$16h$	1.00635	0.125332	1402
$32h$	1.00635	0.125332	4943

Plotted on log-log scale, N versus node width a is approximately a straight line, as shown in Figure 4.1.

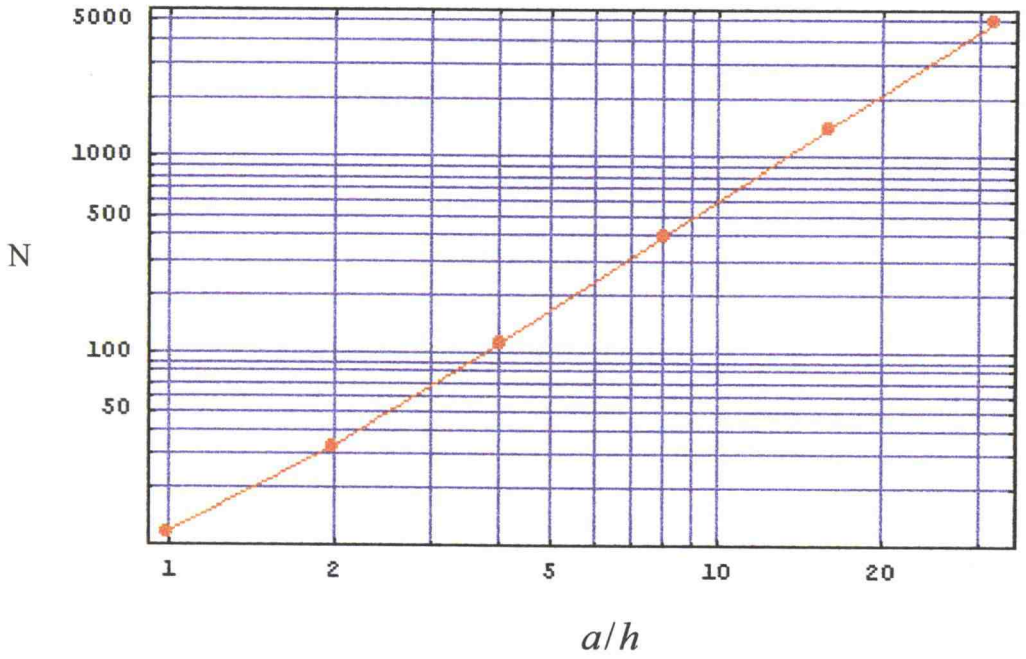

Figure 4.1. Number of iterations plotted versus node width on a log-log scale

4.3. TWO-NODE UO_2-MOX PROBLEMS

This problem assumes two adjacent nodes: a UO_2-fueled assembly, next to a MOX-fueled assembly (Pal 1997). The reasons for considering this configuration is that UO_2 and MOX have different properties, so UO_2 and MOX systems are excellent for investigating the behavior of neutron fluxes at the surface between assemblies of unlike properties. Zero current boundary conditions are applied to the boundaries of the configurations, as shown in Figure 4.2.

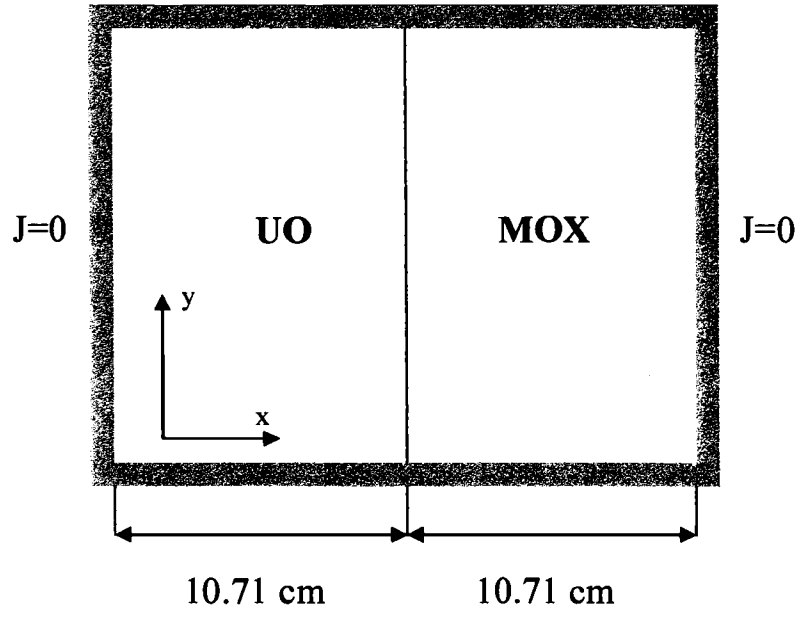

Figure 4.2. UO_2-MOX configuration

Various configurations are obtained by using UO_2 and MOX fuels of various enrichments in ^{235}U and Pu, respectively.

Table 4.6 shows the multiplication factor, the number of iterations required to reach a convergence tolerance $\leq 10^{-6}$, UO_2 assembly power and their relative errors from QDLO calculations using the two-group, single assembly cross sections from Table 4.4 (Pal 1997). Columns 5 and 6 show the relative errors from the advanced nodal diffusion methodology calculations presented in (Pal 1997). Both of these sets of computations are compared to CASMO-4 14-group results (Pal 1997) which are reproduced here in columns 8 and 9. In Table 4.6 U_x and M_y stand for x %-enriched UO_2 and y %-enriched MOX.

Table 4.6. Two-node UO_2-MOX assembly, multiplication factor and power calculations

Config.	k	N	Relative error k (%)	UO_2 assembly power	Relative error (%) UO_2
0	1	2	3	4	5
U_3/U_4	1.29121	18	6.2×10^{-3}	0.93167	0.74
U_4/U_5	1.34542	18	2.2×10^{-3}	0.93569	2.3
U_3/U_5	1.31531	18	8.4×10^{-3}	0.88585	1.2
U_3/M_8	1.20273	20	1.2	0.94333	1.2
U_3/M_{12}	1.20885	21	1.6	0.90974	1.2
U_4/M_8	1.23828	20	0.8	1.01375	2.0
U_4/M_{12}	1.24387	21	1.2	0.98002	2.0
U_5/M_8	1.26385	20	0.52	1.06130	2.3
U_5/M_{12}	1.37004	20	7.0	1.06350	5.9

Table 4.6. Two-node UO_2-MOX assembly, multiplication factor and power calculations (continued)

Config.	Relative error of k (%) , ref. (Pal 1997)	Relative error of UO_2 power (%) ref. (Pal 1997)	Reference k	Reference UO_2 power
0	6	7	8	9
U_3/U_4	2.4×10^{-2}	0.69	1.29113	0.9386
U_4/U_5	1.0×10^{-2}	0.43	1.34545	0.9580
U_3/U_5	6.3×10^{-2}	1.11	1.31520	0.8969
U_3/M_8	0.239	0.87	1.21721	0.9312
U_3/M_{12}	0.306	0.69	1.22896	0.8986
U_4/M_8	0.346	1.64	1.24830	0.994
U_4/M_{12}	0.405	1.47	1.25888	0.9611
U_5/M_8	0.435	2.12	1.27035	1.0372
U_5/M_{12}	0.487	1.96	1.28014	1.0042

Typical fast and thermal neutron flux shapes for the UO_2 (3%)-MOX (12%) configurations of assemblies are presented in Figure 4.3 and Figure 4.4,

respectively. In both figures, the UO_2 fuel assembly is the closest to the viewer. Fast flux is higher in the MOX assembly, due to its higher fission cross-sections. The steepest variation is observed near the surface between the two assemblies, and a smooth flux shape by the reflecting boundaries.

Thermal flux varies strongly at the surface between nodes mainly due to Σ_{a2} higher in UO_2 assembly than in MOX assembly.

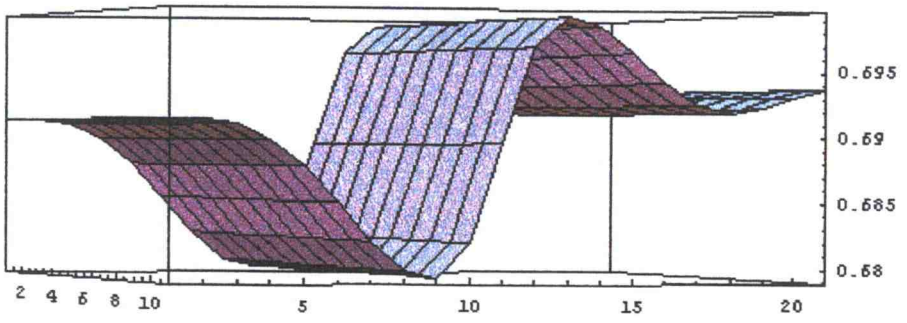

Figure 4.3. Fast neutron flux in UO_2 (3%)-MOX (12%) configuration

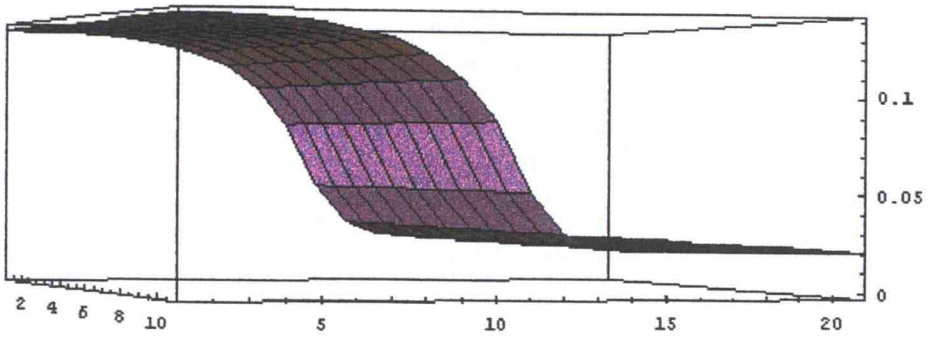

Figure 4.4. Thermal neutron flux in UO_2 (3%)-MOX (12%) configuration

The results show that the smallest errors occur for the case of two UO_2 assemblies. Better results are obtained if, instead of two-group single-assembly cross-sections, 14-group cross-sections are collapsed to two-group with the actual spectrum (Pal 1997).

4.4. MULTIPLE-NODE UO_2-MOX PROBLEMS. DISCONTINUITY FACTORS

In this set of problems, the k-eigenvalues and power distributions are calculated for configurations of UO_2 (UX), MOX (PX), and water (R) (Figure 4.5).

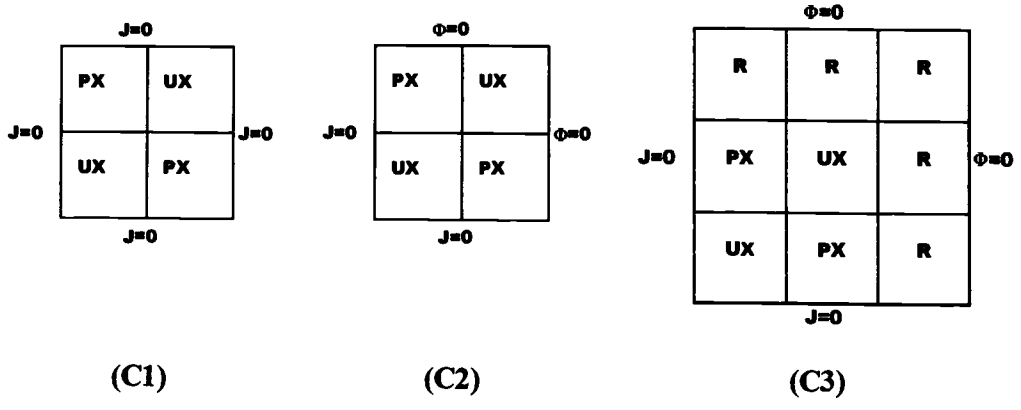

Figure 4.5. UO_2-MOX (C1, C2) and UO_2-MOX-water (C3) configurations

Cross-section data for these problems came from single assembly NEACRP benchmark calculations (zero-current boundary conditions) (Pal 1997), and are presented in Table 4.7. Results from QDLO calculations of these problems are shown in Table 4.8, columns 2 through 4. The relative errors, columns 5 through 7, are calculated with respect to reference eigenvalues and normalized assembly

powers presented in Table 4.9 (Pal 1997). Column 1 of Table 4.8 shows the number of iterations after which a 10^{-6} convergence tolerance for flux and k is reached. The reference solution for each configuration is a 2-D, 2-group, heterogeneous static diffusion calculation performed using one node per fuel pin (Pal 1997).

Compared to STENCIL results presented in (Pal 1997) the QDLO results from Table 4.8 are less accurate in reproducing the reference values, Table 4.9. Reference (Pal 1997) shows also the results produced by other methods (CONQUEST, SIMULATE-3, and PANTHER). QDLO yields results comparable to these for assembly powers, still producing less accurate results for the k-eigenvalues.

Table 4.7. Assembly homogenization results for NEACRP benchmark

Homogenized parameter	**Assembly type**	
	UX	**PX**
k_{inf}	0.998181	1.026669
Σ_{t1}	0.277778	0.277778
Σ_{t2}	0.833333	0.833333
Σ_{a1}	0.009226	0.013791
Σ_{a2}	0.092663	0.231691
$\upsilon\Sigma_{f1}$	0.004570	0.006852
$\upsilon\Sigma_{f2}$	0.113537	0.344583
Σ_{21}	0.020430	0.015864
DF_1	1.004803	0.994570
DC_1	1.006895	0.991336
DF_2	0.951007	1.041629
DC_2	0.930603	1.046322

UX=UO_2; PX=MOX

Table 4.8. NEACRP benchmark, homogenized node calculations

Config.	N	k	Assembly Power		Error (%)		
			UX	PX	k	UX	PX
0	1	2	3	4	5	6	7
C_1	60	1.01974	0.87346	1.1265	5.6×10^{-2}	0.14	0.11
C_2	40	0.91245	1.02145	0.97855	0.62	0.69	0.66
C_3	48	0.940336	0.90558	1.09442	0.24	1.2	1.0

Table 4.9. NEACRP benchmark, homogenized node calculations, reference values

Config.	Reference values (Pal 1997)		
	k	UX	PX
0	7	8	9
C_1	1.01914	0.8747	1.1253
C_2	0.90685	1.0282	0.9718
C_3	0.93806	0.9165	1.0835

A more accurate procedure is based on the Adjusted Current Model (ACM) (Pal 1997). This method defines separate diffusion coefficients for each surface of a node. Surface diffusion coefficients are used everywhere within the nodal diffusion equations: corner balance equations, current, definition of hyperbolic expansion functions for thermal neutron flux. Since diffusion coefficients are used to define hyperbolic expansion functions that are analytic solutions of the source-free thermal balance equation, a single diffusion coefficient is required for each node. This means that ACM can be used only for symmetric nodes (Pal 1997). Table 4.7 (Pal 1997) lists face-discontinuity (DF_g, g=1, 2) and corner-discontinuity (DC_g, g=1, 2) factors calculated using one node per pin and zero-current conditions. In the present work we have used the discontinuity factors to adjust Eddington functionals to be used in the QD code. The weighted moment equations and the surface-averaged flux and current continuity equations are derived with face-discontinuity

factors. Corner balance equations and corner continuity equations are derived with functionals adjusted with corner-discontinuity factors. The use of discontinuity factors from (Pal 1997) is possible because this problem is a diffusion one (the Eddington tensor diagonal components are equal to 1/3 and the off-diagonal components are equal to zero) and the discontinuity factors (Pal 1997) are calculated under this assumption, being compatible with our methodology.

Table 4.10 is similar to Table 4.9 except that columns 2, 3 and 4 are calculated with adjusted Eddington functionals.

Table 4.10. NEACRP benchmark, adjusted Eddington functional calculations

Config.	N	k	Assembly Power		Error (%)		
			UX	PX	k	UX	PX
0	1	2	3	4	5	6	7
C_1	52	1.01916	0.87717	1.12283	2.0×10^{-3}	0.28	0.22
C_2	40	0.907862	1.029931	0.970072	0.11	0.17	0.18
C_3	48	0.939781	0.911162	1.088838	0.18	0.58	0.49

The use of the adjusted Eddington functionals improves the accuracy of calculated values of k for all three configurations and the accuracy of UX and PX power distributions for configurations C_2 and C_3. Compared to reference data shown in Table 4.9 (Pal 1997), the QD code with adjusted functionals led to more accurate results then those given in (Pal 1997) for k in configuration C_1, UX assembly power in C_2 and C_4, and for PX assembly power in configuration C_2. Table 4.11 summarizes this comparison by listing the QDLO method relative errors with and without adjusted Eddington functionals (ε^{DCF} and ε) and ACM nodal diffusion method relative errors (ε^{ACM}), as given in (Pal 1997).

Table 4.11. Comparison between the solutions of NEACRP benchmark problem

Parameter	Config.	ε (%)	ε^{DCF} (%)	ε^{ACM} (%)
k	C_1	5.6×10^{-2}	2.0×10^{-3}	1.3×10^{-2}
	C_2	0.62	0.11	0.11
	C_3	0.24	0.18	4.7×10^{-2}
UX	C_1	0.14	0.28	0.10
	C_2	0.69	0.17	0.26
	C_3	1.2	0.58	0.40
PX	C_1	0.11	0.22	0.10
	C_2	0.66	0.18	0.19
	C_3	1.0	0.49	0.19

4.5. NINE-NODE PROBLEM, CENTRAL REFLECTOR NODE

This subsection presents the results of QDLO calculations for two nine-node configurations, shown in Figure 4.6 (a) and (b).

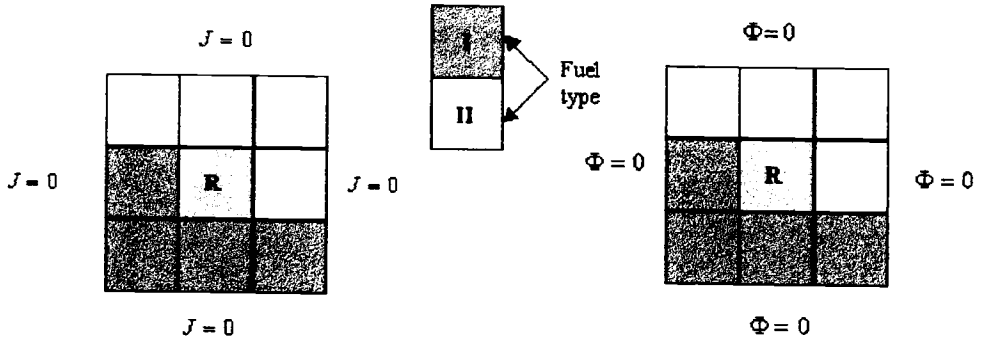

Figure 4.6. Nine-node, two fuel type central reflector node, (a) zero-current boundary conditions, (b) zero-flux boundary conditions

The node-averaged fast and thermal neutron flux and node-averaged power distribution are summarized in Figure 4.7 (a) and (b).

0.175173	0.163905	0.202591
0.006852	0.006475	0.007917
0.054516	0.048678	0.063304
0.089903	0.000000	0.134044
0.004839	0.009945	0.005304
0.030567	0.011976	0.039504
0.075407	0.068166	0.090811
0.004024	0.003678	0.004840
0.026888	0.022868	0.032571

(a)

Power
Thermal flux
Fast flux

0.113499	0.216281	0.143085
0.001276	0.002474	0.001605
0.010302	0.018042	0.013085
0.112636	0.000000	0.194869
0.001756	0.007185	0.002232
0.010685	0.008584	0.016151
0.051896	0.097038	0.070696
0.000796	0.001516	0.001082
0.005405	0.009095	0.007449

(b)

Figure 4.7. Node-averaged neutron fluxes and node-averaged power for nine-node problem with (a) zero-current boundary conditions and (b) zero-flux boundary conditions

The calculated multiplication factors are k=0.926803 for the zero-current boundary condition configuration, and k=0.623707 for the zero-flux boundary condition configuration.

The number of iterations required for the iteration scheme to reach a relative error of 10^{-6} in k and flux is greater for reflecting boundary conditions than for zero-flux, i.e. 133 iterations compared to 66. Thermal neutron flux shows a peak in the central node that is filled with water, as expected.

For zero-flux boundary conditions the nine-node averaged fluxes and power, their standard deviation and relative errors are summarized in Table 4.12.

Table 4.12. Nine-node averaged fast and thermal neutron flux and power for zero-current and zero-flux boundary conditions

Config.	Quantity	Nine-node average	Standard deviation	Relative error (%)
J=0	Fast flux	$3.68\text{x}10^{-2}$	$1.63\text{x}10^{-2}$	44.4
	Thermal flux	$5.99\text{x}10^{-3}$	$2.02\text{x}10^{-3}$	33.8
	Power	$1.11\text{x}10^{-1}$	$0.63\text{x}10^{-1}$	57.0
Φ=0	Fast flux	$1.10\text{x}10^{-2}$	$0.41\text{x}10^{-2}$	37.3
	Thermal flux	$2.21\text{x}10^{-2}$	$1.94\text{x}10^{-2}$	87.5
	Power	$1.11\text{x}10^{-1}$	$0.68\text{x}10^{-1}$	61.0

For zero-flux boundary conditions the peak thermal flux is higher than in zero-current boundary conditions configuration. The zero-current boundary condition problem the thermal flux peak in the central node is 351% higher than the average thermal flux in the other eight nodes. In the zero-flux boundary condition problem, this peak is only with 81% higher.

In both problems, the corresponding ratio Γ_{ij} of the node-averaged thermal flux in node ij and the node-averaged fast flux in the same node is close to the

infinite-medium analytical value, respectively $\frac{\Sigma_{12}^{ij}}{\Sigma_{r2}^{ij}}$. This is possible because the node width of the problem is large compared to neutron mean-free-path, ensuring conditions similar to infinite media. In the fueled nodes that have a surface in common with the reflector-filled central node Γ_{ij} is greater than $\frac{\Sigma_{12}^{ij}}{\Sigma_{r2}^{ij}}$ because of the reflecting and moderating properties of water: fast neutrons that have crossed the surface are moderated and scattered back into the node in which they originated. In these nodes Γ_{ij} for the zero-flux boundary condition problems is greater than for the zero-current boundary condition problems. Here, the thermal neutron flux is being amplified by the presence of the reflector and fast neutrons are in disadvantage because of their stronger tendency to leave the node due to diffusion.

Figure 4.8 shows Γ_{ij} for the zero-current boundary condition, zero-flux boundary condition, and analytic, infinite-medium problems.

0.1253	0.1253	0.1253
0.1239	0.1371	0.1226
0.1257	0.1330	0.1251
0.1494	1.250	0.1253
0.1643	0.8370	0.1239
0.1588	0.8301	0.1343
0.1494	0.1494	0.1494
0.1472	0.1667	0.1453
0.1496	0.1609	0.1486

Analytic
$\Phi = 0$ b.c.
$J = 0$ b.c.

Figure 4.8. Thermal to fast node-averaged neutron fluxes resulted from computations compared to the infinite medium values

3-D plots of the QDLO fast and thermal neutron fluxes are shown in Figure 4.9 and Figure 4.10 for the configuration presented in Figure 4.6(a). The plots show the thermal flux peak in the central node and in the same region a valley for the fast flux.

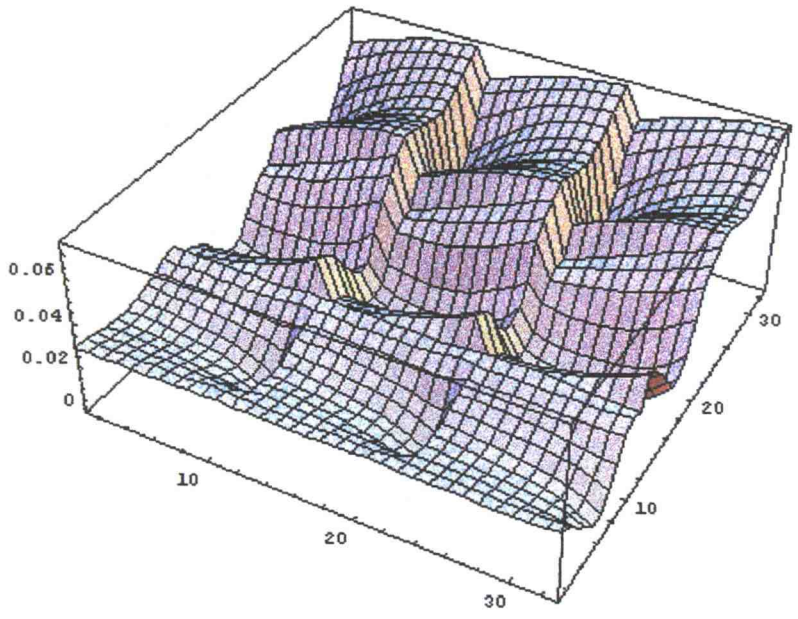

Figure 4.9. 3-D plots of the fast neutron flux, QD code calculations

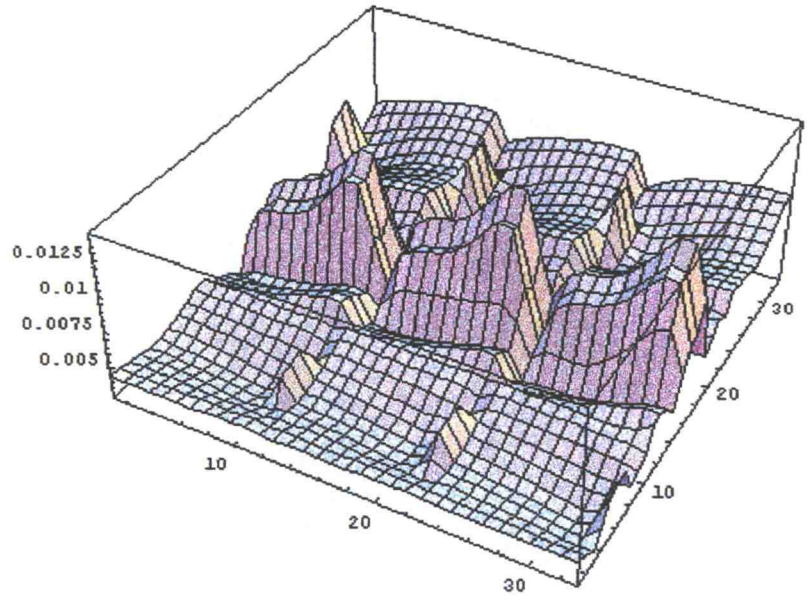

Figure 4.10. 3-D plots of the thermal neutron flux, QD code calculations

4.6. FOUR-NODE QD PROBLEM: REALISTIC EDDINGTON FUNCTIONALS

In this problem, we consider a 4-node domain with semi-reflecting boundaries as shown in Figure 4.11. Each node corresponds to a fuel assembly, all assemblies being identical.

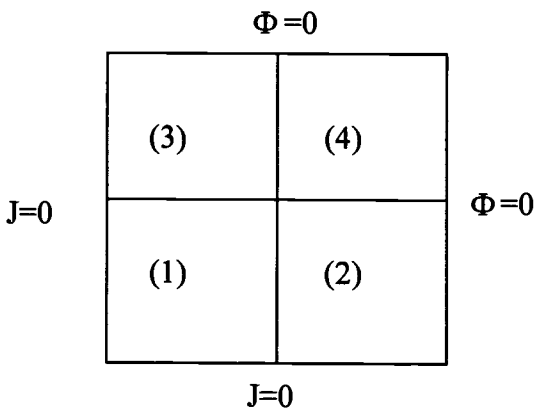

Figure 4.11. Semi-reflecting boundaries, four-node problem

The multiplication factor k of this configuration by using the nodal QDLO methodology for $E^{ij}_{g,xx} = E^{ij}_{g,yy}$ from 0.30 to 0.36 and $E^{ij}_{g,xy} = E^{ij}_{g,yx}$ from 0.0 to 0.04. The results show that k decreases when Eddington functionals increase. This behavior is due to increased leakage, directly related to bigger functional values. The calculated values for k and the dependence of k on **E** are shown in Table 4.13 and Figure 4.12.

Table 4.13. Calculated multiplication factors for various Eddington functionals

$E^{ij}_{g,xy}$	$E^{ij}_{g,xx} = E^{ij}_{g,yy}$			
	0.30	0.32	0.34	0.36
0.00	0.928595	0.922699	0.916875	0.911121
0.01	0.927200	0.921318	0.915508	0.909769
0.02	0.925912	0.920036	0.914233	0.908502
0.03	0.924729	0.918852	0.913050	0.907321
0.04	0.923653	0.917766	0.911958	0.906225

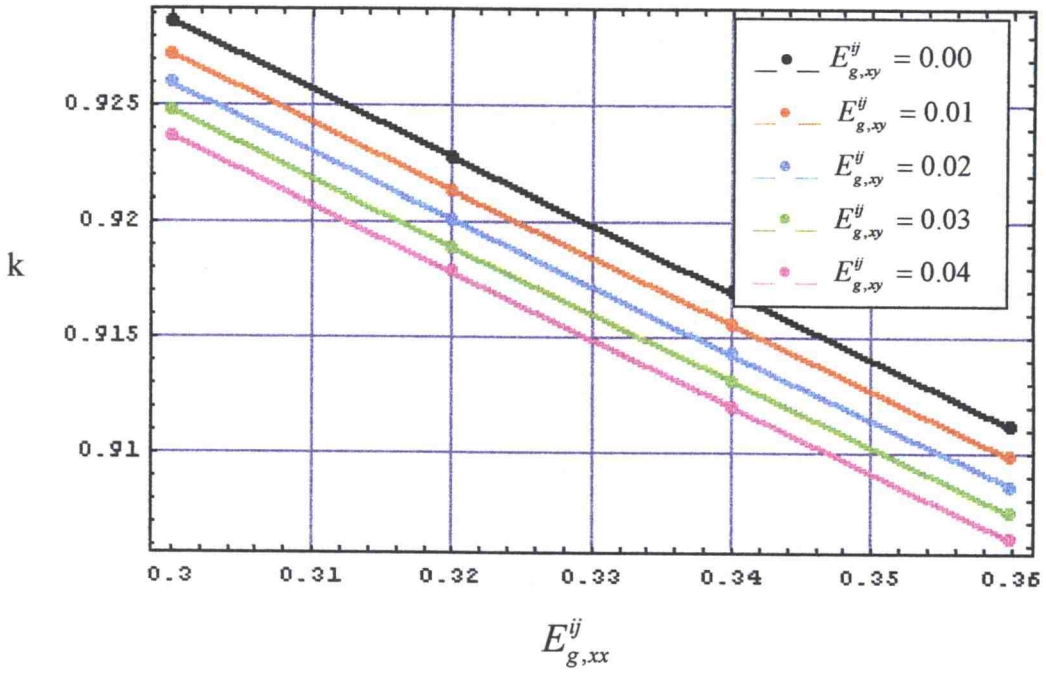

Figure 4.12. Multiplication factor versus diagonal components at various values of off-diagonal components of Eddington tensor

Increased off-diagonal Eddington tensor components also affect the power distribution between nodes by enhancing the flow of neutrons towards certain nodes. For example in our problem the power in node 4 increases with increasing

$E^{ij}_{g,xy}$, while power in nodes 1, 2 and 3 decreases. Table 4.14 summarizes these results, showing the variation of node-averaged power (P) and its relative rate of variation $\left(\frac{1}{P}\frac{dP}{dE^{ij}_{g,xy}}\right)$.

Table 4.14. The effect of off-diagonal Eddington tensor components on the power distribution

$E^{ij}_{g,xy}$	Node 1		Node 2, 3		Node 4	
	P	$\frac{1}{P}\frac{dP}{dE^{ij}_{g,xy}}$	P	$\frac{1}{P}\frac{dP}{dE^{ij}_{g,xy}}$	P	$\frac{1}{P}\frac{dP}{dE^{ij}_{g,xy}}$
0.00	4.99998	-0.323	2.07107	-0.140	8.57873	2.55
0.01	4.98446	-0.299	2.06789	-0.167	8.79730	2.48
0.02	4.97020	-0.274	2.06415	-0.194	9.01471	2.40
0.03	4.95719	-0.250	2.05984	-0.224	9.23107	2.34
0.04	4.94544	-0.225	2.05494	-0.253	9.44652	2.28

In Figure 4.13 node averaged power is plotted against off-diagonal Eddington functionals.

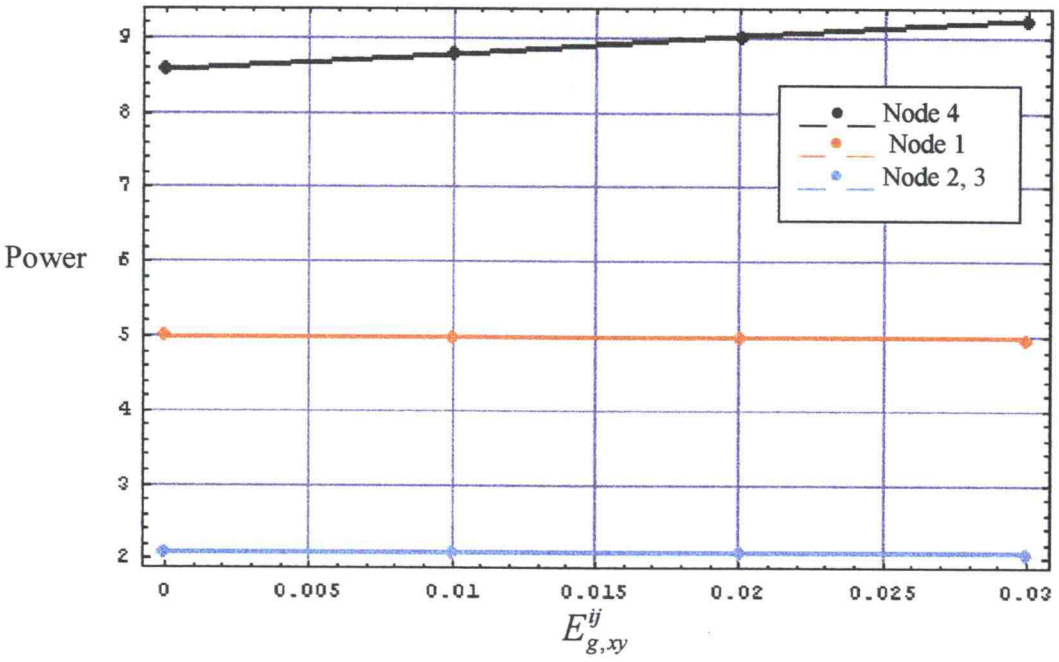

Figure 4.13. Node-averaged power versus off-diagonal Eddington tensor elements

4.7. SUMMARY

The results of the one-node, zero-current boundary condition diffusion problems are in excellent agreement with the benchmark and analytic solutions. Solutions of two-node, zero-current boundary condition problems with UO_2-UO_2 configurations show the same good agreement benchmark solutions (both k-eigenvalue and power distribution) , while UO_2-MOX configurations show more important discrepancies due to the single-assembly homogenized cross-sections used in the calculations. Four and nine-node problem results show power distribution discrepancies comparable with the results presented by other authors (Pal 1997). Larger discrepancies in k-eigenvalue are present in four and nine-node problems, but these discrepancies can be diminished by adjusting diffusion

coefficients (Pal 1997). Finally, the results of the "transport" problems show the influence of Eddington functionals on the multiplication factor k and the power distribution between nodes.

5. CONCLUSIONS AND FUTURE WORK

Two-group nodal diffusion approximations, along with single-assembly transport-generated cross section sets are currently used to calculate full-core eigenvalues (core multiplication factors) and power distribution. The inaccuracy of the diffusion approximation at interfaces between significantly different fuel assemblies can be overcome by using the quasi-diffusion transport formalism. Here, transport equations are solved to compute "functionals" of the angular flux (Eddington tensors, boundary conditions, etc.) and this data is then used in the solution of low-order diffusion-like equations. One important advantage of this technique is that, if the data used in the low-order equations comes from the correct transport solution, the solution of the low-order equations will be the transport scalar flux and current. In this case full-core calculations are capturing transport effects to an arbitrary degree of precision (Nes 2002). We have adapted the advanced nodal methodology developed by Palmtag (Pal 1997) for the two-group, 2-D diffusion equations with MOX and UO_2 fuel assemblies to the QDLO equations in Cartesian coordinates.

A discretization of the QDLO equations with constant nodal cross-sections and Eddington tensors was developed. The two-dimensional QDLO equations are solved by using the weighted residuals method, with non-separable polynomial and hyperbolic basis functions expansions of the fast and thermal neutron fluxes. However, we had to derive new hyperbolic basis functions of the thermal flux expansion different from those used with the diffusion equation (Pal 1997). To form a set of equations which, when solved, will yield the flux expansion coefficients, several conditions are imposed: weighted moment equations, flux and current continuity, node balance and boundary conditions. This yields to 23 equations for 23 flux expansion coefficients for each node of the problem. To perform these calculations we developed a code, written in "Mathematica", which

allows us to generate matrices for multiple-node problems, solve for flux expansion coefficients, and k-eigenvalues. A number of diffusion test problems (Eddington tensor with diagonal entries equal to 1/3, and zero-off-diagonal entries), and "transport" problems (Eddington tensor with diagonal entries different from one-third and zero or positive off-diagonal components) are solved. In the transport problems, the Eddington functionals are chosen to be within the range of values representative for two-node UO_2-MOX fuel assembly transport calculations. The results show that, for fuel assemblies characterized by "diffusive" data ($E_{xx} = E_{yy} = 1/3$, $E_{xy} = E_{yx} = 0$), the QDLO nodal discretization limits to the nodal diffusion discretization derived by Palmtag (Pal 1997).

While the QDLO calculations performed on one-node, zero-current, boundary condition diffusion problems and two-node, zero-current boundary condition problems with UO_2-UO_2 assemblies are in excellent agreement with the benchmark and analytic solutions, UO_2-MOX configurations show more important discrepancies that are due to the single-assembly homogenized cross-sections used in the calculations.

Compared to other authors' results, four- and nine-node problems show similar power distribution discrepancies. Multiple-node k-eigenvalue problems exhibit larger discrepancies, but these can be diminished by using adjusted diffusion coefficients (Pal 1997). The results of the "transport" problems demonstrate the influence of Eddington functionals on homogenized flux and on the multiplication factor k.

The assumption of constant nodal data is a significant limitation of this work. Transport codes, however, can provide with great accuracy the flux profile and, subsequently, space-dependent values for the homogenized cross-sections and the components of the Eddington tensor. An accurate reproduction of fine mesh transport results requires the incorporation of both higher spatial moments of the cross-sections and assembly-surface Eddington tensor data.

Future work will address these limitations by incorporating space-dependent assembly Eddington tensor and cross-sections in a FORTRAN code that will perform flux and k-eigenvalue calculations. We will also extend the methodology based on QDLO equations, developing a 3-D reactor core model.

BIBLIOGRAPHY

(Ada 1994) Adams, M.L., "Computational Methods for Particle-Transport Problems-Course Notes" (1994)

(Ada 2002) Adams, M.L. and Larsen, E.W., "Fast Iterative Methods for Discrete Ordinates Particle Transport Calculations", Progress in Nuclear Energy, Vol.40, No.1, pp 3-159 (2002)

(Aks 1979) Aksenov, N.N. and Gol'din, V.Ya., "Computation of the Two-Dimensional Stationary Equation of Neutron Transfer by the Quasi-Diffusion Method", USSR Comp. Math. and Math. Phys., v.19 pp263-266 (1979)

(Ame 1992) Ames, W.F., "Numerical Methods for Partial Differential Equations", Academic Press, Inc., New York (1992)

(Ani 1999) Anistratov, D.Y., Adams, M.L., Palmer, T.S., and Smith K.S., "An Innovative Reactor Analysis Methodology Based on Quasidiffusion Nodal Core Model", DOE NERI Proposal (1999)

(Ani 2001) Anistratov, D.Y., Private Communication (2001)

(Ari 1993) Aristova, E.N. and Kolpakov, A.V., "A Combined Finite Difference Scheme for an Elliptic Operator in an Oblique-Angled Cell", *Math. Modeling Comp. Exp.* 1, 187 (1993)

(Dud 1976) Duderstadt, J.J. and Hamilton, L.J., "Nuclear Reactor Analysis", John Wiley & Sons, Inc., New York (1976)

(Gol 1967) Gol'din, V.Ya., "A Quasi-Diffusion Method of Solving the Kinetic Equation", USSR Comp. Math. and Math. Phys., v.4 (1967)

(Gol 1972) Gol'din, V.Ya. and Chetverushkin, B.N., "Methods of Solving One-Dimensional Problems of Radiation Gas Dynamics", USSR Comp. Math. and Math. Phys., v.12 (4) (1972)

(Law 1986) Lawrence, R.D., "Progress in Nodal Methods for the Solutions of the Neutron Diffusion and Transport Equations", *Progress in Nuclear Energy*, Vol.17, No.3, pp.271-301 (1986)

(Lew 1993) Lewis, E.E. and Miller, W.F. Jr., "Computational Methods of Neutron Transport", American Nuclear Society, Inc., La Grange Park, Illinois (1993)

(Mif 1993) Miften, M.M. and Larsen, E.W., "A Symmetrized Quasidiffusion Method for Solving Transport Problems in Multidimensional Geometries", Proc. ANS Topical Meeting, *Mathematical Methods and Supercomputing in Nuclear Applications, M&C+SNA '93*, April 19-23, 1993, Karlsruhe, Germany, 1, 707

(Nes 2002) Nes, R and Palmer, T.S., "An Advanced Nodal Discretization for the Quasi-Diffusion Low-Order Equations", Summary submitted to The 2002 ANS RPD Topical Meeting –PHYSOR 2002, Seoul, Korea (2002)

(Pal 2001) Palmer, T.S., Private Communication (2001)

(Pal 1997) Palmtag, S.P., "Advanced Nodal Methods for MOX Fuel Analysis", PhD Thesis, Massachusetts Institute of Technology (1997)

(Rad 1992) Rade, L. and Westergren, B., "Beta Mathematics Handbook", CRC Press, Boca Raton (1992)

(Smi 1986) Smith, K.S., "Assembly Homogenization Techniques for Light Water Reactor Analysis", *Progress in Nuclear Energy*, Vol.17, No.3 , pp.303-335 (1986)

APPENDICES

A. WEIGHTED MOMENTS OF THE LOQD EQUATION OF THE FAST FLUX

A.1. ZERO-TH WEIGHTED MOMENT

- QD operator term:

$$Sr_{1,i,j}\, a_{0,0,i,j} - \frac{6\, a_{2,0,i,j}\, e_{1,xx,i,j}}{h^2\, St_{1,i,j}} - \frac{2\, a_{4,0,i,j}\, e_{1,xx,i,j}}{5\, h^2\, St_{1,i,j}} - \frac{2\, a_{1,1,i,j}\, e_{1,xy,i,j}}{h^2\, St_{1,i,j}} - \frac{6\, a_{0,2,i,j}\, e_{1,yy,i,j}}{h^2\, St_{1,i,j}} - \frac{2\, a_{0,4,i,j}\, e_{1,yy,i,j}}{5\, h^2\, St_{1,i,j}}$$

- Fission source term:

$$\frac{2\,\mathrm{Sinh}\left[\frac{1}{2}\,\gamma_{1,i,j}\right]\, c_{1,i,j}\, Sf_{2,i,j}}{\gamma_{1,i,j}} + \frac{2\,\mathrm{Sinh}\left[\frac{1}{2}\,\gamma_{2,i,j}\right]\, c_{3,i,j}\, Sf_{2,i,j}}{\gamma_{2,i,j}} +$$

$$c_{5,i,j}\left(-\frac{4\,\mathrm{Cosh}\left[\frac{\gamma_{3,i,j}}{2\sqrt{2}} - \frac{\gamma_{3,i,j}\theta_{1,i,j}}{2\sqrt{2}}\right] Sf_{2,i,j}}{\gamma_{3,i,j}^2\,\theta_{1,i,j}} + \frac{4\,\mathrm{Cosh}\left[\frac{\gamma_{3,i,j}}{2\sqrt{2}} + \frac{\gamma_{3,i,j}\theta_{1,i,j}}{2\sqrt{2}}\right] Sf_{2,i,j}}{\gamma_{3,i,j}^2\,\theta_{1,i,j}}\right) +$$

$$c_{7,i,j}\left(-\frac{4\,\mathrm{Cosh}\left[\frac{\gamma_{3,i,j}}{2\sqrt{2}} - \frac{\gamma_{3,i,j}\theta_{2,i,j}}{2\sqrt{2}}\right] Sf_{2,i,j}}{\gamma_{3,i,j}^2\,\theta_{2,i,j}} + \frac{4\,\mathrm{Cosh}\left[\frac{\gamma_{3,i,j}}{2\sqrt{2}} + \frac{\gamma_{3,i,j}\theta_{2,i,j}}{2\sqrt{2}}\right] Sf_{2,i,j}}{\gamma_{3,i,j}^2\,\theta_{2,i,j}}\right) +$$

$$Sf_{1,i,j}\, a_{0,0,i,j} + Sf_{2,i,j}\, b_{0,0,i,j}$$

A.2. FIRST WEIGHTED MOMENT

- QD operator term:

$$\frac{1}{12}\, Sr_{1,i,j}\, a_{1,0,i,j} - \frac{1}{30}\, Sr_{1,i,j}\, a_{3,0,i,j} - \frac{2\, a_{3,0,i,j}\, e_{1,xx,i,j}}{h^2\, St_{1,i,j}} - \frac{a_{2,1,i,j}\, e_{1,xy,i,j}}{h^2\, St_{1,i,j}} - \frac{a_{1,2,i,j}\, e_{1,yy,i,j}}{2\, h^2\, St_{1,i,j}}$$

- Fission source term:

$$c_{2,i,j}\,Sf_{2,i,j}\left(-\frac{2\,\mathrm{Sinh}\left[\frac{1}{2}\,\gamma_{1,i,j}\right]}{\gamma_{1,i,j}^2}+\frac{\mathrm{Cosh}\left[\frac{1}{2}\,\gamma_{1,i,j}\right]}{\gamma_{1,i,j}}\right)-$$

$$\frac{2\sqrt{2}\,\mathrm{Sinh}\left[\frac{\gamma_{3,i,j}}{2\sqrt{2}}\right]c_{6,i,j}\,Sf_{2,i,j}\left(-\frac{4\,\mathrm{Sinh}\left[\frac{\gamma_{3,i,j}\theta_{1,i,j}}{2\sqrt{2}}\right]}{\gamma_{3,i,j}^2\theta_{1,i,j}^2}+\frac{\sqrt{2}\,\mathrm{Cosh}\left[\frac{\gamma_{3,i,j}\theta_{1,i,j}}{2\sqrt{2}}\right]}{\gamma_{3,i,j}\theta_{1,i,j}}\right)}{\gamma_{3,i,j}}-$$

$$\frac{2\sqrt{2}\,\mathrm{Sinh}\left[\frac{\gamma_{3,i,j}}{2\sqrt{2}}\right]c_{8,i,j}\,Sf_{2,i,j}\left(-\frac{4\,\mathrm{Sinh}\left[\frac{\gamma_{3,i,j}\theta_{2,i,j}}{2\sqrt{2}}\right]}{\gamma_{3,i,j}^2\theta_{2,i,j}^2}+\frac{\sqrt{2}\,\mathrm{Cosh}\left[\frac{\gamma_{3,i,j}\theta_{2,i,j}}{2\sqrt{2}}\right]}{\gamma_{3,i,j}\theta_{2,i,j}}\right)}{\gamma_{3,i,j}}+$$

$$\frac{1}{12}\,Sf_{1,i,j}\,a_{1,0,i,j}-\frac{1}{30}\,Sf_{1,i,j}\,a_{3,0,i,j}+\frac{1}{12}\,Sf_{2,i,j}\,b_{1,0,i,j}-\frac{1}{30}\,Sf_{2,i,j}\,b_{3,0,i,j}$$

A.3. SECOND WEIGHTED MOMENT

- QD operator term:

$$\frac{1}{12}\,Sr_{1,i,j}\,a_{0,1,i,j}-\frac{1}{30}\,Sr_{1,i,j}\,a_{0,3,i,j}-\frac{a_{2,1,i,j}\,e_{1,xx,i,j}}{2\,h^2\,St_{1,i,j}}-\frac{a_{1,2,i,j}\,e_{1,xy,i,j}}{h^2\,St_{1,i,j}}-\frac{2\,a_{0,3,i,j}\,e_{1,yy,i,j}}{h^2\,St_{1,i,j}}$$

- Fission source term:

$$\frac{c_{4,i,j}\,Sf_{2,i,j}\left(-2\,\mathrm{Sinh}\left[\frac{1}{2}\,\gamma_{2,i,j}\right]+\mathrm{Cosh}\left[\frac{1}{2}\,\gamma_{2,i,j}\right]\gamma_{2,i,j}\right)}{\gamma_{2,i,j}^2}-$$

$$\frac{4\,\mathrm{Sinh}\left[\frac{\gamma_{3,i,j}\theta_{1,i,j}}{2\sqrt{2}}\right]c_{6,i,j}\,Sf_{2,i,j}\left(2\sqrt{2}\,\mathrm{Sinh}\left[\frac{\gamma_{3,i,j}}{2\sqrt{2}}\right]-\mathrm{Cosh}\left[\frac{\gamma_{3,i,j}}{2\sqrt{2}}\right]\gamma_{3,i,j}\right)}{\gamma_{3,i,j}^3\theta_{1,i,j}}-$$

$$\frac{4\,\mathrm{Sinh}\left[\frac{\gamma_{3,i,j}\theta_{2,i,j}}{2\sqrt{2}}\right]c_{8,i,j}\,Sf_{2,i,j}\left(2\sqrt{2}\,\mathrm{Sinh}\left[\frac{\gamma_{3,i,j}}{2\sqrt{2}}\right]-\mathrm{Cosh}\left[\frac{\gamma_{3,i,j}}{2\sqrt{2}}\right]\gamma_{3,i,j}\right)}{\gamma_{3,i,j}^3\theta_{2,i,j}}+$$

$$\frac{1}{12}\,Sf_{1,i,j}\,a_{0,1,i,j}-\frac{1}{30}\,Sf_{1,i,j}\,a_{0,3,i,j}+\frac{1}{12}\,Sf_{2,i,j}\,b_{0,1,i,j}-\frac{1}{30}\,Sf_{2,i,j}\,b_{0,3,i,j}$$

A.4. THIRD WEIGHTED MOMENT

- QD operator term:

$$Sr_{1,i,j}\, a_{1,1,i,j} - \frac{72\, a_{2,2,i,j}\, e_{1,xy,i,j}}{h^2\, St_{1,i,j}} + \frac{a_{3,3,i,j}\,(4\,h^2\, Sr_{1,i,j}\, St_{1,i,j} + 240\,(e_{1,xx,i,j} + e_{1,yy,i,j}))}{25\,h^2\, St_{1,i,j}}$$

- Fission source term:

$$\frac{1}{\gamma_{3,i,j}^4\, \theta_{1,i,j}^2}\left(144\sqrt{2}\, c_{5,i,j}\, Sf_{2,i,j}\left(-4\,\text{Sinh}\left[\frac{\gamma_{3,i,j}\,\theta_{1,i,j}}{2\sqrt{2}}\right]\left(2\sqrt{2}\,\text{Sinh}\left[\frac{\gamma_{3,i,j}}{2\sqrt{2}}\right] - \text{Cosh}\left[\frac{\gamma_{3,i,j}}{2\sqrt{2}}\right]\gamma_{3,i,j}\right) - \text{Cosh}\left[\frac{\gamma_{3,i,j}\,\theta_{1,i,j}}{2\sqrt{2}}\right]\gamma_{3,i,j}\left(-4\,\text{Sinh}\left[\frac{\gamma_{3,i,j}}{2\sqrt{2}}\right] + \sqrt{2}\,\text{Cosh}\left[\frac{\gamma_{3,i,j}}{2\sqrt{2}}\right]\gamma_{3,i,j}\right)\theta_{1,i,j}\right)\right) +$$

$$\frac{1}{\gamma_{3,i,j}^4\, \theta_{2,i,j}^2}\left(144\sqrt{2}\, c_{7,i,j}\, Sf_{2,i,j}\left(-4\,\text{Sinh}\left[\frac{\gamma_{3,i,j}\,\theta_{2,i,j}}{2\sqrt{2}}\right]\left(2\sqrt{2}\,\text{Sinh}\left[\frac{\gamma_{3,i,j}}{2\sqrt{2}}\right] - \text{Cosh}\left[\frac{\gamma_{3,i,j}}{2\sqrt{2}}\right]\gamma_{3,i,j}\right) - \text{Cosh}\left[\frac{\gamma_{3,i,j}\,\theta_{2,i,j}}{2\sqrt{2}}\right]\gamma_{3,i,j}\left(-4\,\text{Sinh}\left[\frac{\gamma_{3,i,j}}{2\sqrt{2}}\right] + \sqrt{2}\,\text{Cosh}\left[\frac{\gamma_{3,i,j}}{2\sqrt{2}}\right]\gamma_{3,i,j}\right)\theta_{2,i,j}\right)\right) +$$

$$Sf_{1,i,j}\, a_{1,1,i,j} + \frac{4}{25}\, Sf_{1,i,j}\, a_{3,3,i,j} + Sf_{2,i,j}\, b_{1,1,i,j} - \frac{2}{5}\, Sf_{2,i,j}\, b_{1,3,i,j} -$$

$$\frac{2}{5}\, Sf_{2,i,j}\, b_{3,1,i,j} +$$

$$\frac{4}{25}\, Sf_{2,i,j}\, b_{3,3,i,j}$$

A.5. FOURTH WEIGHTED MOMENT

- QD operator term:

$$\frac{1}{5}\, Sr_{1,i,j}\, a_{2,0,i,j} + \frac{a_{4,0,i,j}\,(-5\,h^2\, Sr_{1,i,j}\, St_{1,i,j} - 700\, e_{1,xx,i,j})}{875\,h^2\, St_{1,i,j}} - \frac{6\, a_{2,2,i,j}\, e_{1,yy,i,j}}{5\,h^2\, St_{1,i,j}} + \frac{2\, a_{4,4,i,j}\, e_{1,yy,i,j}}{875\,h^2\, St_{1,i,j}}$$

- Fission source term:

$$\frac{2\,c_{1,i,j}\,Sf_{2,i,j}\left(-12\,\mathrm{Cosh}\left[\frac{1}{2}\,\gamma_{1,i,j}\right]\gamma_{1,i,j}+2\,\mathrm{Sinh}\left[\frac{1}{2}\,\gamma_{1,i,j}\right]\left(12+\gamma_{1,i,j}^2\right)\right)}{\gamma_{1,i,j}^3}+$$

$$\frac{1}{\gamma_{3,i,j}^4\,\theta_{1,i,j}^3}\left(4\sqrt{2}\,\mathrm{Sinh}\left[\frac{\gamma_{3,i,j}}{2\sqrt{2}}\right]c_{5,i,j}\,Sf_{2,i,j}\left(-24\,\mathrm{Cosh}\left[\frac{\gamma_{3,i,j}\theta_{1,i,j}}{2\sqrt{2}}\right]\gamma_{3,i,j}\,\theta_{1,i,j}+2\sqrt{2}\,\mathrm{Sinh}\left[\frac{\gamma_{3,i,j}\theta_{1,i,j}}{2\sqrt{2}}\right]\left(24+\gamma_{3,i,j}^2\,\theta_{1,i,j}^2\right)\right)\right)+$$

$$\frac{1}{\gamma_{3,i,j}^4\,\theta_{2,i,j}^3}\left(4\sqrt{2}\,\mathrm{Sinh}\left[\frac{\gamma_{3,i,j}}{2\sqrt{2}}\right]c_{7,i,j}\,Sf_{2,i,j}\left(-24\,\mathrm{Cosh}\left[\frac{\gamma_{3,i,j}\theta_{2,i,j}}{2\sqrt{2}}\right]\gamma_{3,i,j}\,\theta_{2,i,j}+2\sqrt{2}\,\mathrm{Sinh}\left[\frac{\gamma_{3,i,j}\theta_{2,i,j}}{2\sqrt{2}}\right]\left(24+\gamma_{3,i,j}^2\,\theta_{2,i,j}^2\right)\right)\right)+$$

$$\frac{1}{5}\,Sf_{1,i,j}\,a_{2,0,i,j}-\frac{1}{175}\,Sf_{1,i,j}\,a_{4,0,i,j}+\frac{1}{5}\,Sf_{2,i,j}\,b_{2,0,i,j}-\frac{1}{175}\,Sf_{2,i,j}\,b_{4,0,i,j}$$

A.6. FIFTH WEIGHTED MOMENT

- QD operator term:

$$\frac{1}{5}\,Sr_{1,i,j}\,a_{0,2,i,j}-\frac{6\,a_{2,2,i,j}\,e_{1,xx,i,j}}{5\,h^2\,St_{1,i,j}}+\frac{2\,a_{4,4,i,j}\,e_{1,xx,i,j}}{875\,h^2\,St_{1,i,j}}+\frac{a_{0,4,i,j}\left(-5\,h^2\,Sr_{1,i,j}\,St_{1,i,j}-700\,e_{1,yy,i,j}\right)}{875\,h^2\,St_{1,i,j}}$$

- Fission source term:

$$\frac{4\,c_{3,i,j}\,Sf_{2,i,j}\left(12\,\mathrm{Sinh}\left[\frac{1}{2}\,\gamma_{2,i,j}\right]-6\,\mathrm{Cosh}\left[\frac{1}{2}\,\gamma_{2,i,j}\right]\gamma_{2,i,j}+\mathrm{Sinh}\left[\frac{1}{2}\,\gamma_{2,i,j}\right]\gamma_{2,i,j}^2\right)}{\gamma_{2,i,j}^3}+$$

$$\frac{16\,\mathrm{Sinh}\left[\frac{\gamma_{3,i,j}\theta_{1,i,j}}{2\sqrt{2}}\right]c_{5,i,j}\,Sf_{2,i,j}\left(24\,\mathrm{Sinh}\left[\frac{\gamma_{3,i,j}}{2\sqrt{2}}\right]-6\sqrt{2}\,\mathrm{Cosh}\left[\frac{\gamma_{3,i,j}}{2\sqrt{2}}\right]\gamma_{3,i,j}+\mathrm{Sinh}\left[\frac{\gamma_{3,i,j}}{2\sqrt{2}}\right]\gamma_{3,i,j}^2\right)}{\gamma_{3,i,j}^4\,\theta_{1,i,j}}+$$

$$\frac{16\,\mathrm{Sinh}\left[\frac{\gamma_{3,i,j}\theta_{2,i,j}}{2\sqrt{2}}\right]c_{7,i,j}\,Sf_{2,i,j}\left(24\,\mathrm{Sinh}\left[\frac{\gamma_{3,i,j}}{2\sqrt{2}}\right]-6\sqrt{2}\,\mathrm{Cosh}\left[\frac{\gamma_{3,i,j}}{2\sqrt{2}}\right]\gamma_{3,i,j}+\mathrm{Sinh}\left[\frac{\gamma_{3,i,j}}{2\sqrt{2}}\right]\gamma_{3,i,j}^2\right)}{\gamma_{3,i,j}^4\,\theta_{2,i,j}}+$$

$$\frac{1}{5}\,Sf_{1,i,j}\,a_{0,2,i,j}-\frac{1}{175}\,Sf_{1,i,j}\,a_{0,4,i,j}+\frac{1}{5}\,Sf_{2,i,j}\,b_{0,2,i,j}-\frac{1}{175}\,Sf_{2,i,j}\,b_{0,4,i,j}$$

A.7. SIXTH WEIGHTED MOMENT

- QD operator term:

$$\frac{1}{25} Sr_{1,i,j} a_{2,2,i,j} - \frac{32\, a_{3,3,i,j}\, e_{1,xy,i,j}}{25\, h^2\, St_{1,i,j}} + \frac{a_{4,4,i,j}\,(h^2\, Sr_{1,i,j}\, St_{1,i,j} + 140\,(e_{1,xx,i,j} + e_{1,yy,i,j}))}{30625\, h^2\, St_{1,i,j}}$$

- Fission source term:

$$\frac{1}{\gamma_{3,i,j}^{6}\theta_{1,i,j}^{3}}\left(32\,c_{5,i,j}\,Sf_{2,i,j}\left(576\,\text{Sinh}\left[\frac{\gamma_{3,i,j}}{2\sqrt{2}}\right]\text{Sinh}\left[\frac{\gamma_{3,i,j}\theta_{1,i,j}}{2\sqrt{2}}\right]+\text{Sinh}\left[\frac{\gamma_{3,i,j}}{2\sqrt{2}}\right]\text{Sinh}\left[\frac{\gamma_{3,i,j}\theta_{1,i,j}}{2\sqrt{2}}\right]\gamma_{3,i,j}^{4}\theta_{1,i,j}^{2}-\right.\right.$$
$$144\sqrt{2}\,\gamma_{3,i,j}\left(\text{Cosh}\left[\frac{\gamma_{3,i,j}}{2\sqrt{2}}\right]\text{Sinh}\left[\frac{\gamma_{3,i,j}\theta_{1,i,j}}{2\sqrt{2}}\right]+\text{Cosh}\left[\frac{\gamma_{3,i,j}\theta_{1,i,j}}{2\sqrt{2}}\right]\text{Sinh}\left[\frac{\gamma_{3,i,j}}{2\sqrt{2}}\right]\theta_{1,i,j}\right)-$$
$$6\sqrt{2}\,\gamma_{3,i,j}^{3}\theta_{1,i,j}\left(\text{Cosh}\left[\frac{\gamma_{3,i,j}\theta_{1,i,j}}{2\sqrt{2}}\right]\text{Sinh}\left[\frac{\gamma_{3,i,j}}{2\sqrt{2}}\right]+\text{Cosh}\left[\frac{\gamma_{3,i,j}}{2\sqrt{2}}\right]\text{Sinh}\left[\frac{\gamma_{3,i,j}\theta_{1,i,j}}{2\sqrt{2}}\right]\theta_{1,i,j}\right)+$$
$$24\,\gamma_{3,i,j}^{2}\left(\text{Sinh}\left[\frac{\gamma_{3,i,j}}{2\sqrt{2}}\right]\text{Sinh}\left[\frac{\gamma_{3,i,j}\theta_{1,i,j}}{2\sqrt{2}}\right]+3\,\text{Cosh}\left[\frac{\gamma_{3,i,j}}{2\sqrt{2}}\right]\text{Cosh}\left[\frac{\gamma_{3,i,j}\theta_{1,i,j}}{2\sqrt{2}}\right]\theta_{1,i,j}+\right.$$
$$\left.\left.\left.\text{Sinh}\left[\frac{\gamma_{3,i,j}}{2\sqrt{2}}\right]\text{Sinh}\left[\frac{\gamma_{3,i,j}\theta_{1,i,j}}{2\sqrt{2}}\right]\theta_{1,i,j}^{2}\right)\right)\right)+\frac{1}{\gamma_{3,i,j}^{6}\theta_{2,i,j}^{3}}$$
$$\left(32\,c_{7,i,j}\,Sf_{2,i,j}\left(576\,\text{Sinh}\left[\frac{\gamma_{3,i,j}}{2\sqrt{2}}\right]\text{Sinh}\left[\frac{\gamma_{3,i,j}\theta_{2,i,j}}{2\sqrt{2}}\right]+\text{Sinh}\left[\frac{\gamma_{3,i,j}}{2\sqrt{2}}\right]\text{Sinh}\left[\frac{\gamma_{3,i,j}\theta_{2,i,j}}{2\sqrt{2}}\right]\gamma_{3,i,j}^{4}\theta_{2,i,j}^{2}-\right.\right.$$
$$144\sqrt{2}\,\gamma_{3,i,j}\left(\text{Cosh}\left[\frac{\gamma_{3,i,j}}{2\sqrt{2}}\right]\text{Sinh}\left[\frac{\gamma_{3,i,j}\theta_{2,i,j}}{2\sqrt{2}}\right]+\text{Cosh}\left[\frac{\gamma_{3,i,j}\theta_{2,i,j}}{2\sqrt{2}}\right]\text{Sinh}\left[\frac{\gamma_{3,i,j}}{2\sqrt{2}}\right]\theta_{2,i,j}\right)-$$
$$6\sqrt{2}\,\gamma_{3,i,j}^{3}\theta_{2,i,j}\left(\text{Cosh}\left[\frac{\gamma_{3,i,j}\theta_{2,i,j}}{2\sqrt{2}}\right]\text{Sinh}\left[\frac{\gamma_{3,i,j}}{2\sqrt{2}}\right]+\text{Cosh}\left[\frac{\gamma_{3,i,j}}{2\sqrt{2}}\right]\text{Sinh}\left[\frac{\gamma_{3,i,j}\theta_{2,i,j}}{2\sqrt{2}}\right]\theta_{2,i,j}\right)+$$
$$24\,\gamma_{3,i,j}^{2}\left(\text{Sinh}\left[\frac{\gamma_{3,i,j}}{2\sqrt{2}}\right]\text{Sinh}\left[\frac{\gamma_{3,i,j}\theta_{2,i,j}}{2\sqrt{2}}\right]+\right.$$
$$\left.\left.\left.\left.3\,\text{Cosh}\left[\frac{\gamma_{3,i,j}}{2\sqrt{2}}\right]\text{Cosh}\left[\frac{\gamma_{3,i,j}\theta_{2,i,j}}{2\sqrt{2}}\right]\theta_{2,i,j}+\text{Sinh}\left[\frac{\gamma_{3,i,j}}{2\sqrt{2}}\right]\text{Sinh}\left[\frac{\gamma_{3,i,j}\theta_{2,i,j}}{2\sqrt{2}}\right]\theta_{2,i,j}^{2}\right)\right)\right)+$$
$$\frac{1}{25}\,Sf_{1,i,j}\,a_{2,2,i,j}+\frac{Sf_{1,i,j}\,a_{4,4,i,j}}{30625}+\frac{1}{25}\,Sf_{2,i,j}\,b_{2,2,i,j}-$$
$$\frac{1}{875}$$
$$Sf_{2,i,j}$$
$$b_{2,4,i,j}-\frac{1}{875}$$
$$Sf_{2,i,j}$$
$$b_{4,2,i,j}+$$
$$\frac{Sf_{2,i,j}\,b_{4,4,i,j}}{30625}$$

B. SURFACE-AVERAGED FLUXES AND CURRENTS

B.1. SURFACE-AVERAGED FLUXES

- Fast group

$$\bar{\Phi}^{ij}_{1x+} =$$

$$a_{0,0,i,j} + \frac{1}{2} a_{1,0,i,j} + \frac{1}{2} a_{2,0,i,j}$$

$$\bar{\Phi}^{ij}_{1x-} =$$

$$a_{0,0,i,j} - \frac{1}{2} a_{1,0,i,j} + \frac{1}{2} a_{2,0,i,j}$$

$$\bar{\Phi}^{ij}_{1y+} =$$

$$a_{0,0,i,j} + \frac{1}{2} a_{0,1,i,j} + \frac{1}{2} a_{0,2,i,j}$$

$$\bar{\Phi}^{ij}_{1y-} =$$

$$a_{0,0,i,j} - \frac{1}{2} a_{0,1,i,j} + \frac{1}{2} a_{0,2,i,j}$$

- Thermal group

$$\bar{\Phi}^{ij}_{2x+} =$$

$$\mathrm{Cosh}\left[\frac{1}{2}\gamma_{1,i,j}\right] c_{1,i,j} + \mathrm{Sinh}\left[\frac{1}{2}\gamma_{1,i,j}\right] c_{2,i,j} +$$

$$\frac{2\,\mathrm{Sinh}\left[\frac{1}{2}\gamma_{2,i,j}\right] c_{3,i,j}}{\gamma_{2,i,j}} + \frac{2\sqrt{2}\,\mathrm{Cosh}\left[\frac{\gamma_{3,i,j}\theta_{1,i,j}}{2\sqrt{2}}\right]\mathrm{Sinh}\left[\frac{\gamma_{3,i,j}}{2\sqrt{2}}\right] c_{5,i,j}}{\gamma_{3,i,j}} -$$

$$\frac{2\sqrt{2}\,\mathrm{Sinh}\left[\frac{\gamma_{3,i,j}}{2\sqrt{2}}\right]\mathrm{Sinh}\left[\frac{\gamma_{3,i,j}\theta_{1,i,j}}{2\sqrt{2}}\right] c_{6,i,j}}{\gamma_{3,i,j}} + \frac{2\sqrt{2}\,\mathrm{Cosh}\left[\frac{\gamma_{3,i,j}\theta_{2,i,j}}{2\sqrt{2}}\right]\mathrm{Sinh}\left[\frac{\gamma_{3,i,j}}{2\sqrt{2}}\right] c_{7,i,j}}{\gamma_{3,i,j}} -$$

$$\frac{2\sqrt{2}\,\mathrm{Sinh}\left[\frac{\gamma_{3,i,j}}{2\sqrt{2}}\right]\mathrm{Sinh}\left[\frac{\gamma_{3,i,j}\theta_{2,i,j}}{2\sqrt{2}}\right] c_{8,i,j}}{\gamma_{3,i,j}} + b_{0,0,i,j} + \frac{1}{2} b_{1,0,i,j} + \frac{1}{2} b_{2,0,i,j}$$

$$\bar{\Phi}^{ij}_{2x-} =$$

$$\cosh\left[\frac{1}{2}\gamma_{1,i,j}\right] c_{1,i,j} - \sinh\left[\frac{1}{2}\gamma_{1,i,j}\right] c_{2,i,j} +$$

$$\frac{2\sinh\left[\frac{1}{2}\gamma_{2,i,j}\right] c_{3,i,j}}{\gamma_{2,i,j}} + \frac{2\sqrt{2}\cosh\left[\frac{\gamma_{3,i,j}\theta_{1,i,j}}{2\sqrt{2}}\right]\sinh\left[\frac{\gamma_{3,i,j}}{2\sqrt{2}}\right] c_{5,i,j}}{\gamma_{3,i,j}} +$$

$$\frac{2\sqrt{2}\sinh\left[\frac{\gamma_{3,i,j}}{2\sqrt{2}}\right]\sinh\left[\frac{\gamma_{3,i,j}\theta_{1,i,j}}{2\sqrt{2}}\right] c_{6,i,j}}{\gamma_{3,i,j}} + \frac{2\sqrt{2}\cosh\left[\frac{\gamma_{3,i,j}\theta_{2,i,j}}{2\sqrt{2}}\right]\sinh\left[\frac{\gamma_{3,i,j}}{2\sqrt{2}}\right] c_{7,i,j}}{\gamma_{3,i,j}} +$$

$$\frac{2\sqrt{2}\sinh\left[\frac{\gamma_{3,i,j}}{2\sqrt{2}}\right]\sinh\left[\frac{\gamma_{3,i,j}\theta_{2,i,j}}{2\sqrt{2}}\right] c_{8,i,j}}{\gamma_{3,i,j}} + b_{0,0,i,j} - \frac{1}{2} b_{1,0,i,j} + \frac{1}{2} b_{2,0,i,j}$$

$$\bar{\Phi}^{ij}_{2y+} =$$

$$\cosh\left[\frac{1}{2}\gamma_{2,i,j}\right] c_{3,i,j} + \sinh\left[\frac{1}{2}\gamma_{2,i,j}\right] c_{4,i,j} +$$

$$\frac{2\sinh\left[\frac{1}{2}\gamma_{1,i,j}\right] c_{1,i,j}}{\gamma_{1,i,j}} - \frac{\sqrt{2}\sinh\left[\frac{\gamma_{3,i,j}}{2\sqrt{2}} - \frac{\gamma_{3,i,j}\theta_{1,i,j}}{2\sqrt{2}}\right] c_{5,i,j}}{\gamma_{3,i,j}\theta_{1,i,j}} +$$

$$\frac{\sqrt{2}\sinh\left[\frac{\gamma_{3,i,j}}{2\sqrt{2}} + \frac{\gamma_{3,i,j}\theta_{1,i,j}}{2\sqrt{2}}\right] c_{5,i,j}}{\gamma_{3,i,j}\theta_{1,i,j}} - \frac{\sqrt{2}\cosh\left[\frac{\gamma_{3,i,j}}{2\sqrt{2}} - \frac{\gamma_{3,i,j}\theta_{1,i,j}}{2\sqrt{2}}\right] c_{6,i,j}}{\gamma_{3,i,j}\theta_{1,i,j}} +$$

$$\frac{\sqrt{2}\cosh\left[\frac{\gamma_{3,i,j}}{2\sqrt{2}} + \frac{\gamma_{3,i,j}\theta_{1,i,j}}{2\sqrt{2}}\right] c_{6,i,j}}{\gamma_{3,i,j}\theta_{1,i,j}} - \frac{\sqrt{2}\sinh\left[\frac{\gamma_{3,i,j}}{2\sqrt{2}} - \frac{\gamma_{3,i,j}\theta_{2,i,j}}{2\sqrt{2}}\right] c_{7,i,j}}{\gamma_{3,i,j}\theta_{2,i,j}} +$$

$$\frac{\sqrt{2}\sinh\left[\frac{\gamma_{3,i,j}}{2\sqrt{2}} + \frac{\gamma_{3,i,j}\theta_{2,i,j}}{2\sqrt{2}}\right] c_{7,i,j}}{\gamma_{3,i,j}\theta_{2,i,j}} - \frac{\sqrt{2}\cosh\left[\frac{\gamma_{3,i,j}}{2\sqrt{2}} - \frac{\gamma_{3,i,j}\theta_{2,i,j}}{2\sqrt{2}}\right] c_{8,i,j}}{\gamma_{3,i,j}\theta_{2,i,j}} +$$

$$\frac{\sqrt{2}\cosh\left[\frac{\gamma_{3,i,j}}{2\sqrt{2}} + \frac{\gamma_{3,i,j}\theta_{2,i,j}}{2\sqrt{2}}\right] c_{8,i,j}}{\gamma_{3,i,j}\theta_{2,i,j}} + b_{0,0,i,j} + \frac{1}{2} b_{0,1,i,j} + \frac{1}{2} b_{0,2,i,j}$$

$$\bar{\Phi}^{ij}_{2y-} =$$

$$\cosh\left[\frac{1}{2}\gamma_{2,i,j}\right] c_{3,i,j} - \sinh\left[\frac{1}{2}\gamma_{2,i,j}\right] c_{4,i,j} +$$

$$\frac{2\sinh\left[\frac{1}{2}\gamma_{1,i,j}\right] c_{1,i,j}}{\gamma_{1,i,j}} - \frac{\sqrt{2}\sinh\left[\frac{\gamma_{3,i,j}}{2\sqrt{2}} - \frac{\gamma_{3,i,j}\theta_{1,i,j}}{2\sqrt{2}}\right] c_{5,i,j}}{\gamma_{3,i,j}\theta_{1,i,j}} +$$

$$\frac{\sqrt{2}\sinh\left[\frac{\gamma_{3,i,j}}{2\sqrt{2}} + \frac{\gamma_{3,i,j}\theta_{1,i,j}}{2\sqrt{2}}\right] c_{5,i,j}}{\gamma_{3,i,j}\theta_{1,i,j}} + \frac{\sqrt{2}\cosh\left[\frac{\gamma_{3,i,j}}{2\sqrt{2}} - \frac{\gamma_{3,i,j}\theta_{1,i,j}}{2\sqrt{2}}\right] c_{6,i,j}}{\gamma_{3,i,j}\theta_{1,i,j}} -$$

$$\frac{\sqrt{2}\cosh\left[\frac{\gamma_{3,i,j}}{2\sqrt{2}} + \frac{\gamma_{3,i,j}\theta_{1,i,j}}{2\sqrt{2}}\right] c_{6,i,j}}{\gamma_{3,i,j}\theta_{1,i,j}} - \frac{\sqrt{2}\sinh\left[\frac{\gamma_{3,i,j}}{2\sqrt{2}} - \frac{\gamma_{3,i,j}\theta_{2,i,j}}{2\sqrt{2}}\right] c_{7,i,j}}{\gamma_{3,i,j}\theta_{2,i,j}} +$$

$$\frac{\sqrt{2}\sinh\left[\frac{\gamma_{3,i,j}}{2\sqrt{2}} + \frac{\gamma_{3,i,j}\theta_{2,i,j}}{2\sqrt{2}}\right] c_{7,i,j}}{\gamma_{3,i,j}\theta_{2,i,j}} + \frac{\sqrt{2}\cosh\left[\frac{\gamma_{3,i,j}}{2\sqrt{2}} - \frac{\gamma_{3,i,j}\theta_{2,i,j}}{2\sqrt{2}}\right] c_{8,i,j}}{\gamma_{3,i,j}\theta_{2,i,j}} -$$

$$\frac{\sqrt{2}\cosh\left[\frac{\gamma_{3,i,j}}{2\sqrt{2}} + \frac{\gamma_{3,i,j}\theta_{2,i,j}}{2\sqrt{2}}\right] c_{8,i,j}}{\gamma_{3,i,j}\theta_{2,i,j}} + b_{0,0,i,j} - \frac{1}{2} b_{0,1,i,j} + \frac{1}{2} b_{0,2,i,j}$$

B.2. SURFACE-AVERAGED CURRENTS

- Fast group

$$\bar{J}^{ij}_{1x+} =$$

$$-\frac{St_{1,i,j}\, a_{1,0,i,j}\, e_{1,xx,i,j}}{h} - \frac{3\, St_{1,i,j}\, a_{2,0,i,j}\, e_{1,xx,i,j}}{h} -$$

$$\frac{2\, St_{1,i,j}\, a_{3,0,i,j}\, e_{1,xx,i,j}}{h} - \frac{St_{1,i,j}\, a_{4,0,i,j}\, e_{1,xx,i,j}}{5h} -$$

$$\frac{St_{1,i,j}\, a_{0,1,i,j}\, e_{1,xy,i,j}}{h} - \frac{St_{1,i,j}\, a_{1,1,i,j}\, e_{1,xy,i,j}}{2h} - \frac{St_{1,i,j}\, a_{2,1,i,j}\, e_{1,xy,i,j}}{2h}$$

$$\bar{J}^{ij}_{1x-} =$$

$$-\frac{St_{1,i,j}\, a_{1,0,i,j}\, e_{1,xx,i,j}}{h} + \frac{3\, St_{1,i,j}\, a_{2,0,i,j}\, e_{1,xx,i,j}}{h} -$$
$$\frac{2\, St_{1,i,j}\, a_{3,0,i,j}\, e_{1,xx,i,j}}{h} + \frac{St_{1,i,j}\, a_{4,0,i,j}\, e_{1,xx,i,j}}{5h} -$$
$$\frac{St_{1,i,j}\, a_{0,1,i,j}\, e_{1,xy,i,j}}{h} + \frac{St_{1,i,j}\, a_{1,1,i,j}\, e_{1,xy,i,j}}{2h} - \frac{St_{1,i,j}\, a_{2,1,i,j}\, e_{1,xy,i,j}}{2h}$$

$$\bar{J}^{ij}_{1y+} =$$

$$-\frac{St_{1,i,j}\, a_{1,0,i,j}\, e_{1,xy,i,j}}{h} - \frac{St_{1,i,j}\, a_{1,1,i,j}\, e_{1,xy,i,j}}{2h} -$$
$$\frac{St_{1,i,j}\, a_{1,2,i,j}\, e_{1,xy,i,j}}{2h} - \frac{St_{1,i,j}\, a_{0,1,i,j}\, e_{1,yy,i,j}}{h} -$$
$$\frac{3\, St_{1,i,j}\, a_{0,2,i,j}\, e_{1,yy,i,j}}{h} - \frac{2\, St_{1,i,j}\, a_{0,3,i,j}\, e_{1,yy,i,j}}{h} - \frac{St_{1,i,j}\, a_{0,4,i,j}\, e_{1,yy,i,j}}{5h}$$

$$\bar{J}^{ij}_{1y-} =$$

$$-\frac{St_{1,i,j}\, a_{1,0,i,j}\, e_{1,xy,i,j}}{h} + \frac{St_{1,i,j}\, a_{1,1,i,j}\, e_{1,xy,i,j}}{2h} -$$
$$\frac{St_{1,i,j}\, a_{1,2,i,j}\, e_{1,xy,i,j}}{2h} - \frac{St_{1,i,j}\, a_{0,1,i,j}\, e_{1,yy,i,j}}{h} +$$
$$\frac{3\, St_{1,i,j}\, a_{0,2,i,j}\, e_{1,yy,i,j}}{h} - \frac{2\, St_{1,i,j}\, a_{0,3,i,j}\, e_{1,yy,i,j}}{h} + \frac{St_{1,i,j}\, a_{0,4,i,j}\, e_{1,yy,i,j}}{5h}$$

- Thermal group

$$\bar{J}^{ij}_{2x+} =$$

$$-\frac{\text{Sinh}\left[\frac{1}{2}\,\gamma_{1,i,j}\right]\,c_{1,i,j}\,St_{2,i,j}\,\gamma_{1,i,j}\,e_{2,xx,i,j}}{h} - \frac{\text{Cosh}\left[\frac{1}{2}\,\gamma_{1,i,j}\right]\,c_{2,i,j}\,St_{2,i,j}\,\gamma_{1,i,j}\,e_{2,xx,i,j}}{h} -$$

$$\frac{St_{2,i,j}\,b_{1,0,i,j}\,e_{2,xx,i,j}}{h} - \frac{3\,St_{2,i,j}\,b_{2,0,i,j}\,e_{2,xx,i,j}}{h} - \frac{2\,St_{2,i,j}\,b_{3,0,i,j}\,e_{2,xx,i,j}}{h} -$$

$$\frac{St_{2,i,j}\,b_{4,0,i,j}\,e_{2,xx,i,j}}{5\,h} - \frac{2\,\text{Sinh}\left[\frac{1}{2}\,\gamma_{2,i,j}\right]\,c_{4,i,j}\,St_{2,i,j}\,e_{2,xy,i,j}}{h} -$$

$$\frac{St_{2,i,j}\,b_{0,1,i,j}\,e_{2,xy,i,j}}{h} - \frac{St_{2,i,j}\,b_{1,1,i,j}\,e_{2,xy,i,j}}{2\,h} - \frac{St_{2,i,j}\,b_{2,1,i,j}\,e_{2,xy,i,j}}{2\,h} -$$

$$\frac{1}{10\,h}\left(c_{6,i,j}\,St_{2,i,j}\left(-20\,\text{Cosh}\left[\frac{\gamma_{3,i,j}\,\theta_{1,i,j}}{2\sqrt{2}}\right]\,\text{Sinh}\left[\frac{\gamma_{3,i,j}}{2\sqrt{2}}\right]\,\theta_{1,i,j}\,e_{2,xx,i,j} + \right.\right.$$

$$\left.\left.20\,\text{Cosh}\left[\frac{\gamma_{3,i,j}\,\theta_{1,i,j}}{2\sqrt{2}}\right]\,\text{Sinh}\left[\frac{\gamma_{3,i,j}}{2\sqrt{2}}\right]\,e_{2,xy,i,j}\right)\right) -$$

$$\frac{1}{10\,h}\left(c_{8,i,j}\,St_{2,i,j}\left(-20\,\text{Cosh}\left[\frac{\gamma_{3,i,j}\,\theta_{2,i,j}}{2\sqrt{2}}\right]\,\text{Sinh}\left[\frac{\gamma_{3,i,j}}{2\sqrt{2}}\right]\,\theta_{2,i,j}\,e_{2,xx,i,j} + \right.\right.$$

$$\left.\left.20\,\text{Cosh}\left[\frac{\gamma_{3,i,j}\,\theta_{2,i,j}}{2\sqrt{2}}\right]\,\text{Sinh}\left[\frac{\gamma_{3,i,j}}{2\sqrt{2}}\right]\,e_{2,xy,i,j}\right)\right) -$$

$$\frac{1}{10\,h}\left(c_{5,i,j}\,St_{2,i,j}\left(20\,\text{Sinh}\left[\frac{\gamma_{3,i,j}}{2\sqrt{2}}\right]\,\text{Sinh}\left[\frac{\gamma_{3,i,j}\,\theta_{1,i,j}}{2\sqrt{2}}\right]\,\theta_{1,i,j}\,e_{2,xx,i,j} - \right.\right.$$

$$\left.\left.20\,\text{Sinh}\left[\frac{\gamma_{3,i,j}}{2\sqrt{2}}\right]\,\text{Sinh}\left[\frac{\gamma_{3,i,j}\,\theta_{1,i,j}}{2\sqrt{2}}\right]\,e_{2,xy,i,j}\right)\right) -$$

$$\frac{1}{10\,h}\left(c_{7,i,j}\,St_{2,i,j}\left(20\,\text{Sinh}\left[\frac{\gamma_{3,i,j}}{2\sqrt{2}}\right]\,\text{Sinh}\left[\frac{\gamma_{3,i,j}\,\theta_{2,i,j}}{2\sqrt{2}}\right]\,\theta_{2,i,j}\,e_{2,xx,i,j} - \right.\right.$$

$$\left.\left.20\,\text{Sinh}\left[\frac{\gamma_{3,i,j}}{2\sqrt{2}}\right]\,\text{Sinh}\left[\frac{\gamma_{3,i,j}\,\theta_{2,i,j}}{2\sqrt{2}}\right]\,e_{2,xy,i,j}\right)\right)$$

$$\bar{J}^{ij}_{2x-} =$$

$$\frac{\text{Sinh}\left[\frac{1}{2}\,\gamma_{1,i,j}\right] c_{1,i,j}\,St_{2,i,j}\,\gamma_{1,i,j}\,e_{2,xx,i,j}}{h} - \frac{\text{Cosh}\left[\frac{1}{2}\,\gamma_{1,i,j}\right] c_{2,i,j}\,St_{2,i,j}\,\gamma_{1,i,j}\,e_{2,xx,i,j}}{h} -$$

$$\frac{St_{2,i,j}\,b_{1,0,i,j}\,e_{2,xx,i,j}}{h} + \frac{3\,St_{2,i,j}\,b_{2,0,i,j}\,e_{2,xx,i,j}}{h} - \frac{2\,St_{2,i,j}\,b_{3,0,i,j}\,e_{2,xx,i,j}}{h} +$$

$$\frac{St_{2,i,j}\,b_{4,0,i,j}\,e_{2,xx,i,j}}{5\,h} - \frac{2\,\text{Sinh}\left[\frac{1}{2}\,\gamma_{2,i,j}\right] c_{4,i,j}\,St_{2,i,j}\,e_{2,xy,i,j}}{h} -$$

$$\frac{St_{2,i,j}\,b_{0,1,i,j}\,e_{2,xy,i,j}}{h} + \frac{St_{2,i,j}\,b_{1,1,i,j}\,e_{2,xy,i,j}}{2\,h} - \frac{St_{2,i,j}\,b_{2,1,i,j}\,e_{2,xy,i,j}}{2\,h} +$$

$$\frac{1}{10\,h}\left(c_{6,i,j}\,St_{2,i,j}\left(20\,\text{Cosh}\left[\frac{\gamma_{3,i,j}\,\theta_{1,i,j}}{2\sqrt{2}}\right]\text{Sinh}\left[\frac{\gamma_{3,i,j}}{2\sqrt{2}}\right]\theta_{1,i,j}\,e_{2,xx,i,j} -\right.\right.$$

$$\left.\left.20\,\text{Cosh}\left[\frac{\gamma_{3,i,j}\,\theta_{1,i,j}}{2\sqrt{2}}\right]\text{Sinh}\left[\frac{\gamma_{3,i,j}}{2\sqrt{2}}\right]e_{2,xy,i,j}\right)\right) +$$

$$\frac{1}{10\,h}\left(c_{8,i,j}\,St_{2,i,j}\left(20\,\text{Cosh}\left[\frac{\gamma_{3,i,j}\,\theta_{2,i,j}}{2\sqrt{2}}\right]\text{Sinh}\left[\frac{\gamma_{3,i,j}}{2\sqrt{2}}\right]\theta_{2,i,j}\,e_{2,xx,i,j} -\right.\right.$$

$$\left.\left.20\,\text{Cosh}\left[\frac{\gamma_{3,i,j}\,\theta_{2,i,j}}{2\sqrt{2}}\right]\text{Sinh}\left[\frac{\gamma_{3,i,j}}{2\sqrt{2}}\right]e_{2,xy,i,j}\right)\right) +$$

$$\frac{1}{10\,h}\left(c_{5,i,j}\,St_{2,i,j}\left(20\,\text{Sinh}\left[\frac{\gamma_{3,i,j}}{2\sqrt{2}}\right]\text{Sinh}\left[\frac{\gamma_{3,i,j}\,\theta_{1,i,j}}{2\sqrt{2}}\right]\theta_{1,i,j}\,e_{2,xx,i,j} -\right.\right.$$

$$\left.\left.20\,\text{Sinh}\left[\frac{\gamma_{3,i,j}}{2\sqrt{2}}\right]\text{Sinh}\left[\frac{\gamma_{3,i,j}\,\theta_{1,i,j}}{2\sqrt{2}}\right]e_{2,xy,i,j}\right)\right) +$$

$$\frac{1}{10\,h}\left(c_{7,i,j}\,St_{2,i,j}\left(20\,\text{Sinh}\left[\frac{\gamma_{3,i,j}}{2\sqrt{2}}\right]\text{Sinh}\left[\frac{\gamma_{3,i,j}\,\theta_{2,i,j}}{2\sqrt{2}}\right]\theta_{2,i,j}\,e_{2,xx,i,j} -\right.\right.$$

$$\left.\left.20\,\text{Sinh}\left[\frac{\gamma_{3,i,j}}{2\sqrt{2}}\right]\text{Sinh}\left[\frac{\gamma_{3,i,j}\,\theta_{2,i,j}}{2\sqrt{2}}\right]e_{2,xy,i,j}\right)\right)$$

$$\bar{J}^{ij}_{2y+} =$$

$$-\frac{2\,\mathrm{Sinh}\left[\frac{1}{2}\gamma_{1,i,j}\right]\,c_{2,i,j}\,St_{2,i,j}\,e_{2,xy,i,j}}{h} -$$

$$\frac{St_{2,i,j}\,b_{1,0,i,j}\,e_{2,xy,i,j}}{h} - \frac{St_{2,i,j}\,b_{1,1,i,j}\,e_{2,xy,i,j}}{2h} - \frac{St_{2,i,j}\,b_{1,2,i,j}\,e_{2,xy,i,j}}{2h} +$$

$$\frac{2\,\mathrm{Sinh}\left[\frac{\gamma_{3,i,j}}{2\sqrt{2}}\right]\,\mathrm{Sinh}\left[\frac{\gamma_{3,i,j}\theta_{1,i,j}}{2\sqrt{2}}\right]\,c_{5,i,j}\,St_{2,i,j}\,(\theta_{1,i,j}\,e_{2,xy,i,j} - e_{2,yy,i,j})}{h\theta_{1,i,j}} -$$

$$\frac{\mathrm{Sinh}\left[\frac{1}{2}\gamma_{2,i,j}\right]\,c_{3,i,j}\,St_{2,i,j}\,\gamma_{2,i,j}\,e_{2,yy,i,j}}{h} -$$

$$\frac{\mathrm{Cosh}\left[\frac{1}{2}\gamma_{2,i,j}\right]\,c_{4,i,j}\,St_{2,i,j}\,\gamma_{2,i,j}\,e_{2,yy,i,j}}{h} - \frac{St_{2,i,j}\,b_{0,1,i,j}\,e_{2,yy,i,j}}{h} -$$

$$\frac{3\,St_{2,i,j}\,b_{0,2,i,j}\,e_{2,yy,i,j}}{h} - \frac{2\,St_{2,i,j}\,b_{0,3,i,j}\,e_{2,yy,i,j}}{h} - \frac{St_{2,i,j}\,b_{0,4,i,j}\,e_{2,yy,i,j}}{5h} -$$

$$\frac{1}{10h\theta_{1,i,j}\,\theta_{2,i,j}}\left(c_{8,i,j}\,St_{2,i,j}\left(-20\,\mathrm{Cosh}\left[\frac{\gamma_{3,i,j}}{2\sqrt{2}}\right]\,\mathrm{Sinh}\left[\frac{\gamma_{3,i,j}\theta_{2,i,j}}{2\sqrt{2}}\right]\,\theta_{1,i,j}\,\theta_{2,i,j}\,e_{2,xy,i,j} + \right.\right.$$

$$\left.\left.20\,\mathrm{Cosh}\left[\frac{\gamma_{3,i,j}}{2\sqrt{2}}\right]\,\mathrm{Sinh}\left[\frac{\gamma_{3,i,j}\theta_{2,i,j}}{2\sqrt{2}}\right]\,\theta_{1,i,j}\,e_{2,yy,i,j}\right)\right) -$$

$$\frac{1}{10h\theta_{1,i,j}\,\theta_{2,i,j}}\left(c_{7,i,j}\,St_{2,i,j}\left(-20\,\mathrm{Sinh}\left[\frac{\gamma_{3,i,j}}{2\sqrt{2}}\right]\,\mathrm{Sinh}\left[\frac{\gamma_{3,i,j}\theta_{2,i,j}}{2\sqrt{2}}\right]\,\theta_{1,i,j}\,\theta_{2,i,j}\,e_{2,xy,i,j} + \right.\right.$$

$$\left.\left.20\,\mathrm{Sinh}\left[\frac{\gamma_{3,i,j}}{2\sqrt{2}}\right]\,\mathrm{Sinh}\left[\frac{\gamma_{3,i,j}\theta_{2,i,j}}{2\sqrt{2}}\right]\,\theta_{1,i,j}\,e_{2,yy,i,j}\right)\right) -$$

$$\frac{1}{10h\theta_{1,i,j}\,\theta_{2,i,j}}\left(c_{6,i,j}\,St_{2,i,j}\left(-20\,\mathrm{Cosh}\left[\frac{\gamma_{3,i,j}}{2\sqrt{2}}\right]\,\mathrm{Sinh}\left[\frac{\gamma_{3,i,j}\theta_{1,i,j}}{2\sqrt{2}}\right]\,\theta_{1,i,j}\,\theta_{2,i,j}\,e_{2,xy,i,j} + \right.\right.$$

$$\left.\left.20\,\mathrm{Cosh}\left[\frac{\gamma_{3,i,j}}{2\sqrt{2}}\right]\,\mathrm{Sinh}\left[\frac{\gamma_{3,i,j}\theta_{1,i,j}}{2\sqrt{2}}\right]\,\theta_{2,i,j}\,e_{2,yy,i,j}\right)\right)$$

$$\bar{J}^{ij}_{2y-} =$$

$$-\frac{2\,\mathrm{Sinh}\left[\frac{1}{2}\gamma_{1,i,j}\right] c_{2,i,j}\,St_{2,i,j}\,e_{2,xy,i,j}}{h} -$$

$$\frac{St_{2,i,j}\,b_{1,0,i,j}\,e_{2,xy,i,j}}{h} + \frac{St_{2,i,j}\,b_{1,1,i,j}\,e_{2,xy,i,j}}{2h} - \frac{St_{2,i,j}\,b_{1,2,i,j}\,e_{2,xy,i,j}}{2h} -$$

$$\frac{2\,\mathrm{Sinh}\left[\frac{\gamma_{3,i,j}}{2\sqrt{2}}\right]\mathrm{Sinh}\left[\frac{\gamma_{3,i,j}\theta_{1,i,j}}{2\sqrt{2}}\right] c_{5,i,j}\,St_{2,i,j}\,(\theta_{1,i,j}\,e_{2,xy,i,j} - e_{2,yy,i,j})}{h\theta_{1,i,j}} +$$

$$\frac{\mathrm{Sinh}\left[\frac{1}{2}\gamma_{2,i,j}\right] c_{3,i,j}\,St_{2,i,j}\,\gamma_{2,i,j}\,e_{2,yy,i,j}}{h} -$$

$$\frac{\mathrm{Cosh}\left[\frac{1}{2}\gamma_{2,i,j}\right] c_{4,i,j}\,St_{2,i,j}\,\gamma_{2,i,j}\,e_{2,yy,i,j}}{h} - \frac{St_{2,i,j}\,b_{0,1,i,j}\,e_{2,yy,i,j}}{h} +$$

$$\frac{3\,St_{2,i,j}\,b_{0,2,i,j}\,e_{2,yy,i,j}}{h} - \frac{2\,St_{2,i,j}\,b_{0,3,i,j}\,e_{2,yy,i,j}}{h} + \frac{St_{2,i,j}\,b_{0,4,i,j}\,e_{2,yy,i,j}}{5h} -$$

$$\frac{1}{10h\theta_{1,i,j}\theta_{2,i,j}}\left(c_{8,i,j}\,St_{2,i,j}\left(-20\,\mathrm{Cosh}\left[\frac{\gamma_{3,i,j}}{2\sqrt{2}}\right]\mathrm{Sinh}\left[\frac{\gamma_{3,i,j}\theta_{2,i,j}}{2\sqrt{2}}\right]\theta_{1,i,j}\,\theta_{2,i,j}\,e_{2,xy,i,j} + \right.\right.$$

$$\left.\left.20\,\mathrm{Cosh}\left[\frac{\gamma_{3,i,j}}{2\sqrt{2}}\right]\mathrm{Sinh}\left[\frac{\gamma_{3,i,j}\theta_{2,i,j}}{2\sqrt{2}}\right]\theta_{1,i,j}\,e_{2,yy,i,j}\right)\right) -$$

$$\frac{1}{10h\theta_{1,i,j}\theta_{2,i,j}}\left(c_{7,i,j}\,St_{2,i,j}\left(20\,\mathrm{Sinh}\left[\frac{\gamma_{3,i,j}}{2\sqrt{2}}\right]\mathrm{Sinh}\left[\frac{\gamma_{3,i,j}\theta_{2,i,j}}{2\sqrt{2}}\right]\theta_{1,i,j}\,\theta_{2,i,j}\,e_{2,xy,i,j} - \right.\right.$$

$$\left.\left.20\,\mathrm{Sinh}\left[\frac{\gamma_{3,i,j}}{2\sqrt{2}}\right]\mathrm{Sinh}\left[\frac{\gamma_{3,i,j}\theta_{2,i,j}}{2\sqrt{2}}\right]\theta_{1,i,j}\,e_{2,yy,i,j}\right)\right) -$$

$$\frac{1}{10h\theta_{1,i,j}\theta_{2,i,j}}\left(c_{6,i,j}\,St_{2,i,j}\left(-20\,\mathrm{Cosh}\left[\frac{\gamma_{3,i,j}}{2\sqrt{2}}\right]\mathrm{Sinh}\left[\frac{\gamma_{3,i,j}\theta_{1,i,j}}{2\sqrt{2}}\right]\theta_{1,i,j}\,\theta_{2,i,j}\,e_{2,xy,i,j} + \right.\right.$$

$$\left.\left.20\,\mathrm{Cosh}\left[\frac{\gamma_{3,i,j}}{2\sqrt{2}}\right]\mathrm{Sinh}\left[\frac{\gamma_{3,i,j}\theta_{1,i,j}}{2\sqrt{2}}\right]\theta_{2,i,j}\,e_{2,yy,i,j}\right)\right)$$

C. CONTINUITY EQUATIONS OF SURFACE-AVERAGED FLUXES AND CURRENTS

C.1. FLUX CONTINUITY EQUATIONS

- Fast flux

$$\bar{\Phi}_{1x+}^{i-1,j} - \bar{\Phi}_{1x-}^{i,j} = 0$$

$$a_{0,0,-1+i,j} - a_{0,0,i,j} + \frac{1}{2} a_{1,0,-1+i,j} + \frac{1}{2} a_{1,0,i,j} + \frac{1}{2} a_{2,0,-1+i,j} - \frac{1}{2} a_{2,0,i,j} == 0$$

$$\bar{\Phi}_{1x+}^{i-1,j-1} - \bar{\Phi}_{1x-}^{i,j-1} = 0$$

$$a_{0,0,-1+i,-1+j} - a_{0,0,i,-1+j} + \frac{1}{2} a_{1,0,-1+i,-1+j} + \frac{1}{2} a_{1,0,i,-1+j} + \frac{1}{2} a_{2,0,-1+i,-1+j} - \frac{1}{2} a_{2,0,i,-1+j} == 0$$

$$\bar{\Phi}_{1y+}^{i-1,j-1} - \bar{\Phi}_{1y-}^{i-1,j} = 0$$

$$a_{0,0,-1+i,-1+j} - a_{0,0,-1+i,j} + \frac{1}{2} a_{0,1,-1+i,-1+j} + \frac{1}{2} a_{0,1,-1+i,j} + \frac{1}{2} a_{0,2,-1+i,-1+j} - \frac{1}{2} a_{0,2,-1+i,j} == 0$$

$$\bar{\Phi}_{1y+}^{i,j-1} - \bar{\Phi}_{1y-}^{i,j} = 0$$

$$a_{0,0,i,-1+j} - a_{0,0,i,j} + \frac{1}{2} a_{0,1,i,-1+j} + \frac{1}{2} a_{0,1,i,j} + \frac{1}{2} a_{0,2,i,-1+j} - \frac{1}{2} a_{0,2,i,j} == 0$$

- Thermal flux

$$\bar{\Phi}_{2x+}^{i-1,j} - \bar{\Phi}_{2x-}^{i,j} = 0$$

$$\text{Cosh}\left[\frac{1}{2}\,\gamma_{1,-1+i,j}\right] c_{1,-1+i,j} - \text{Cosh}\left[\frac{1}{2}\,\gamma_{1,i,j}\right] c_{1,i,j} +$$

$$\text{Sinh}\left[\frac{1}{2}\,\gamma_{1,-1+i,j}\right] c_{2,-1+i,j} + \text{Sinh}\left[\frac{1}{2}\,\gamma_{1,i,j}\right] c_{2,i,j} + \frac{2\,\text{Sinh}\left[\frac{1}{2}\,\gamma_{2,-1+i,j}\right] c_{3,-1+i,j}}{\gamma_{2,-1+i,j}} -$$

$$\frac{2\,\text{Sinh}\left[\frac{1}{2}\,\gamma_{2,i,j}\right] c_{3,i,j}}{\gamma_{2,i,j}} + \frac{2\sqrt{2}\,\text{Cosh}\left[\frac{\gamma_{3,-1+i,j}\Theta_{1,-1+i,j}}{2\sqrt{2}}\right] \text{Sinh}\left[\frac{\gamma_{3,-1+i,j}}{2\sqrt{2}}\right] c_{5,-1+i,j}}{\gamma_{3,-1+i,j}} -$$

$$\frac{2\sqrt{2}\,\text{Sinh}\left[\frac{\gamma_{3,-1+i,j}}{2\sqrt{2}}\right] \text{Sinh}\left[\frac{\gamma_{3,-1+i,j}\Theta_{1,-1+i,j}}{2\sqrt{2}}\right] c_{6,-1+i,j}}{\gamma_{3,-1+i,j}} +$$

$$\frac{2\sqrt{2}\,\text{Cosh}\left[\frac{\gamma_{3,-1+i,j}\Theta_{2,-1+i,j}}{2\sqrt{2}}\right] \text{Sinh}\left[\frac{\gamma_{3,-1+i,j}}{2\sqrt{2}}\right] c_{7,-1+i,j}}{\gamma_{3,-1+i,j}} -$$

$$\frac{2\sqrt{2}\,\text{Sinh}\left[\frac{\gamma_{3,-1+i,j}}{2\sqrt{2}}\right] \text{Sinh}\left[\frac{\gamma_{3,-1+i,j}\Theta_{2,-1+i,j}}{2\sqrt{2}}\right] c_{8,-1+i,j}}{\gamma_{3,-1+i,j}} -$$

$$\frac{2\sqrt{2}\,\text{Cosh}\left[\frac{\gamma_{3,i,j}\Theta_{1,i,j}}{2\sqrt{2}}\right] \text{Sinh}\left[\frac{\gamma_{3,i,j}}{2\sqrt{2}}\right] c_{5,i,j}}{\gamma_{3,i,j}} - \frac{2\sqrt{2}\,\text{Sinh}\left[\frac{\gamma_{3,i,j}}{2\sqrt{2}}\right] \text{Sinh}\left[\frac{\gamma_{3,i,j}\Theta_{1,i,j}}{2\sqrt{2}}\right] c_{6,i,j}}{\gamma_{3,i,j}} -$$

$$\frac{2\sqrt{2}\,\text{Cosh}\left[\frac{\gamma_{3,i,j}\Theta_{2,i,j}}{2\sqrt{2}}\right] \text{Sinh}\left[\frac{\gamma_{3,i,j}}{2\sqrt{2}}\right] c_{7,i,j}}{\gamma_{3,i,j}} - \frac{2\sqrt{2}\,\text{Sinh}\left[\frac{\gamma_{3,i,j}}{2\sqrt{2}}\right] \text{Sinh}\left[\frac{\gamma_{3,i,j}\Theta_{2,i,j}}{2\sqrt{2}}\right] c_{8,i,j}}{\gamma_{3,i,j}} +$$

$$b_{0,0,-1+i,j} - b_{0,0,i,j} + \frac{1}{2}\,b_{1,0,-1+i,j} + \frac{1}{2}\,b_{1,0,i,j} + \frac{1}{2}\,b_{2,0,-1+i,j} - \frac{1}{2}\,b_{2,0,i,j} == 0$$

$$\bar{\Phi}^{i-1,j-1}_{2x+} - \bar{\Phi}^{i,j-1}_{2x-} = 0$$

$$\text{Cosh}\left[\frac{1}{2}\,\gamma_{1,-1+i,-1+j}\right] c_{1,-1+i,-1+j} - \text{Cosh}\left[\frac{1}{2}\,\gamma_{1,i,-1+j}\right] c_{1,i,-1+j} +$$

$$\text{Sinh}\left[\frac{1}{2}\,\gamma_{1,-1+i,-1+j}\right] c_{2,-1+i,-1+j} + \text{Sinh}\left[\frac{1}{2}\,\gamma_{1,i,-1+j}\right] c_{2,i,-1+j} + \frac{2\,\text{Sinh}\left[\frac{1}{2}\,\gamma_{2,-1+i,-1+j}\right] c_{3,-1+i,-1+j}}{\gamma_{2,-1+i,-1+j}} -$$

$$\frac{2\,\text{Sinh}\left[\frac{1}{2}\,\gamma_{2,i,-1+j}\right] c_{3,i,-1+j}}{\gamma_{2,i,-1+j}} + \frac{2\sqrt{2}\,\text{Cosh}\left[\frac{\gamma_{3,-1+i,-1+j}\Theta_{1,-1+i,-1+j}}{2\sqrt{2}}\right] \text{Sinh}\left[\frac{\gamma_{3,-1+i,-1+j}}{2\sqrt{2}}\right] c_{5,-1+i,-1+j}}{\gamma_{3,-1+i,-1+j}} -$$

$$\frac{2\sqrt{2}\,\text{Sinh}\left[\frac{\gamma_{3,-1+i,-1+j}}{2\sqrt{2}}\right] \text{Sinh}\left[\frac{\gamma_{3,-1+i,-1+j}\Theta_{1,-1+i,-1+j}}{2\sqrt{2}}\right] c_{6,-1+i,-1+j}}{\gamma_{3,-1+i,-1+j}} +$$

$$\frac{2\sqrt{2}\,\text{Cosh}\left[\frac{\gamma_{3,-1+i,-1+j}\Theta_{2,-1+i,-1+j}}{2\sqrt{2}}\right] \text{Sinh}\left[\frac{\gamma_{3,-1+i,-1+j}}{2\sqrt{2}}\right] c_{7,-1+i,-1+j}}{\gamma_{3,-1+i,-1+j}} -$$

$$\frac{2\sqrt{2}\,\text{Sinh}\left[\frac{\gamma_{3,-1+i,-1+j}}{2\sqrt{2}}\right] \text{Sinh}\left[\frac{\gamma_{3,-1+i,-1+j}\Theta_{2,-1+i,-1+j}}{2\sqrt{2}}\right] c_{8,-1+i,-1+j}}{\gamma_{3,-1+i,-1+j}} -$$

$$\frac{2\sqrt{2}\,\text{Cosh}\left[\frac{\gamma_{3,i,-1+j}\Theta_{1,i,-1+j}}{2\sqrt{2}}\right] \text{Sinh}\left[\frac{\gamma_{3,i,-1+j}}{2\sqrt{2}}\right] c_{5,i,-1+j}}{\gamma_{3,i,-1+j}} -$$

$$\frac{2\sqrt{2}\,\text{Sinh}\left[\frac{\gamma_{3,i,-1+j}}{2\sqrt{2}}\right] \text{Sinh}\left[\frac{\gamma_{3,i,-1+j}\Theta_{1,i,-1+j}}{2\sqrt{2}}\right] c_{6,i,-1+j}}{\gamma_{3,i,-1+j}} -$$

$$\frac{2\sqrt{2}\,\text{Cosh}\left[\frac{\gamma_{3,i,-1+j}\Theta_{2,i,-1+j}}{2\sqrt{2}}\right] \text{Sinh}\left[\frac{\gamma_{3,i,-1+j}}{2\sqrt{2}}\right] c_{7,i,-1+j}}{\gamma_{3,i,-1+j}} -$$

$$\frac{2\sqrt{2}\,\text{Sinh}\left[\frac{\gamma_{3,i,-1+j}}{2\sqrt{2}}\right] \text{Sinh}\left[\frac{\gamma_{3,i,-1+j}\Theta_{2,i,-1+j}}{2\sqrt{2}}\right] c_{8,i,-1+j}}{\gamma_{3,i,-1+j}} + b_{0,0,-1+i,-1+j} -$$

$$b_{0,0,i,-1+j} + \frac{1}{2}\,b_{1,0,-1+i,-1+j} + \frac{1}{2}\,b_{1,0,i,-1+j} + \frac{1}{2}\,b_{2,0,-1+i,-1+j} - \frac{1}{2}\,b_{2,0,i,-1+j} == 0$$

$$\bar{\Phi}_{2y+}^{i-1,j-1} - \bar{\Phi}_{2y-}^{i-1,j} = 0$$

$$\text{Cosh}\left[\frac{1}{2}\,\gamma_{2,-1+i,-1+j}\right] c_{3,-1+i,-1+j} - \text{Cosh}\left[\frac{1}{2}\,\gamma_{2,-1+i,j}\right] c_{3,-1+i,j} +$$

$$\text{Sinh}\left[\frac{1}{2}\,\gamma_{2,-1+i,-1+j}\right] c_{4,-1+i,-1+j} + \text{Sinh}\left[\frac{1}{2}\,\gamma_{2,-1+i,j}\right] c_{4,-1+i,j} + \frac{2\,\text{Sinh}\left[\frac{1}{2}\,\gamma_{1,-1+i,-1+j}\right] c_{1,-1+i,-1+j}}{\gamma_{1,-1+i,-1+j}} -$$

$$\frac{2\,\text{Sinh}\left[\frac{1}{2}\,\gamma_{1,-1+i,j}\right] c_{1,-1+i,j}}{\gamma_{1,-1+i,j}} + \frac{2\sqrt{2}\,\text{Cosh}\left[\frac{\gamma_{3,-1+i,-1+j}}{2\sqrt{2}}\right] \text{Sinh}\left[\frac{\gamma_{3,-1+i,-1+j}\theta_{1,-1+i,-1+j}}{2\sqrt{2}}\right] c_{5,-1+i,-1+j}}{\gamma_{3,-1+i,-1+j}\,\theta_{1,-1+i,-1+j}} +$$

$$\frac{2\sqrt{2}\,\text{Sinh}\left[\frac{\gamma_{3,-1+i,-1+j}}{2\sqrt{2}}\right] \text{Sinh}\left[\frac{\gamma_{3,-1+i,-1+j}\theta_{1,-1+i,-1+j}}{2\sqrt{2}}\right] c_{6,-1+i,-1+j}}{\gamma_{3,-1+i,-1+j}\,\theta_{1,-1+i,-1+j}} -$$

$$\frac{2\sqrt{2}\,\text{Cosh}\left[\frac{\gamma_{3,-1+i,j}}{2\sqrt{2}}\right] \text{Sinh}\left[\frac{\gamma_{3,-1+i,j}\theta_{1,-1+i,j}}{2\sqrt{2}}\right] c_{5,-1+i,j}}{\gamma_{3,-1+i,j}\,\theta_{1,-1+i,j}} +$$

$$\frac{2\sqrt{2}\,\text{Sinh}\left[\frac{\gamma_{3,-1+i,j}}{2\sqrt{2}}\right] \text{Sinh}\left[\frac{\gamma_{3,-1+i,j}\theta_{1,-1+i,j}}{2\sqrt{2}}\right] c_{6,-1+i,j}}{\gamma_{3,-1+i,j}\,\theta_{1,-1+i,j}} +$$

$$\frac{2\sqrt{2}\,\text{Cosh}\left[\frac{\gamma_{3,-1+i,-1+j}}{2\sqrt{2}}\right] \text{Sinh}\left[\frac{\gamma_{3,-1+i,-1+j}\theta_{2,-1+i,-1+j}}{2\sqrt{2}}\right] c_{7,-1+i,-1+j}}{\gamma_{3,-1+i,-1+j}\,\theta_{2,-1+i,-1+j}} +$$

$$\frac{2\sqrt{2}\,\text{Sinh}\left[\frac{\gamma_{3,-1+i,-1+j}}{2\sqrt{2}}\right] \text{Sinh}\left[\frac{\gamma_{3,-1+i,-1+j}\theta_{2,-1+i,-1+j}}{2\sqrt{2}}\right] c_{8,-1+i,-1+j}}{\gamma_{3,-1+i,-1+j}\,\theta_{2,-1+i,-1+j}} -$$

$$\frac{2\sqrt{2}\,\text{Cosh}\left[\frac{\gamma_{3,-1+i,j}}{2\sqrt{2}}\right] \text{Sinh}\left[\frac{\gamma_{3,-1+i,j}\theta_{2,-1+i,j}}{2\sqrt{2}}\right] c_{7,-1+i,j}}{\gamma_{3,-1+i,j}\,\theta_{2,-1+i,j}} +$$

$$\frac{2\sqrt{2}\,\text{Sinh}\left[\frac{\gamma_{3,-1+i,j}}{2\sqrt{2}}\right] \text{Sinh}\left[\frac{\gamma_{3,-1+i,j}\theta_{2,-1+i,j}}{2\sqrt{2}}\right] c_{8,-1+i,j}}{\gamma_{3,-1+i,j}\,\theta_{2,-1+i,j}} + b_{0,0,-1+i,-1+j} -$$

$$b_{0,0,-1+i,j} + \frac{1}{2}\,b_{0,1,-1+i,-1+j} + \frac{1}{2}\,b_{0,1,-1+i,j} + \frac{1}{2}\,b_{0,2,-1+i,-1+j} - \frac{1}{2}\,b_{0,2,-1+i,j} == 0$$

$$\bar{\Phi}^{i,j-1}_{2y+} - \bar{\Phi}^{i,j}_{2y-} = 0$$

$$\cosh\left[\frac{1}{2}\gamma_{2,i,-1+j}\right] c_{3,i,-1+j} - \cosh\left[\frac{1}{2}\gamma_{2,i,j}\right] c_{3,i,j} +$$

$$\sinh\left[\frac{1}{2}\gamma_{2,i,-1+j}\right] c_{4,i,-1+j} + \sinh\left[\frac{1}{2}\gamma_{2,i,j}\right] c_{4,i,j} + \frac{2\sinh\left[\frac{1}{2}\gamma_{1,i,-1+j}\right] c_{1,i,-1+j}}{\gamma_{1,i,-1+j}} -$$

$$\frac{2\sinh\left[\frac{1}{2}\gamma_{1,i,j}\right] c_{1,i,j}}{\gamma_{1,i,j}} + \frac{2\sqrt{2}\cosh\left[\frac{\gamma_{3,i,-1+j}}{2\sqrt{2}}\right]\sinh\left[\frac{\gamma_{3,i,-1+j}\theta_{1,i,-1+j}}{2\sqrt{2}}\right] c_{5,i,-1+j}}{\gamma_{3,i,-1+j}\theta_{1,i,-1+j}} +$$

$$\frac{2\sqrt{2}\sinh\left[\frac{\gamma_{3,i,-1+j}}{2\sqrt{2}}\right]\sinh\left[\frac{\gamma_{3,i,-1+j}\theta_{1,i,-1+j}}{2\sqrt{2}}\right] c_{6,i,-1+j}}{\gamma_{3,i,-1+j}\theta_{1,i,-1+j}} - \frac{2\sqrt{2}\cosh\left[\frac{\gamma_{3,i,j}}{2\sqrt{2}}\right]\sinh\left[\frac{\gamma_{3,i,j}\theta_{1,i,j}}{2\sqrt{2}}\right] c_{5,i,j}}{\gamma_{3,i,j}\theta_{1,i,j}} +$$

$$\frac{2\sqrt{2}\sinh\left[\frac{\gamma_{3,i,j}}{2\sqrt{2}}\right]\sinh\left[\frac{\gamma_{3,i,j}\theta_{1,i,j}}{2\sqrt{2}}\right] c_{6,i,j}}{\gamma_{3,i,j}\theta_{1,i,j}} + \frac{2\sqrt{2}\cosh\left[\frac{\gamma_{3,i,-1+j}}{2\sqrt{2}}\right]\sinh\left[\frac{\gamma_{3,i,-1+j}\theta_{2,i,-1+j}}{2\sqrt{2}}\right] c_{7,i,-1+j}}{\gamma_{3,i,-1+j}\theta_{2,i,-1+j}} +$$

$$\frac{2\sqrt{2}\sinh\left[\frac{\gamma_{3,i,-1+j}}{2\sqrt{2}}\right]\sinh\left[\frac{\gamma_{3,i,-1+j}\theta_{2,i,-1+j}}{2\sqrt{2}}\right] c_{8,i,-1+j}}{\gamma_{3,i,-1+j}\theta_{2,i,-1+j}} -$$

$$\frac{2\sqrt{2}\cosh\left[\frac{\gamma_{3,i,j}}{2\sqrt{2}}\right]\sinh\left[\frac{\gamma_{3,i,j}\theta_{2,i,j}}{2\sqrt{2}}\right] c_{7,i,j}}{\gamma_{3,i,j}\theta_{2,i,j}} + \frac{2\sqrt{2}\sinh\left[\frac{\gamma_{3,i,j}}{2\sqrt{2}}\right]\sinh\left[\frac{\gamma_{3,i,j}\theta_{2,i,j}}{2\sqrt{2}}\right] c_{8,i,j}}{\gamma_{3,i,j}\theta_{2,i,j}} +$$

$$b_{0,0,i,-1+j} - b_{0,0,i,j} + \frac{1}{2} b_{0,1,i,-1+j} + \frac{1}{2} b_{0,1,i,j} + \frac{1}{2} b_{0,2,i,-1+j} - \frac{1}{2} b_{0,2,i,j} == 0$$

C.2. CURRENT CONTINUITY EQUATIONS

- Fast current

$$\bar{J}^{i-1,j}_{1x+} - \bar{J}^{i,j}_{1x-} = 0$$

$$\frac{1}{h}\left(St_{1,-1+i,j}\left(-a_{1,0,-1+i,j}\, e_{1,xx,-1+i,j} - 3a_{2,0,-1+i,j}\, e_{1,xx,-1+i,j} - 2a_{3,0,-1+i,j}\, e_{1,xx,-1+i,j} - \right.\right.$$

$$\left.\left.\frac{1}{5} a_{4,0,-1+i,j}\, e_{1,xx,-1+i,j} - a_{0,1,-1+i,j}\, e_{1,xy,-1+i,j} - \frac{1}{2} a_{1,1,-1+i,j}\, e_{1,xy,-1+i,j} - \frac{1}{2} a_{2,1,-1+i,j}\, e_{1,xy,-1+i,j}\right)\right) -$$

$$\frac{1}{h}\left(St_{1,i,j}\left(-a_{1,0,i,j}\, e_{1,xx,i,j} + 3a_{2,0,i,j}\, e_{1,xx,i,j} - 2a_{3,0,i,j}\, e_{1,xx,i,j} + \frac{1}{5} a_{4,0,i,j}\, e_{1,xx,i,j} - \right.\right.$$

$$\left.\left. a_{0,1,i,j}\, e_{1,xy,i,j} + \frac{1}{2} a_{1,1,i,j}\, e_{1,xy,i,j} - \frac{1}{2} a_{2,1,i,j}\, e_{1,xy,i,j}\right)\right) == 0$$

$$\overline{J}_{1x+}^{i-1,j-1} - \overline{J}_{1x-}^{i,j-1} = 0$$

$$\frac{1}{h}\left(St_{1,-1+i,-1+j}\left(-a_{1,0,-1+i,-1+j}\,e_{1,xx,-1+i,-1+j} - 3\,a_{2,0,-1+i,-1+j}\,e_{1,xx,-1+i,-1+j} - 2\,a_{3,0,-1+i,-1+j}\,e_{1,xx,-1+i,-1+j} - \frac{1}{5}\,a_{4,0,-1+i,-1+j}\,e_{1,xx,-1+i,-1+j} - a_{0,1,-1+i,-1+j}\,e_{1,xy,-1+i,-1+j} - \frac{1}{2}\,a_{1,1,-1+i,-1+j}\,e_{1,xy,-1+i,-1+j} - \frac{1}{2}\,a_{2,1,-1+i,-1+j}\,e_{1,xy,-1+i,-1+j}\right)\right) -$$

$$\frac{1}{h}\left(St_{1,i,-1+j}\left(-a_{1,0,i,-1+j}\,e_{1,xx,i,-1+j} + 3\,a_{2,0,i,-1+j}\,e_{1,xx,i,-1+j} - 2\,a_{3,0,i,-1+j}\,e_{1,xx,i,-1+j} + \frac{1}{5}\,a_{4,0,i,-1+j}\,e_{1,xx,i,-1+j} - a_{0,1,i,-1+j}\,e_{1,xy,i,-1+j} + \frac{1}{2}\,a_{1,1,i,-1+j}\,e_{1,xy,i,-1+j} - \frac{1}{2}\,a_{2,1,i,-1+j}\,e_{1,xy,i,-1+j}\right)\right) == 0$$

$$\overline{J}_{1y+}^{i-1,j-1} - \overline{J}_{1y-}^{i-1,j} = 0$$

$$\frac{1}{h}\left(St_{1,-1+i,-1+j}\left(-a_{1,0,-1+i,-1+j}\,e_{1,xy,-1+i,-1+j} - \frac{1}{2}\,a_{1,1,-1+i,-1+j}\,e_{1,xy,-1+i,-1+j} - \frac{1}{2}\,a_{1,2,-1+i,-1+j}\,e_{1,xy,-1+i,-1+j} - a_{0,1,-1+i,-1+j}\,e_{1,yy,-1+i,-1+j} - 3\,a_{0,2,-1+i,-1+j}\,e_{1,yy,-1+i,-1+j} - 2\,a_{0,3,-1+i,-1+j}\,e_{1,yy,-1+i,-1+j} - \frac{1}{5}\,a_{0,4,-1+i,-1+j}\,e_{1,yy,-1+i,-1+j}\right)\right) -$$

$$\frac{1}{h}\left(St_{1,-1+i,j}\left(-a_{1,0,-1+i,j}\,e_{1,xy,-1+i,j} + \frac{1}{2}\,a_{1,1,-1+i,j}\,e_{1,xy,-1+i,j} - \frac{1}{2}\,a_{1,2,-1+i,j}\,e_{1,xy,-1+i,j} - a_{0,1,-1+i,j}\,e_{1,yy,-1+i,j} + 3\,a_{0,2,-1+i,j}\,e_{1,yy,-1+i,j} - 2\,a_{0,3,-1+i,j}\,e_{1,yy,-1+i,j} + \frac{1}{5}\,a_{0,4,-1+i,j}\,e_{1,yy,-1+i,j}\right)\right) == 0$$

$$\overline{J}_{1y+}^{i,j-1} - \overline{J}_{1y-}^{i,j} = 0$$

$$\frac{1}{h}\left(St_{1,i,-1+j}\left(-a_{1,0,i,-1+j}\,e_{1,xy,i,-1+j} - \frac{1}{2}\,a_{1,1,i,-1+j}\,e_{1,xy,i,-1+j} - \frac{1}{2}\,a_{1,2,i,-1+j}\,e_{1,xy,i,-1+j} - a_{0,1,i,-1+j}\,e_{1,yy,i,-1+j} - 3\,a_{0,2,i,-1+j}\,e_{1,yy,i,-1+j} - 2\,a_{0,3,i,-1+j}\,e_{1,yy,i,-1+j} - \frac{1}{5}\,a_{0,4,i,-1+j}\,e_{1,yy,i,-1+j}\right)\right) -$$

$$\frac{1}{h}\left(St_{1,i,j}\left(-a_{1,0,i,j}\,e_{1,xy,i,j} + \frac{1}{2}\,a_{1,1,i,j}\,e_{1,xy,i,j} - \frac{1}{2}\,a_{1,2,i,j}\,e_{1,xy,i,j} - a_{0,1,i,j}\,e_{1,yy,i,j} + 3\,a_{0,2,i,j}\,e_{1,yy,i,j} - 2\,a_{0,3,i,j}\,e_{1,yy,i,j} + \frac{1}{5}\,a_{0,4,i,j}\,e_{1,yy,i,j}\right)\right) == 0$$

- Thermal current

$$\bar{J}^{i-1,j}_{2x+} - \bar{J}^{i,j}_{2x-} = 0$$

$$-\frac{\text{Sinh}\left[\frac{1}{2}\,\gamma_{1,-1+i,j}\right] c_{1,-1+i,j}\, St_{2,-1+i,j}\, \gamma_{1,-1+i,j}\, e_{2,xx,-1+i,j}}{h} -$$

$$\frac{\text{Cosh}\left[\frac{1}{2}\,\gamma_{1,-1+i,j}\right] c_{2,-1+i,j}\, St_{2,-1+i,j}\, \gamma_{1,-1+i,j}\, e_{2,xx,-1+i,j}}{h} - \frac{St_{2,-1+i,j}\, b_{1,0,-1+i,j}\, e_{2,xx,-1+i,j}}{h} -$$

$$\frac{3\, St_{2,-1+i,j}\, b_{2,0,-1+i,j}\, e_{2,xx,-1+i,j}}{h} - \frac{2\, St_{2,-1+i,j}\, b_{3,0,-1+i,j}\, e_{2,xx,-1+i,j}}{h} - \frac{St_{2,-1+i,j}\, b_{4,0,-1+i,j}\, e_{2,xx,-1+i,j}}{5h} -$$

$$\frac{\text{Sinh}\left[\frac{1}{2}\,\gamma_{1,i,j}\right] c_{1,i,j}\, St_{2,i,j}\, \gamma_{1,i,j}\, e_{2,xx,i,j}}{h} + \frac{\text{Cosh}\left[\frac{1}{2}\,\gamma_{1,i,j}\right] c_{2,i,j}\, St_{2,i,j}\, \gamma_{1,i,j}\, e_{2,xx,i,j}}{h} +$$

$$\frac{St_{2,i,j}\, b_{1,0,i,j}\, e_{2,xx,i,j}}{h} - \frac{3\, St_{2,i,j}\, b_{2,0,i,j}\, e_{2,xx,i,j}}{h} + \frac{2\, St_{2,i,j}\, b_{3,0,i,j}\, e_{2,xx,i,j}}{h} -$$

$$\frac{St_{2,i,j}\, b_{4,0,i,j}\, e_{2,xx,i,j}}{5h} - \frac{2\,\text{Sinh}\left[\frac{1}{2}\,\gamma_{2,-1+i,j}\right] c_{4,-1+i,j}\, St_{2,-1+i,j}\, e_{2,xy,-1+i,j}}{h} -$$

$$\frac{St_{2,-1+i,j}\, b_{0,1,-1+i,j}\, e_{2,xy,-1+i,j}}{h} - \frac{St_{2,-1+i,j}\, b_{1,1,-1+i,j}\, e_{2,xy,-1+i,j}}{2h} - \frac{St_{2,-1+i,j}\, b_{2,1,-1+i,j}\, e_{2,xy,-1+i,j}}{2h} +$$

$$c_{6,-1+i,j}\left(\frac{2\,\text{Cosh}\left[\frac{\gamma_{3,-1+i,j}\theta_{1,-1+i,j}}{2\sqrt{2}}\right]\text{Sinh}\left[\frac{\gamma_{3,-1+i,j}}{2\sqrt{2}}\right] St_{2,-1+i,j}\,\theta_{1,-1+i,j}\, e_{2,xx,-1+i,j}}{h} -\right.$$

$$\left.\frac{2\,\text{Cosh}\left[\frac{\gamma_{3,-1+i,j}\theta_{1,-1+i,j}}{2\sqrt{2}}\right]\text{Sinh}\left[\frac{\gamma_{3,-1+i,j}}{2\sqrt{2}}\right] St_{2,-1+i,j}\, e_{2,xy,-1+i,j}}{h}\right) +$$

$$c_{8,-1+i,j}\left(\frac{2\,\text{Cosh}\left[\frac{\gamma_{3,-1+i,j}\theta_{2,-1+i,j}}{2\sqrt{2}}\right]\text{Sinh}\left[\frac{\gamma_{3,-1+i,j}}{2\sqrt{2}}\right] St_{2,-1+i,j}\,\theta_{2,-1+i,j}\, e_{2,xx,-1+i,j}}{h} -\right.$$

$$\left.\frac{2\,\text{Cosh}\left[\frac{\gamma_{3,-1+i,j}\theta_{2,-1+i,j}}{2\sqrt{2}}\right]\text{Sinh}\left[\frac{\gamma_{3,-1+i,j}}{2\sqrt{2}}\right] St_{2,-1+i,j}\, e_{2,xy,-1+i,j}}{h}\right) +$$

$$c_{5,-1+i,j}\left(-\frac{2\,\text{Sinh}\left[\frac{\gamma_{3,-1+i,j}}{2\sqrt{2}}\right]\text{Sinh}\left[\frac{\gamma_{3,-1+i,j}\theta_{1,-1+i,j}}{2\sqrt{2}}\right] St_{2,-1+i,j}\,\theta_{1,-1+i,j}\, e_{2,xx,-1+i,j}}{h} +\right.$$

$$\left.\frac{2\,\text{Sinh}\left[\frac{\gamma_{3,-1+i,j}}{2\sqrt{2}}\right]\text{Sinh}\left[\frac{\gamma_{3,-1+i,j}\theta_{1,-1+i,j}}{2\sqrt{2}}\right] St_{2,-1+i,j}\, e_{2,xy,-1+i,j}}{h}\right) +$$

$$c_{7,-1+i,j}\left(-\frac{2\,\text{Sinh}\left[\frac{\gamma_{3,-1+i,j}}{2\sqrt{2}}\right]\text{Sinh}\left[\frac{\gamma_{3,-1+i,j}\theta_{2,-1+i,j}}{2\sqrt{2}}\right]\text{St}_{2,-1+i,j}\,\theta_{2,-1+i,j}\,e_{2,xx,-1+i,j}}{h}+\right.$$

$$\left.\frac{2\,\text{Sinh}\left[\frac{\gamma_{3,-1+i,j}}{2\sqrt{2}}\right]\text{Sinh}\left[\frac{\gamma_{3,-1+i,j}\theta_{2,-1+i,j}}{2\sqrt{2}}\right]\text{St}_{2,-1+i,j}\,e_{2,xy,-1+i,j}}{h}\right)+$$

$$\frac{2\,\text{Sinh}\left[\frac{1}{2}\gamma_{2,i,j}\right]c_{4,i,j}\,\text{St}_{2,i,j}\,e_{2,xy,i,j}}{h}+\frac{\text{St}_{2,i,j}\,b_{0,1,i,j}\,e_{2,xy,i,j}}{h}-\frac{\text{St}_{2,i,j}\,b_{1,1,i,j}\,e_{2,xy,i,j}}{2\,h}+$$

$$\frac{\text{St}_{2,i,j}\,b_{2,1,i,j}\,e_{2,xy,i,j}}{2\,h}+c_{6,i,j}\left(-\frac{2\,\text{Cosh}\left[\frac{\gamma_{3,i,j}\theta_{1,i,j}}{2\sqrt{2}}\right]\text{Sinh}\left[\frac{\gamma_{3,i,j}}{2\sqrt{2}}\right]\text{St}_{2,i,j}\,\theta_{1,i,j}\,e_{2,xx,i,j}}{h}+\right.$$

$$\left.\frac{2\,\text{Cosh}\left[\frac{\gamma_{3,i,j}\theta_{1,i,j}}{2\sqrt{2}}\right]\text{Sinh}\left[\frac{\gamma_{3,i,j}}{2\sqrt{2}}\right]\text{St}_{2,i,j}\,e_{2,xy,i,j}}{h}\right)+$$

$$c_{8,i,j}\left(-\frac{2\,\text{Cosh}\left[\frac{\gamma_{3,i,j}\theta_{2,i,j}}{2\sqrt{2}}\right]\text{Sinh}\left[\frac{\gamma_{3,i,j}}{2\sqrt{2}}\right]\text{St}_{2,i,j}\,\theta_{2,i,j}\,e_{2,xx,i,j}}{h}+\right.$$

$$\left.\frac{2\,\text{Cosh}\left[\frac{\gamma_{3,i,j}\theta_{2,i,j}}{2\sqrt{2}}\right]\text{Sinh}\left[\frac{\gamma_{3,i,j}}{2\sqrt{2}}\right]\text{St}_{2,i,j}\,e_{2,xy,i,j}}{h}\right)+$$

$$c_{5,i,j}\left(-\frac{2\,\text{Sinh}\left[\frac{\gamma_{3,i,j}}{2\sqrt{2}}\right]\text{Sinh}\left[\frac{\gamma_{3,i,j}\theta_{1,i,j}}{2\sqrt{2}}\right]\text{St}_{2,i,j}\,\theta_{1,i,j}\,e_{2,xx,i,j}}{h}+\right.$$

$$\left.\frac{2\,\text{Sinh}\left[\frac{\gamma_{3,i,j}}{2\sqrt{2}}\right]\text{Sinh}\left[\frac{\gamma_{3,i,j}\theta_{1,i,j}}{2\sqrt{2}}\right]\text{St}_{2,i,j}\,e_{2,xy,i,j}}{h}\right)+$$

$$c_{7,i,j}\left(-\frac{2\,\text{Sinh}\left[\frac{\gamma_{3,i,j}}{2\sqrt{2}}\right]\text{Sinh}\left[\frac{\gamma_{3,i,j}\theta_{2,i,j}}{2\sqrt{2}}\right]\text{St}_{2,i,j}\,\theta_{2,i,j}\,e_{2,xx,i,j}}{h}+\right.$$

$$\left.\frac{2\,\text{Sinh}\left[\frac{\gamma_{3,i,j}}{2\sqrt{2}}\right]\text{Sinh}\left[\frac{\gamma_{3,i,j}\theta_{2,i,j}}{2\sqrt{2}}\right]\text{St}_{2,i,j}\,e_{2,xy,i,j}}{h}\right)==0$$

$$\overline{J}^{i-1,j-1}_{2x+} - \overline{J}^{i,j-1}_{2x-} = 0$$

$$-\frac{\text{Sinh}\left[\frac{1}{2}\,\gamma_{1,-1+i,-1+j}\right]\,c_{1,-1+i,-1+j}\,St_{2,-1+i,-1+j}\,\gamma_{1,-1+i,-1+j}\,e_{2,xx,-1+i,-1+j}}{h} -$$

$$\frac{\text{Cosh}\left[\frac{1}{2}\,\gamma_{1,-1+i,-1+j}\right]\,c_{2,-1+i,-1+j}\,St_{2,-1+i,-1+j}\,\gamma_{1,-1+i,-1+j}\,e_{2,xx,-1+i,-1+j}}{h} - \frac{St_{2,-1+i,-1+j}\,b_{1,0,-1+i,-1+j}\,e_{2,xx,-1+i,-1+j}}{h} -$$

$$\frac{3\,St_{2,-1+i,-1+j}\,b_{2,0,-1+i,-1+j}\,e_{2,xx,-1+i,-1+j}}{h} - \frac{2\,St_{2,-1+i,-1+j}\,b_{3,0,-1+i,-1+j}\,e_{2,xx,-1+i,-1+j}}{h} -$$

$$\frac{St_{2,-1+i,-1+j}\,b_{4,0,-1+i,-1+j}\,e_{2,xx,-1+i,-1+j}}{5h} - \frac{\text{Sinh}\left[\frac{1}{2}\,\gamma_{1,i,-1+j}\right]\,c_{1,i,-1+j}\,St_{2,i,-1+j}\,\gamma_{1,i,-1+j}\,e_{2,xx,i,-1+j}}{h} +$$

$$\frac{\text{Cosh}\left[\frac{1}{2}\,\gamma_{1,i,-1+j}\right]\,c_{2,i,-1+j}\,St_{2,i,-1+j}\,\gamma_{1,i,-1+j}\,e_{2,xx,i,-1+j}}{h} + \frac{St_{2,i,-1+j}\,b_{1,0,i,-1+j}\,e_{2,xx,i,-1+j}}{h} -$$

$$\frac{3\,St_{2,i,-1+j}\,b_{2,0,i,-1+j}\,e_{2,xx,i,-1+j}}{h} + \frac{2\,St_{2,i,-1+j}\,b_{3,0,i,-1+j}\,e_{2,xx,i,-1+j}}{h} - \frac{St_{2,i,-1+j}\,b_{4,0,i,-1+j}\,e_{2,xx,i,-1+j}}{5h} -$$

$$\frac{2\,\text{Sinh}\left[\frac{1}{2}\,\gamma_{2,-1+i,-1+j}\right]\,c_{4,-1+i,-1+j}\,St_{2,-1+i,-1+j}\,e_{2,xy,-1+i,-1+j}}{h} - \frac{St_{2,-1+i,-1+j}\,b_{0,1,-1+i,-1+j}\,e_{2,xy,-1+i,-1+j}}{h} -$$

$$\frac{St_{2,-1+i,-1+j}\,b_{1,1,-1+i,-1+j}\,e_{2,xy,-1+i,-1+j}}{2h} - \frac{St_{2,-1+i,-1+j}\,b_{2,1,-1+i,-1+j}\,e_{2,xy,-1+i,-1+j}}{2h} +$$

$$c_{6,-1+i,-1+j}\left(\frac{2\,\text{Cosh}\left[\frac{\gamma_{3,-1+i,-1+j}\,\theta_{1,-1+i,-1+j}}{2\sqrt{2}}\right]\,\text{Sinh}\left[\frac{\gamma_{3,-1+i,-1+j}}{2\sqrt{2}}\right]\,St_{2,-1+i,-1+j}\,\theta_{1,-1+i,-1+j}\,e_{2,xx,-1+i,-1+j}}{h} -\right.$$

$$\left.\frac{2\,\text{Cosh}\left[\frac{\gamma_{3,-1+i,-1+j}\,\theta_{1,-1+i,-1+j}}{2\sqrt{2}}\right]\,\text{Sinh}\left[\frac{\gamma_{3,-1+i,-1+j}}{2\sqrt{2}}\right]\,St_{2,-1+i,-1+j}\,e_{2,xy,-1+i,-1+j}}{h}\right) +$$

$$c_{8,-1+i,-1+j}\left(\frac{2\,\text{Cosh}\left[\frac{\gamma_{3,-1+i,-1+j}\,\theta_{2,-1+i,-1+j}}{2\sqrt{2}}\right]\,\text{Sinh}\left[\frac{\gamma_{3,-1+i,-1+j}}{2\sqrt{2}}\right]\,St_{2,-1+i,-1+j}\,\theta_{2,-1+i,-1+j}\,e_{2,xx,-1+i,-1+j}}{h} -\right.$$

$$\left.\frac{2\,\text{Cosh}\left[\frac{\gamma_{3,-1+i,-1+j}\,\theta_{2,-1+i,-1+j}}{2\sqrt{2}}\right]\,\text{Sinh}\left[\frac{\gamma_{3,-1+i,-1+j}}{2\sqrt{2}}\right]\,St_{2,-1+i,-1+j}\,e_{2,xy,-1+i,-1+j}}{h}\right) +$$

$$c_{5,-1+i,-1+j}\left(-\frac{2\,\text{Sinh}\left[\frac{\gamma_{3,-1+i,-1+j}}{2\sqrt{2}}\right]\,\text{Sinh}\left[\frac{\gamma_{3,-1+i,-1+j}\,\theta_{1,-1+i,-1+j}}{2\sqrt{2}}\right]\,St_{2,-1+i,-1+j}\,\theta_{1,-1+i,-1+j}\,e_{2,xx,-1+i,-1+j}}{h} +\right.$$

$$\left.\frac{2\,\text{Sinh}\left[\frac{\gamma_{3,-1+i,-1+j}}{2\sqrt{2}}\right]\,\text{Sinh}\left[\frac{\gamma_{3,-1+i,-1+j}\,\theta_{1,-1+i,-1+j}}{2\sqrt{2}}\right]\,St_{2,-1+i,-1+j}\,e_{2,xy,-1+i,-1+j}}{h}\right) +$$

$$c_{7,-1+i,-1+j}\left(-\frac{2\,\text{Sinh}\left[\frac{\gamma_{3,-1+i,-1+j}}{2\sqrt{2}}\right]\,\text{Sinh}\left[\frac{\gamma_{3,-1+i,-1+j}\,\theta_{2,-1+i,-1+j}}{2\sqrt{2}}\right]\,St_{2,-1+i,-1+j}\,\theta_{2,-1+i,-1+j}\,e_{2,xx,-1+i,-1+j}}{h} +\right.$$

$$\frac{2\,\text{Sinh}\left[\frac{\gamma_{3,-1+i,-1+j}}{2\sqrt{2}}\right]\text{Sinh}\left[\frac{\gamma_{3,-1+i,-1+j}\theta_{2,-1+i,-1+j}}{2\sqrt{2}}\right]\text{St}_{2,-1+i,-1+j}\,e_{2,xy,-1+i,-1+j}}{h}+$$

$$\frac{2\,\text{Sinh}\left[\frac{1}{2}\gamma_{2,i,-1+j}\right]c_{4,i,-1+j}\,\text{St}_{2,i,-1+j}\,e_{2,xy,i,-1+j}}{h}+\frac{\text{St}_{2,i,-1+j}\,b_{0,1,i,-1+j}\,e_{2,xy,i,-1+j}}{h}-$$

$$\frac{\text{St}_{2,i,-1+j}\,b_{1,1,i,-1+j}\,e_{2,xy,i,-1+j}}{2h}+\frac{\text{St}_{2,i,-1+j}\,b_{2,1,i,-1+j}\,e_{2,xy,i,-1+j}}{2h}+$$

$$c_{6,i,-1+j}\left(-\frac{2\,\text{Cosh}\left[\frac{\gamma_{3,i,-1+j}\theta_{1,i,-1+j}}{2\sqrt{2}}\right]\text{Sinh}\left[\frac{\gamma_{3,i,-1+j}}{2\sqrt{2}}\right]\text{St}_{2,i,-1+j}\,\theta_{1,i,-1+j}\,e_{2,xx,i,-1+j}}{h}+\right.$$

$$\left.\frac{2\,\text{Cosh}\left[\frac{\gamma_{3,i,-1+j}\theta_{1,i,-1+j}}{2\sqrt{2}}\right]\text{Sinh}\left[\frac{\gamma_{3,i,-1+j}}{2\sqrt{2}}\right]\text{St}_{2,i,-1+j}\,e_{2,xy,i,-1+j}}{h}\right)+$$

$$c_{8,i,-1+j}\left(-\frac{2\,\text{Cosh}\left[\frac{\gamma_{3,i,-1+j}\theta_{2,i,-1+j}}{2\sqrt{2}}\right]\text{Sinh}\left[\frac{\gamma_{3,i,-1+j}}{2\sqrt{2}}\right]\text{St}_{2,i,-1+j}\,\theta_{2,i,-1+j}\,e_{2,xx,i,-1+j}}{h}+\right.$$

$$\left.\frac{2\,\text{Cosh}\left[\frac{\gamma_{3,i,-1+j}\theta_{2,i,-1+j}}{2\sqrt{2}}\right]\text{Sinh}\left[\frac{\gamma_{3,i,-1+j}}{2\sqrt{2}}\right]\text{St}_{2,i,-1+j}\,e_{2,xy,i,-1+j}}{h}\right)+$$

$$c_{5,i,-1+j}\left(-\frac{2\,\text{Sinh}\left[\frac{\gamma_{3,i,-1+j}}{2\sqrt{2}}\right]\text{Sinh}\left[\frac{\gamma_{3,i,-1+j}\theta_{1,i,-1+j}}{2\sqrt{2}}\right]\text{St}_{2,i,-1+j}\,\theta_{1,i,-1+j}\,e_{2,xx,i,-1+j}}{h}+\right.$$

$$\left.\frac{2\,\text{Sinh}\left[\frac{\gamma_{3,i,-1+j}}{2\sqrt{2}}\right]\text{Sinh}\left[\frac{\gamma_{3,i,-1+j}\theta_{1,i,-1+j}}{2\sqrt{2}}\right]\text{St}_{2,i,-1+j}\,e_{2,xy,i,-1+j}}{h}\right)+$$

$$c_{7,i,-1+j}\left(-\frac{2\,\text{Sinh}\left[\frac{\gamma_{3,i,-1+j}}{2\sqrt{2}}\right]\text{Sinh}\left[\frac{\gamma_{3,i,-1+j}\theta_{2,i,-1+j}}{2\sqrt{2}}\right]\text{St}_{2,i,-1+j}\,\theta_{2,i,-1+j}\,e_{2,xx,i,-1+j}}{h}+\right.$$

$$\left.\frac{2\,\text{Sinh}\left[\frac{\gamma_{3,i,-1+j}}{2\sqrt{2}}\right]\text{Sinh}\left[\frac{\gamma_{3,i,-1+j}\theta_{2,i,-1+j}}{2\sqrt{2}}\right]\text{St}_{2,i,-1+j}\,e_{2,xy,i,-1+j}}{h}\right)==0$$

$$\overline{J}^{i-1,j-1}_{2y+} - \overline{J}^{i-1,j}_{2y-} = 0$$

$$-\frac{2\,\mathrm{Sinh}\left[\frac{1}{2}\,\gamma_{1,-1+i,-1+j}\right]\,c_{2,-1+i,-1+j}\,St_{2,-1+i,-1+j}\,e_{2,xy,-1+i,-1+j}}{h} -$$

$$\frac{St_{2,-1+i,-1+j}\,b_{1,0,-1+i,-1+j}\,e_{2,xy,-1+i,-1+j}}{h} - \frac{St_{2,-1+i,-1+j}\,b_{1,1,-1+i,-1+j}\,e_{2,xy,-1+i,-1+j}}{2\,h} -$$

$$\frac{St_{2,-1+i,-1+j}\,b_{1,2,-1+i,-1+j}\,e_{2,xy,-1+i,-1+j}}{2\,h} + \frac{2\,\mathrm{Sinh}\left[\frac{1}{2}\,\gamma_{1,-1+i,j}\right]\,c_{2,-1+i,j}\,St_{2,-1+i,j}\,e_{2,xy,-1+i,j}}{h} +$$

$$\frac{St_{2,-1+i,j}\,b_{1,0,-1+i,j}\,e_{2,xy,-1+i,j}}{h} - \frac{St_{2,-1+i,j}\,b_{1,1,-1+i,j}\,e_{2,xy,-1+i,j}}{2\,h} + \frac{St_{2,-1+i,j}\,b_{1,2,-1+i,j}\,e_{2,xy,-1+i,j}}{2\,h} -$$

$$\frac{\mathrm{Sinh}\left[\frac{1}{2}\,\gamma_{2,-1+i,-1+j}\right]\,c_{3,-1+i,-1+j}\,St_{2,-1+i,-1+j}\,\gamma_{2,-1+i,-1+j}\,e_{2,yy,-1+i,-1+j}}{h} -$$

$$\frac{\mathrm{Cosh}\left[\frac{1}{2}\,\gamma_{2,-1+i,-1+j}\right]\,c_{4,-1+i,-1+j}\,St_{2,-1+i,-1+j}\,\gamma_{2,-1+i,-1+j}\,e_{2,yy,-1+i,-1+j}}{h} -$$

$$\frac{St_{2,-1+i,-1+j}\,b_{0,1,-1+i,-1+j}\,e_{2,yy,-1+i,-1+j}}{h} - \frac{3\,St_{2,-1+i,-1+j}\,b_{0,2,-1+i,-1+j}\,e_{2,yy,-1+i,-1+j}}{h} -$$

$$\frac{2\,St_{2,-1+i,-1+j}\,b_{0,3,-1+i,-1+j}\,e_{2,yy,-1+i,-1+j}}{h} - \frac{St_{2,-1+i,-1+j}\,b_{0,4,-1+i,-1+j}\,e_{2,yy,-1+i,-1+j}}{5\,h} +$$

$$c_{6,-1+i,-1+j}\left(\frac{2\,\mathrm{Cosh}\left[\frac{\gamma_{3,-1+i,-1+j}}{2\sqrt{2}}\right]\,\mathrm{Sinh}\left[\frac{\gamma_{3,-1+i,-1+j}\,\theta_{1,-1+i,-1+j}}{2\sqrt{2}}\right]\,St_{2,-1+i,-1+j}\,e_{2,xy,-1+i,-1+j}}{h} -\right.$$

$$\left.\frac{2\,\mathrm{Cosh}\left[\frac{\gamma_{3,-1+i,-1+j}}{2\sqrt{2}}\right]\,\mathrm{Sinh}\left[\frac{\gamma_{3,-1+i,-1+j}\,\theta_{1,-1+i,-1+j}}{2\sqrt{2}}\right]\,St_{2,-1+i,-1+j}\,e_{2,yy,-1+i,-1+j}}{h\,\theta_{1,-1+i,-1+j}}\right) +$$

$$c_{5,-1+i,-1+j}\left(\frac{2\,\mathrm{Sinh}\left[\frac{\gamma_{3,-1+i,-1+j}}{2\sqrt{2}}\right]\,\mathrm{Sinh}\left[\frac{\gamma_{3,-1+i,-1+j}\,\theta_{1,-1+i,-1+j}}{2\sqrt{2}}\right]\,St_{2,-1+i,-1+j}\,e_{2,xy,-1+i,-1+j}}{h} -\right.$$

$$\left.\frac{2\,\mathrm{Sinh}\left[\frac{\gamma_{3,-1+i,-1+j}}{2\sqrt{2}}\right]\,\mathrm{Sinh}\left[\frac{\gamma_{3,-1+i,-1+j}\,\theta_{1,-1+i,-1+j}}{2\sqrt{2}}\right]\,St_{2,-1+i,-1+j}\,e_{2,yy,-1+i,-1+j}}{h\,\theta_{1,-1+i,-1+j}}\right) +$$

$$c_{8,-1+i,-1+j}\left(\frac{2\,\mathrm{Cosh}\left[\frac{\gamma_{3,-1+i,-1+j}}{2\sqrt{2}}\right]\,\mathrm{Sinh}\left[\frac{\gamma_{3,-1+i,-1+j}\,\theta_{2,-1+i,-1+j}}{2\sqrt{2}}\right]\,St_{2,-1+i,-1+j}\,e_{2,xy,-1+i,-1+j}}{h} -\right.$$

$$\left.\frac{2\,\mathrm{Cosh}\left[\frac{\gamma_{3,-1+i,-1+j}}{2\sqrt{2}}\right]\,\mathrm{Sinh}\left[\frac{\gamma_{3,-1+i,-1+j}\,\theta_{2,-1+i,-1+j}}{2\sqrt{2}}\right]\,St_{2,-1+i,-1+j}\,e_{2,yy,-1+i,-1+j}}{h\,\theta_{2,-1+i,-1+j}}\right) +$$

$$c_{7,-1+i,-1+j}\left(\frac{2\,\mathrm{Sinh}\left[\frac{\gamma_{3,-1+i,-1+j}}{2\sqrt{2}}\right]\,\mathrm{Sinh}\left[\frac{\gamma_{3,-1+i,-1+j}\,\theta_{2,-1+i,-1+j}}{2\sqrt{2}}\right]\,St_{2,-1+i,-1+j}\,e_{2,xy,-1+i,-1+j}}{h} -\right.$$

$$\frac{2\,\mathrm{Sinh}\left[\frac{\gamma_{3,-1+i,-1+j}}{2\sqrt{2}}\right]\mathrm{Sinh}\left[\frac{\gamma_{3,-1+i,-1+j}\theta_{2,-1+i,-1+j}}{2\sqrt{2}}\right]\mathrm{St}_{2,-1+i,-1+j}\,e_{2,yy,-1+i,-1+j}}{h\theta_{2,-1+i,-1+j}} -$$

$$\frac{\mathrm{Sinh}\left[\frac{1}{2}\gamma_{2,-1+i,j}\right]c_{3,-1+i,j}\,\mathrm{St}_{2,-1+i,j}\,\gamma_{2,-1+i,j}\,e_{2,yy,-1+i,j}}{h} +$$

$$\frac{\mathrm{Cosh}\left[\frac{1}{2}\gamma_{2,-1+i,j}\right]c_{4,-1+i,j}\,\mathrm{St}_{2,-1+i,j}\,\gamma_{2,-1+i,j}\,e_{2,yy,-1+i,j}}{h} + \frac{\mathrm{St}_{2,-1+i,j}\,b_{0,1,-1+i,j}\,e_{2,yy,-1+i,j}}{h} -$$

$$\frac{3\,\mathrm{St}_{2,-1+i,j}\,b_{0,2,-1+i,j}\,e_{2,yy,-1+i,j}}{h} + \frac{2\,\mathrm{St}_{2,-1+i,j}\,b_{0,3,-1+i,j}\,e_{2,yy,-1+i,j}}{h} - \frac{\mathrm{St}_{2,-1+i,j}\,b_{0,4,-1+i,j}\,e_{2,yy,-1+i,j}}{5h} +$$

$$c_{6,-1+i,j}\left(-\frac{2\,\mathrm{Cosh}\left[\frac{\gamma_{3,-1+i,j}}{2\sqrt{2}}\right]\mathrm{Sinh}\left[\frac{\gamma_{3,-1+i,j}\theta_{1,-1+i,j}}{2\sqrt{2}}\right]\mathrm{St}_{2,-1+i,j}\,e_{2,xy,-1+i,j}}{h} +\right.$$

$$\left.\frac{2\,\mathrm{Cosh}\left[\frac{\gamma_{3,-1+i,j}}{2\sqrt{2}}\right]\mathrm{Sinh}\left[\frac{\gamma_{3,-1+i,j}\theta_{1,-1+i,j}}{2\sqrt{2}}\right]\mathrm{St}_{2,-1+i,j}\,e_{2,yy,-1+i,j}}{h\theta_{1,-1+i,j}}\right) +$$

$$c_{5,-1+i,j}\left(\frac{2\,\mathrm{Sinh}\left[\frac{\gamma_{3,-1+i,j}}{2\sqrt{2}}\right]\mathrm{Sinh}\left[\frac{\gamma_{3,-1+i,j}\theta_{1,-1+i,j}}{2\sqrt{2}}\right]\mathrm{St}_{2,-1+i,j}\,e_{2,xy,-1+i,j}}{h} -\right.$$

$$\left.\frac{2\,\mathrm{Sinh}\left[\frac{\gamma_{3,-1+i,j}}{2\sqrt{2}}\right]\mathrm{Sinh}\left[\frac{\gamma_{3,-1+i,j}\theta_{1,-1+i,j}}{2\sqrt{2}}\right]\mathrm{St}_{2,-1+i,j}\,e_{2,yy,-1+i,j}}{h\theta_{1,-1+i,j}}\right) +$$

$$c_{8,-1+i,j}\left(-\frac{2\,\mathrm{Cosh}\left[\frac{\gamma_{3,-1+i,j}}{2\sqrt{2}}\right]\mathrm{Sinh}\left[\frac{\gamma_{3,-1+i,j}\theta_{2,-1+i,j}}{2\sqrt{2}}\right]\mathrm{St}_{2,-1+i,j}\,e_{2,xy,-1+i,j}}{h} +\right.$$

$$\left.\frac{2\,\mathrm{Cosh}\left[\frac{\gamma_{3,-1+i,j}}{2\sqrt{2}}\right]\mathrm{Sinh}\left[\frac{\gamma_{3,-1+i,j}\theta_{2,-1+i,j}}{2\sqrt{2}}\right]\mathrm{St}_{2,-1+i,j}\,e_{2,yy,-1+i,j}}{h\theta_{2,-1+i,j}}\right) +$$

$$c_{7,-1+i,j}\left(\frac{2\,\mathrm{Sinh}\left[\frac{\gamma_{3,-1+i,j}}{2\sqrt{2}}\right]\mathrm{Sinh}\left[\frac{\gamma_{3,-1+i,j}\theta_{2,-1+i,j}}{2\sqrt{2}}\right]\mathrm{St}_{2,-1+i,j}\,e_{2,xy,-1+i,j}}{h} -\right.$$

$$\left.\frac{2\,\mathrm{Sinh}\left[\frac{\gamma_{3,-1+i,j}}{2\sqrt{2}}\right]\mathrm{Sinh}\left[\frac{\gamma_{3,-1+i,j}\theta_{2,-1+i,j}}{2\sqrt{2}}\right]\mathrm{St}_{2,-1+i,j}\,e_{2,yy,-1+i,j}}{h\theta_{2,-1+i,j}}\right) == 0$$

$$\bar{J}^{i,j-1}_{2y+} - \bar{J}^{i,j}_{2y-} = 0$$

$$-\frac{2\,\mathrm{Sinh}\left[\frac{1}{2}\,\gamma_{1,i,-1+j}\right]\,c_{2,i,-1+j}\,St_{2,i,-1+j}\,e_{2,xy,i,-1+j}}{h} - \frac{St_{2,i,-1+j}\,b_{1,0,i,-1+j}\,e_{2,xy,i,-1+j}}{h} -$$

$$\frac{St_{2,i,-1+j}\,b_{1,1,i,-1+j}\,e_{2,xy,i,-1+j}}{2h} - \frac{St_{2,i,-1+j}\,b_{1,2,i,-1+j}\,e_{2,xy,i,-1+j}}{2h} +$$

$$\frac{2\,\mathrm{Sinh}\left[\frac{1}{2}\,\gamma_{1,i,j}\right]\,c_{2,i,j}\,St_{2,i,j}\,e_{2,xy,i,j}}{h} + \frac{St_{2,i,j}\,b_{1,0,i,j}\,e_{2,xy,i,j}}{h} - \frac{St_{2,i,j}\,b_{1,1,i,j}\,e_{2,xy,i,j}}{2h} +$$

$$\frac{St_{2,i,j}\,b_{1,2,i,j}\,e_{2,xy,i,j}}{2h} - \frac{\mathrm{Sinh}\left[\frac{1}{2}\,\gamma_{2,i,-1+j}\right]\,c_{3,i,-1+j}\,St_{2,i,-1+j}\,\gamma_{2,i,-1+j}\,e_{2,yy,i,-1+j}}{h} -$$

$$\frac{\mathrm{Cosh}\left[\frac{1}{2}\,\gamma_{2,i,-1+j}\right]\,c_{4,i,-1+j}\,St_{2,i,-1+j}\,\gamma_{2,i,-1+j}\,e_{2,yy,i,-1+j}}{h} - \frac{St_{2,i,-1+j}\,b_{0,1,i,-1+j}\,e_{2,yy,i,-1+j}}{h} -$$

$$\frac{3\,St_{2,i,-1+j}\,b_{0,2,i,-1+j}\,e_{2,yy,i,-1+j}}{h} - \frac{2\,St_{2,i,-1+j}\,b_{0,3,i,-1+j}\,e_{2,yy,i,-1+j}}{h} - \frac{St_{2,i,-1+j}\,b_{0,4,i,-1+j}\,e_{2,yy,i,-1+j}}{5h} +$$

$$c_{6,i,-1+j}\left(\frac{2\,\mathrm{Cosh}\left[\frac{\gamma_{3,i,-1+j}}{2\sqrt{2}}\right]\,\mathrm{Sinh}\left[\frac{\gamma_{3,i,-1+j}\,\theta_{1,i,-1+j}}{2\sqrt{2}}\right]\,St_{2,i,-1+j}\,e_{2,xy,i,-1+j}}{h} -\right.$$

$$\left.\frac{2\,\mathrm{Cosh}\left[\frac{\gamma_{3,i,-1+j}}{2\sqrt{2}}\right]\,\mathrm{Sinh}\left[\frac{\gamma_{3,i,-1+j}\,\theta_{1,i,-1+j}}{2\sqrt{2}}\right]\,St_{2,i,-1+j}\,e_{2,yy,i,-1+j}}{h\,\theta_{1,i,-1+j}}\right) +$$

$$c_{5,i,-1+j}\left(\frac{2\,\mathrm{Sinh}\left[\frac{\gamma_{3,i,-1+j}}{2\sqrt{2}}\right]\,\mathrm{Sinh}\left[\frac{\gamma_{3,i,-1+j}\,\theta_{1,i,-1+j}}{2\sqrt{2}}\right]\,St_{2,i,-1+j}\,e_{2,xy,i,-1+j}}{h} -\right.$$

$$\left.\frac{2\,\mathrm{Sinh}\left[\frac{\gamma_{3,i,-1+j}}{2\sqrt{2}}\right]\,\mathrm{Sinh}\left[\frac{\gamma_{3,i,-1+j}\,\theta_{1,i,-1+j}}{2\sqrt{2}}\right]\,St_{2,i,-1+j}\,e_{2,yy,i,-1+j}}{h\,\theta_{1,i,-1+j}}\right) +$$

$$c_{8,i,-1+j}\left(\frac{2\,\mathrm{Cosh}\left[\frac{\gamma_{3,i,-1+j}}{2\sqrt{2}}\right]\,\mathrm{Sinh}\left[\frac{\gamma_{3,i,-1+j}\,\theta_{2,i,-1+j}}{2\sqrt{2}}\right]\,St_{2,i,-1+j}\,e_{2,xy,i,-1+j}}{h} -\right.$$

$$\left.\frac{2\,\mathrm{Cosh}\left[\frac{\gamma_{3,i,-1+j}}{2\sqrt{2}}\right]\,\mathrm{Sinh}\left[\frac{\gamma_{3,i,-1+j}\,\theta_{2,i,-1+j}}{2\sqrt{2}}\right]\,St_{2,i,-1+j}\,e_{2,yy,i,-1+j}}{h\,\theta_{2,i,-1+j}}\right) +$$

$$c_{7,i,-1+j}\left(\frac{2\,\mathrm{Sinh}\left[\frac{\gamma_{3,i,-1+j}}{2\sqrt{2}}\right]\,\mathrm{Sinh}\left[\frac{\gamma_{3,i,-1+j}\,\theta_{2,i,-1+j}}{2\sqrt{2}}\right]\,St_{2,i,-1+j}\,e_{2,xy,i,-1+j}}{h} -\right.$$

$$\left.\frac{2\,\mathrm{Sinh}\left[\frac{\gamma_{3,i,-1+j}}{2\sqrt{2}}\right]\,\mathrm{Sinh}\left[\frac{\gamma_{3,i,-1+j}\,\theta_{2,i,-1+j}}{2\sqrt{2}}\right]\,St_{2,i,-1+j}\,e_{2,yy,i,-1+j}}{h\,\theta_{2,i,-1+j}}\right) -$$

$$\frac{\text{Sinh}\left[\frac{1}{2}\gamma_{2,i,j}\right] c_{3,i,j}\, St_{2,i,j}\, \gamma_{2,i,j}\, e_{2,yy,i,j}}{h} +$$

$$\frac{\text{Cosh}\left[\frac{1}{2}\gamma_{2,i,j}\right] c_{4,i,j}\, St_{2,i,j}\, \gamma_{2,i,j}\, e_{2,yy,i,j}}{h} + \frac{St_{2,i,j}\, b_{0,1,i,j}\, e_{2,yy,i,j}}{h} -$$

$$\frac{3\, St_{2,i,j}\, b_{0,2,i,j}\, e_{2,yy,i,j}}{h} + \frac{2\, St_{2,i,j}\, b_{0,3,i,j}\, e_{2,yy,i,j}}{h} - \frac{St_{2,i,j}\, b_{0,4,i,j}\, e_{2,yy,i,j}}{5h} + c_{6,i,j}$$

$$\left(-\frac{2\,\text{Cosh}\left[\frac{\gamma_{3,i,j}}{2\sqrt{2}}\right] \text{Sinh}\left[\frac{\gamma_{3,i,j}\theta_{1,i,j}}{2\sqrt{2}}\right] St_{2,i,j}\, e_{2,xy,i,j}}{h} + \frac{2\,\text{Cosh}\left[\frac{\gamma_{3,i,j}}{2\sqrt{2}}\right] \text{Sinh}\left[\frac{\gamma_{3,i,j}\theta_{1,i,j}}{2\sqrt{2}}\right] St_{2,i,j}\, e_{2,yy,i,j}}{h\theta_{1,i,j}} \right) +$$

$$c_{5,i,j} \left(\frac{2\,\text{Sinh}\left[\frac{\gamma_{3,i,j}}{2\sqrt{2}}\right] \text{Sinh}\left[\frac{\gamma_{3,i,j}\theta_{1,i,j}}{2\sqrt{2}}\right] St_{2,i,j}\, e_{2,xy,i,j}}{h} - \right.$$

$$\left. \frac{2\,\text{Sinh}\left[\frac{\gamma_{3,i,j}}{2\sqrt{2}}\right] \text{Sinh}\left[\frac{\gamma_{3,i,j}\theta_{1,i,j}}{2\sqrt{2}}\right] St_{2,i,j}\, e_{2,yy,i,j}}{h\theta_{1,i,j}} \right) + c_{8,i,j}$$

$$\left(-\frac{2\,\text{Cosh}\left[\frac{\gamma_{3,i,j}}{2\sqrt{2}}\right] \text{Sinh}\left[\frac{\gamma_{3,i,j}\theta_{2,i,j}}{2\sqrt{2}}\right] St_{2,i,j}\, e_{2,xy,i,j}}{h} + \frac{2\,\text{Cosh}\left[\frac{\gamma_{3,i,j}}{2\sqrt{2}}\right] \text{Sinh}\left[\frac{\gamma_{3,i,j}\theta_{2,i,j}}{2\sqrt{2}}\right] St_{2,i,j}\, e_{2,yy,i,j}}{h\theta_{2,i,j}} \right) +$$

$$c_{7,i,j} \left(\frac{2\,\text{Sinh}\left[\frac{\gamma_{3,i,j}}{2\sqrt{2}}\right] \text{Sinh}\left[\frac{\gamma_{3,i,j}\theta_{2,i,j}}{2\sqrt{2}}\right] St_{2,i,j}\, e_{2,xy,i,j}}{h} - \right.$$

$$\left. \frac{2\,\text{Sinh}\left[\frac{\gamma_{3,i,j}}{2\sqrt{2}}\right] \text{Sinh}\left[\frac{\gamma_{3,i,j}\theta_{2,i,j}}{2\sqrt{2}}\right] St_{2,i,j}\, e_{2,yy,i,j}}{h\theta_{2,i,j}} \right) == 0$$

NOTE: Appendices A, B, and C are included to illustrate the complexity of the linear equations in expansion coefficients a_{mn} and c_l. Some equations are omitted for brevity.